Title
Accumulation of Toxic Trace Elements in Evaporites in Agricultural Evaporation Ponds

Authors
Tanji, Kenneth K
Dahlgren, Randy A
Ong, Colin
et al.

Publication Date
1994-12-01

ACCUMULATION OF TOXIC TRACE ELEMENTS IN EVAPORITES IN AGRICULTURAL EVAPORATION PONDS

by

Kenneth K. Tanji and Randy A. Dahlgren

Principal Investigators

Department of Land, Air and Water Resources

University of California, Davis

and

Colin Ong, Mitchell Herbel, Ann Quek, Suduan Gao

Research Staff

Department of Land, Air and Water Resources

University of California, Davis

TECHNICAL COMPLETION REPORT

Project Number UCAL-WRC-W-742

December 1994

University of California Water Resources Center

The research leading to this report was supported by the University of California Water Resources Center, as part of Water Resources Center Project UCAL-WRC-W-742

Abstract

Evaporation ponds are utilized to dispose of saline agricultural drainage waters where there are no surface drainage outlets to the San Joaquin River. Presently, 22 ponds in the San Joaquin Valley's west side are receiving about 32,000 acre-feet per year of tile drainage effluents and about 0.8 million tons per year of salt are being deposited. This project investigates the incorporation of potentially toxic trace elements (selenium, boron, arsenic, molybdenum) into evaporite minerals forming by desiccation of drainage waters.

Over 50 samples of salt deposits (evaporites) obtained from seven ponds show that the predominant minerals are either halite (NaCl), thenardite (Na_2SO_4) or mirabilite ($Na_2SO_4 \cdot 10H_2O$), reflecting the dominant dissolved mineral salts in the drain water. The highest selenium concentrations in evaporites were found in Peck pond, ranging from 3 to 33 mg/kg (ppm) with a mean value of 12 mg/kg for six samples. Evaporite samples from all other ponds contained a maximum selenium level of 1.8 mg/kg and mean value of 0.22 mg/kg or less. The values are well below the 100 mg/kg threshold level of selenium for wastes to be considered hazardous. The concentrations of boron in evaporites ranged from a low of 16 in Barbizon pond to as high as 975 mg/kg in Lost Hills pond. The mean concentration of boron in evaporites from seven ponds ranged from 73 to 690 mg/kg. There are no hazardous criterion for boron threshold level in waste solids.

Laboratory studies indicate that association of boron with halite or mirabilite are influenced by both the nature of the salt crystal surface and the chemical species of boron. For example, boron association occurs mainly by surface adsorption on halite and by both surface adsorption and internal absorption (by diffusion into the crystal lattice) for mirabilite.

Keywords: Trace elements, subsurface drainage, evaporation, mineralogy, geochemistry, hazardous wastes.

List of Tables

List of Figures

* PROBLEM STATEMENT:

The presence of toxic trace elements (e.g., selenium, boron, arsenic, and molybdenum) in collected subsurface drainage waters and shallow ground waters in the San Joaquin Valley's west side has resulted in a critical agricultural and environmental problem. Where there is no surface drainage outlet to the San Joaquin River (i.e., south of Firebaugh to Bakersfield), saline tile effluents from drainage-impacted farmlands are disposed into agricultural evaporation ponds. The 22 active ponds are receiving about 32,000 acre-feet of effluents from about 56,500 acres of tile-drained fields. About 25% of the 3.3 million tons of salt per year accumulating in the west side are disposed into these ponds.

The use of evaporation ponds is of concern because they may potentially result in hazardous levels of trace elements to waterfowl and other wildlife attracted to these ponds. Several ponds in the environs of Tulare Lake Basin have already approached functionally hazardous status to waterfowl, similar to the selenium poisoning of waterfowl at Kesterson National Wildlife Refuge. The Regional Water Quality Control board recently ordered the closure of the Sumner Peck evaporation pond facility located south of Mendota due to elevated concentrations of selenium. The closure order requires the pond operator to dry up the 120 acre pond facility by January 1993 or line them with plastic.

A previous study showed that trace elements accumulated differentially in pond waters during the evapoconcentration process due to different immobilization mechanisms. The question of what kinds of trace elements and how much are present in the precipitated salt deposits (evaporites) had not been previously addressed. This question is of importance in the ultimate disposal and/or recycling of the 0.8 million tons/year of salts deposited in the ponds. The alternatives include salt harvesting for commercial use (industrial and agricultural) and burial. Ponds could be filled in and new ones constructed. In the event that the salts contain hazardous levels of toxicants such that it would be classified as toxic waste, burial at Class I waste disposal sites may be necessary. Therefore, it is important to determine if these salts accumulate trace elements to the point of becoming hazardous wastes.

*RESEARCH OBJECTIVES

(1) Determine the quantity of selenium, boron, arsenic and molybdenum immobilized in evaporite minerals (salt crusts) found in seven representative evaporation pond facilities in the San Joaquin Valley.

(2) Determine the partitioning of trace elements between the evaporite minerals and the ponds waters.

(3) Develop a laboratory method of simulating evapoconcentration of salt solutions and drainage waters to enhance evaporite mineral precipitation.

(4) Examine mechanisms of trace element incorporation by halite and mirabilite, e.g. sorption, occlusion, co-precipitation.

*MATERIALS AND METHODS (general overview)

This project involves the integration of field and laboratory studies. In August 1990 and February 1991, 50 samples of evaporite minerals and 18 brine solutions in equilibrium with the evaporite minerals were obtained from 7 evaporation ponds (Peck, Pryse, Meyers, Barbizon, Lost Hills, Westlake South and Westlake North). The evaporites were analyzed by x-ray powder diffraction analysis (XRD) to identify the dominant mineral phases. The evaporites were dissolved in distilled deionized water, filtered through a 0.45 μm membrane filter to remove particulate matter, and the filtrate analyzed for the major cations (sodium, calcium, potassium, magnesium) and anions (chloride, nitrate, sulfate) as well as trace elements (selenium, boron, arsenic, molybdenum). The pond waters were analyzed for the same elemental constituents. This data was used to ascertain the principal mineral phases formed in the ponds from evapoconcentration and their trace element content. The data was also used to determine partitioning of trace elements between the evaporite minerals and the pond waters (i.e. to determine whether trace elements concentrate in the evaporite minerals or if they are excluded from the evaporite minerals).

Laboratory evapoconcentration studies were conducted using several pure salt solutions spiked with either Se or B. The salt solutions utilized were sodium sulfate (Na_2SO_4) and sodium chloride (NaCl) to represent the dominant dissolved mineral salts present in the pond waters. Field evapoconcentration (desiccation) of pond waters was simulated by passing dry air over salt solution samples placed in evaporation chambers. In one evaporation study, salt solution mixtures of Na_2SO_4 and sodium selenite (Na_2SeO_3) as well as Na_2SO_4 and sodium selenate (Na_2SeO_4) were desiccated at 40°C with dry air. The results of this experiment show variations in the chemical composition of the mineral precipitated along particular desiccation pathways.

In a second laboratory evapoconcentration study, the association of B with halite and mirabilite, the two dominant minerals found in evaporation ponds, was investigated. One approach was to evapoconcentrate NaCl or Na_2SO_4 solutions containing B to form halite (NaCl) or mirabilite ($Na_2SO_4 \cdot 10H_2O$). The other approach was to equilibrate boron-free halite and mirabilite with saline boron solutions. The data collected was used to assess how much B becomes associated with these two evaporites and possible mechanisms of B removal (immobilization) from the solution by the minerals.

NATURE OF EVAPORITES FORMED IN EVAPORATION PONDS

Twenty eight evaporation basins were installed in the San Joaquin Valley of California between 1974 and 1985. These occupy about 7,170 acres and vary in size from 10 to 1,800 acres (Chilcott et al., 1990). Six are currently not in operation. Desiccation of pond waters has led to the accumulation of vast

quantities of evaporites, the solid waste by-product of the evaporation of agricultural drainage water. The most common evaporite minerals found at evaporation ponds are halite (NaCl), thenardite (Na_2SO_4) and mirabilite ($Na_2SO_4 \cdot 10H_2O$).

The evaporation ponds receive about 32,000 acre-feet of subsurface drainage annually which contain approximately 810,100 tons of dissolved salt. The annual net weight of salts accumulating in the ponds when seepage losses are considered has been estimated to be 630,500 tons/year. This vast mass of salt suggests the possibility for commercial salt harvesting, but the presence of Se, As, B, Mo and other potentially toxic elements may constrain the commercial value of these salts. Furthermore, accumulation of high concentrations of trace elements by the evaporite minerals may result in designation of these salts as hazardous wastes.

The type of evaporites that form depends on the chemical composition of the pond water and degree of desiccation (Smith, 1989). The principal cation is Na while Cl and SO_4 are the major anions. Sodium and Cl combine to form NaCl (halite) while Na and SO_4 combine to form either mirabilite or thenardite. Incorporation of water into the $NaSO_4$ mineral to results in formation of mirabilite, $Na_2SO_4 \cdot 10H_2O$, a hydrated form of thenardite. Mirabilite forms under wet and cool (<30°C) conditions. Thenardite forms from the dehydration of mirabilite or precipitation under warm (>30°C) conditions. Pond waters have an ambient EC between 90 and 100 dS/m when mirabilite or thenardite forms, while halite, a more soluble salt, maintains the ambient solution EC between 165 and 200 dS/m.

Salts form in evaporation ponds when the salinity rises such that the amount of dissolved ions comprising a particular salt exceed the solubility product of this salt. The salinity typically rises in response to a loss of water via evaporation while ions are generally conserved in solution. Temperature changes in solution may affect the solubility of certain salts. Most evaporites become more soluble at higher temperature (e.g., halite, mirabilite) but some behave conversely (thenardite, calcite). Solution temperatures found during sampling ranged from a low of 6°C in February to a high of 41.1°C in August. Salts typically need a nucleation site to initiate crystal growth. In the ponds, the abundance of suspended particulate matter ensures an ample supply of nucleation sites.

The formation of salts from desiccating pond waters inevitably involves the contamination by trace elements that are also present in the solution. The major concern is over incorporation of potentially toxic trace elements, such as Se, B, As or Mo, since these elements would essentially be "fixed" in the salt as contaminants. Trace elements may co-precipitate as a structural component of the salt, adsorbed onto evaporite surfaces, or be occluded in structural defects or between crystal surface planes. Salts also may contain particulate matter (clay, organic matter) with adsorbed trace elements. Lastly, crystals removed from a solution will contain trace elements in the wetness film on the outer surface. Salts formed by desiccating the ponds to complete dryness may contain elevated levels of trace elements if the trace elements remained in solution through to complete evaporation.

MINERAL-SOLUTION COMPOSITIONAL RELATIONSHIPS IN EVAPORITE-FORMING AGRICULTURAL DRAINAGE EVAPORATION PONDS

The major ionic solutes in agricultural drainage waste water deposited in evaporation ponds in the San Joaquin Valley of California include sodium (Na), magnesium (Mg), calcium (Ca), sulfate (SO_4) and chloride (Cl). The dominant cation is by far Na while SO_4 and Cl vary in dominance according to region (Westcot et al., 1989; Tanji and Dahlgren, 1990). Evaporative concentration at the ponds results in hypersaline solution conditions which, given the dominant ions, favor the formation of evaporite minerals including thenardite (Na_2SO_4), mirabilite ($Na_2SO_4 \bullet 10H_2O$) and halite (NaCl). The complex composition of the pond solutions poses the question of whether pure salts are forming, and if not, whether impure salts are easily characterized for environmental monitoring purposes. Characterization is necessary to design disposal alternatives for the solid evaporite by-product which must be removed to maintain a high evaporation rate and high operating efficiency.

This section describes a survey of the evaporite minerals present in evaporation ponds located in the San Joaquin Valley. The minerals were analyzed for major ion composition, water content, insoluble matter content, and mineral-phase identification. Chemical composition was also determined for solution samples in which evaporite minerals coexisted. Both compositions are compared to determine the likelihood that coexisting evaporite minerals and solutions are in equilibrium. The variability of the solubility with temperature of field samples of a halite and a mirabilite-thenardite were determined for comparison of evaporation pond chemistry to published data.

* MATERIALS AND METHODS

Evaporite samples were collected from Lost Hills, Westlake South, Pryse, Barbizon, Meyers, Westlake North, and Peck evaporation ponds in August 1990 and February 1991. Site descriptions may be found in Chilcott et al., (1990). Fifty samples were collected in August while another ten were obtained in February. Solutions saturated with evaporite minerals were also sampled.

Evaporite mineral-phase identification was determined by x-ray powder diffraction (XRPD) with a Diano 8000 x-ray diffractometer. Evaporite minerals were maintained at their ambient temperature and relative humidity by sealing samples in glass vials. As a result, problems with mirabilite dehydrating to thenardite during transportation from the field to the laboratory did not occur as they have elsewhere (Keller et al., 1986b). Previously reported studies from North Dakota involved collection of salt effloresces from soil surfaces which are powdery. The evaporation ponds typically yielded minerals of high crystallinity and often large crystal size.

Subsamples of evaporite (approximately 1 g) were dissolved in 1 L of distilled-deionized water, and analyzed for cations and anions. Cations (Na, Ca, Mg, K) were analyzed with an Applied Research

Laboratories (ARL) Model 3510 Inductively Coupled Plasma (ICP) spectrophotometer, while anions (SO_4, NO_3, Cl) were analyzed on a Ion Chromatograph (Model 4000) with conductivity detector.

The water content was determined by drying known weights of sample at 180°C for 24 hours. The samples were allowed to cool to room temperature in a desiccator, and were then weighed again. The water content was calculated as a percentage:

$$\% \text{ Water} = \frac{\text{initial sample weight - dried sample weight}}{\text{initial sample weight}} \times 100$$

Insoluble matter content was determined by first weighing a known amount of sample in a weighing dish. The sample was mixed with 10 mL distilled-deionized water to dissolve the soluble portion. The mixture was filtered using a Nalgene filter holder and pre-weighed 0.45 µm Gelman membrane filter. Additional water was added to the rinse filter and insoluble matter trapped on the filter. The filter was then removed and dried in an oven at 60°C for 6 hours. The filter was allowed to cool to room temperature in a desiccator then re-weighed. The insoluble matter content was calculated as a percentage:

$$\% \text{ Insoluble Matter} = \frac{\text{final filter weight - initial filter weight}}{\text{initial sample weight}} \times 100$$

The chemical composition as determined by the preceding method was used to verify mineral identification determined by XRPD. Samples high in Na and Cl would be identified as halite while Na and SO_4-dominated samples were identified as thenardite or mirabilite depending on the water content.

The chemical equilibrium program C SALT was used to examine solubility relationships between pond waters and the evaporite assemblage identified in each evaporation pond (Smith, 1989). The model makes use of the Pitzer equations to calculate ionic activities and the percentage breakdown of the element as a specific species. The saturation index (log IAP/Ksp) is calculated for various evaporite mineral phases based on the ion activities of the solution, temperature, and the solubility products of the evaporite minerals. Saturation indices were used to determine whether the pond waters were in equilibrium with the evaporite minerals identified.

* RESULTS

Table 1 summarizes the mineral identification and compares the effectiveness of chemical composition analysis and XRPD for mineral identification. Results of chemical analysis and XRPD were very consistent. **Figures 1** to **8** display the chemical composition of evaporite minerals from the evaporation ponds collected in August 1990 and February 1991. Major solutes, water and insoluble matter

account for most of the solids. Totals ranging from 90-100% suggest that the margin of error in analysis may be as great as 10% (with one case at 20%).

Sodium and Cl clearly dominate the Lost Hills evaporite minerals and some at Westlake South and Peck ponds. In contrast, Na and SO_4 make up most of the solids at Westlake South, Pryse, Barbizon, Meyers, and Peck ponds. Solids containing a significant percentage of water include those from Westlake North, and a few from Peck and Westlake South. Insoluble matter is significant only in isolated cases such as samples 36 and 37 from Pryse pond, samples 39, 40 and 42 from Barbizon pond, sample 46 from Meyers pond, and samples 49 and 68 from Westlake North pond. These sites were mostly dry.

TABLE 1.

Mineral identification of field samples by different methods.

	IDENTIFICATION METHOD	
	Chemical	XRPD
	# of samples identified	
Halite	14	14
Thenardite	24	24
Mirabilite	18	17

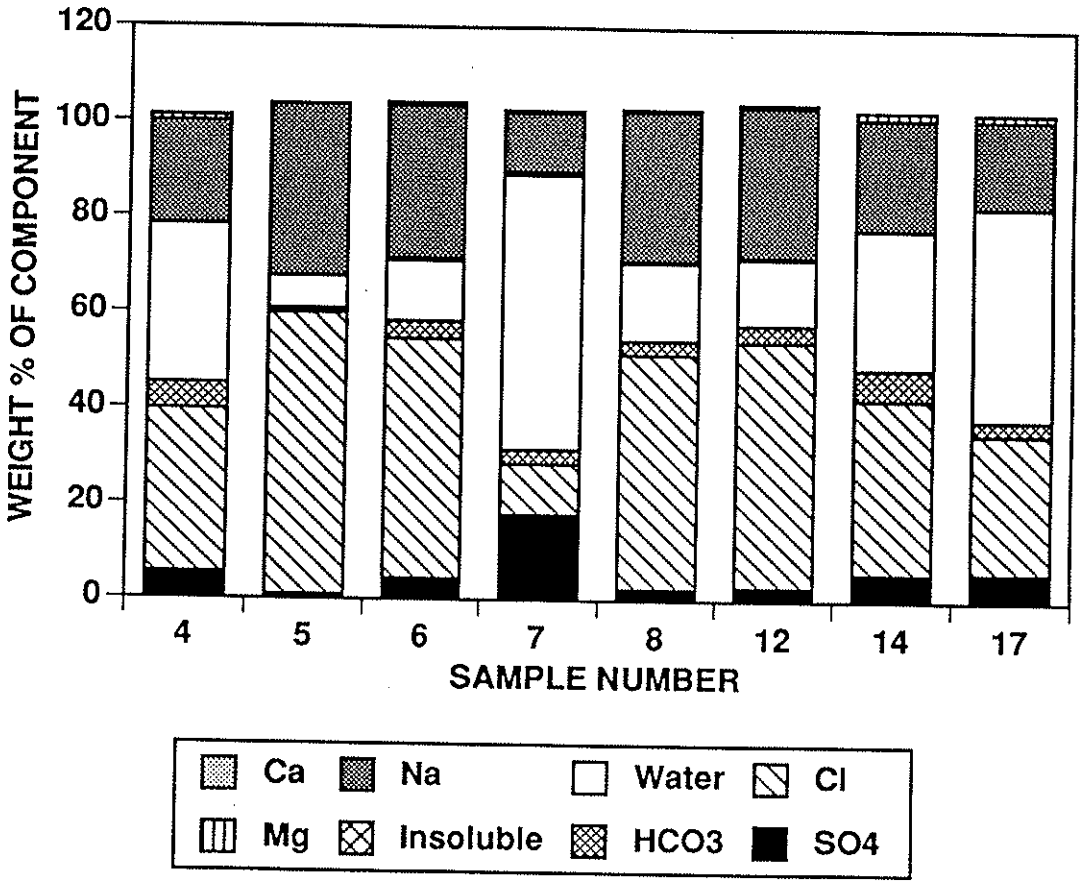

Figure 1. Chemical compositions of evaporite samples from Lost Hills evaporation pond collected on August 17, 1990

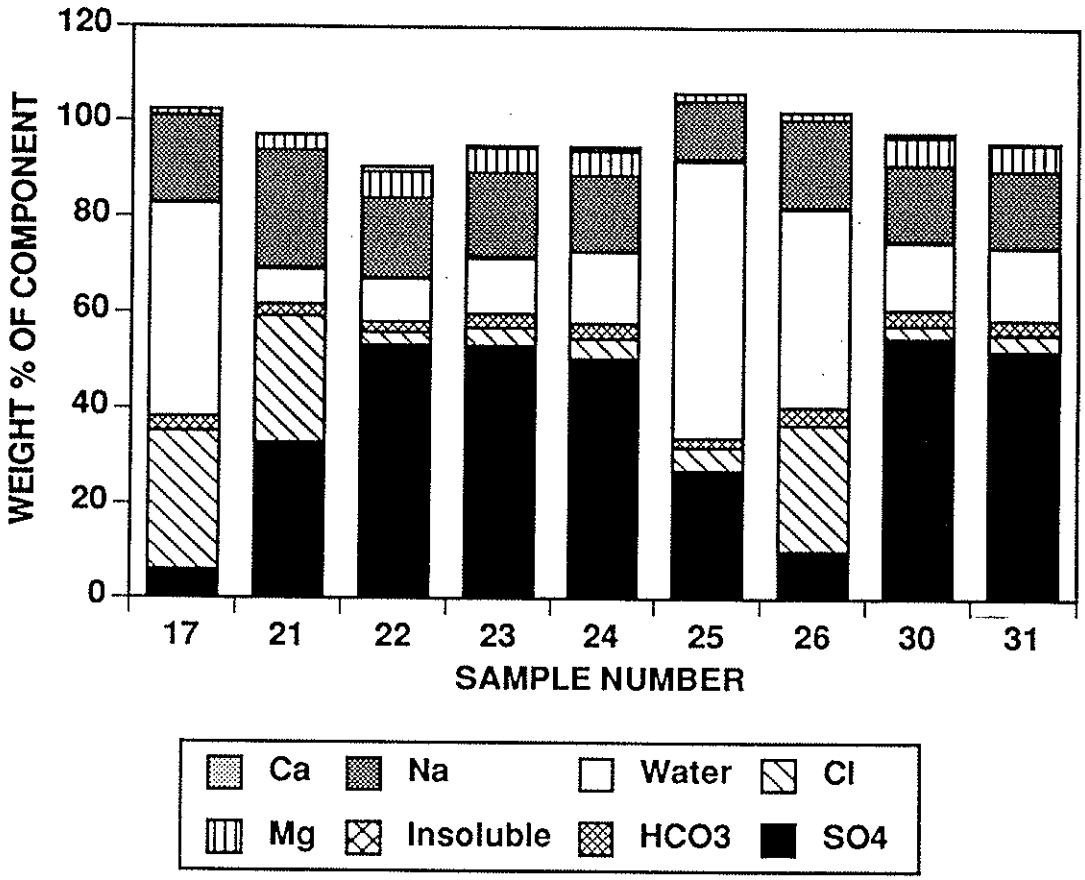

Figure 2. Chemical compositions of evaporite samples from Westlake South evaporation pond collected on August 17, 1990

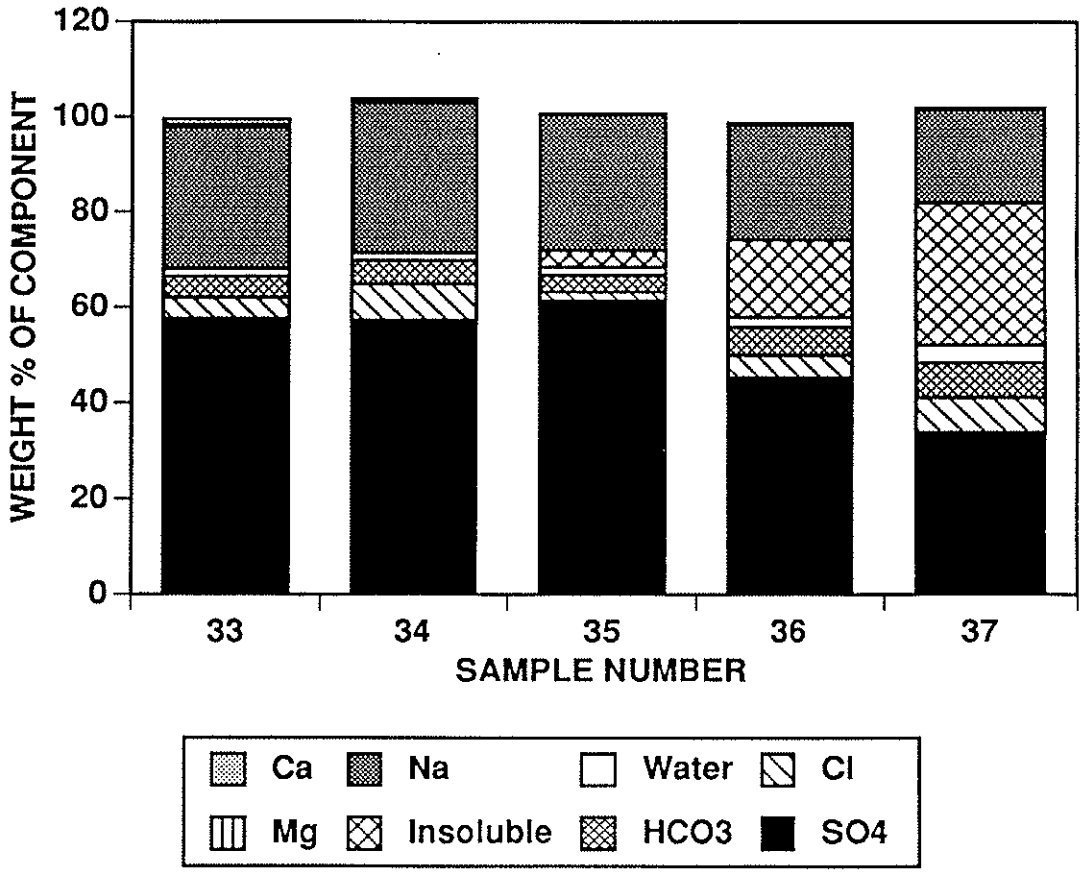

Figure 3. Chemical compositions of evaporite samples from Pryse evaporation pond collected on August 17, 1990

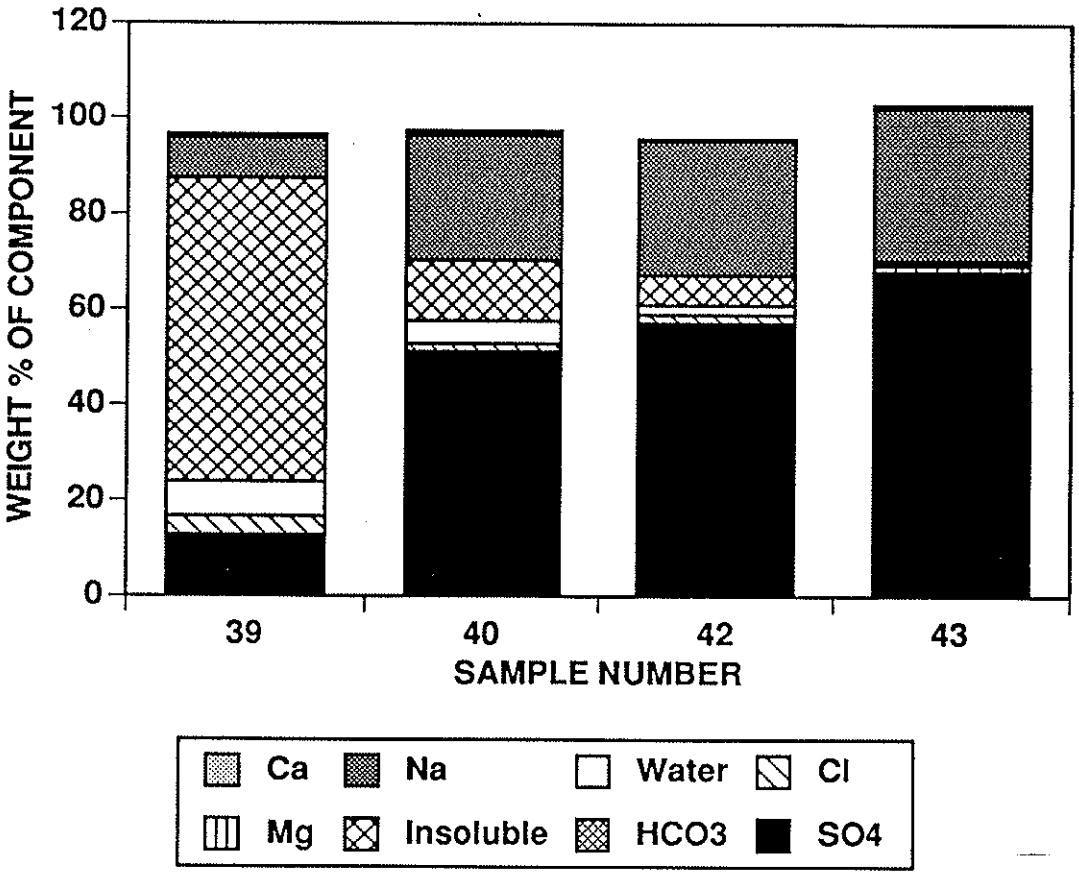

Figure 4. Chemical compositions of evaporite samples from Barbizon evaporation pond collected on August 18, 1990

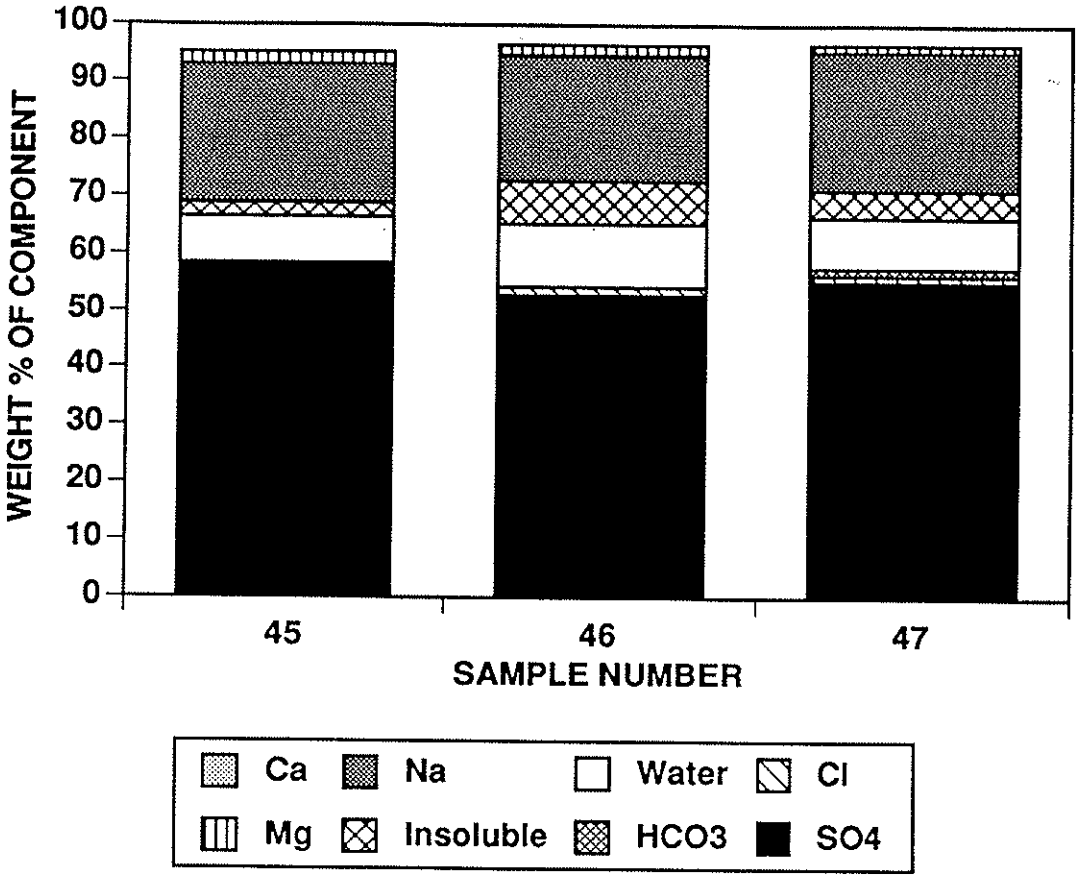

Figure 5. Chemical compositions of evaporite samples from Meyers evaporation pond collected on August 18, 1990

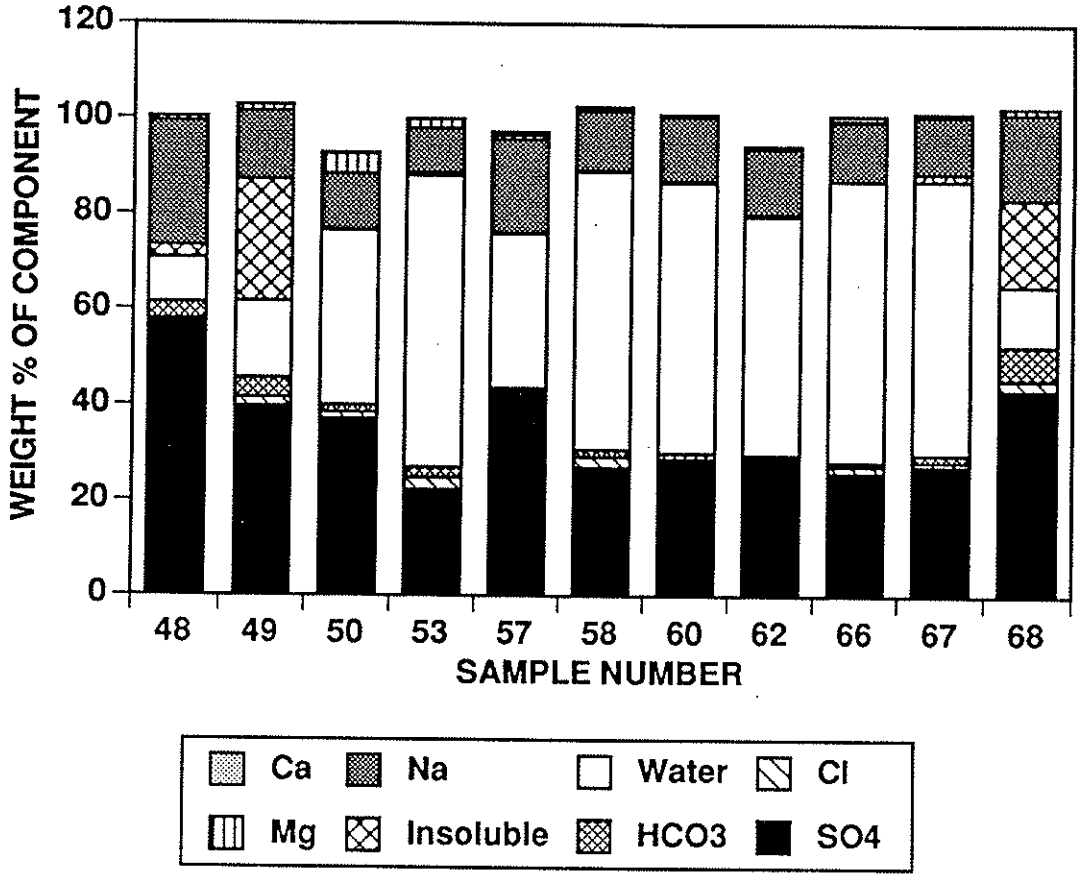

Figure 6. Chemical compositions of evaporite samples from Westlake North evaporation pond collected on August 18, 1990

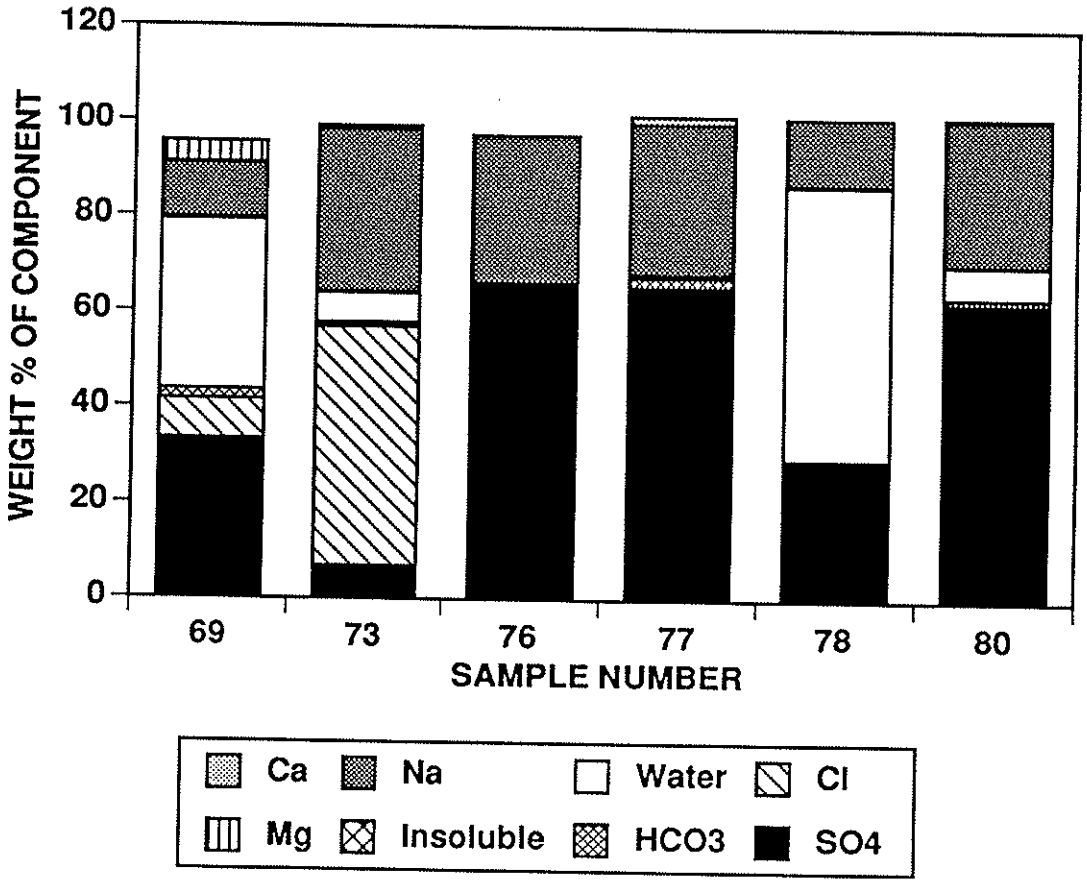

Figure 7. Chemical compositions of evaporite samples from Peck evaporation pond collected on August 18, 1990

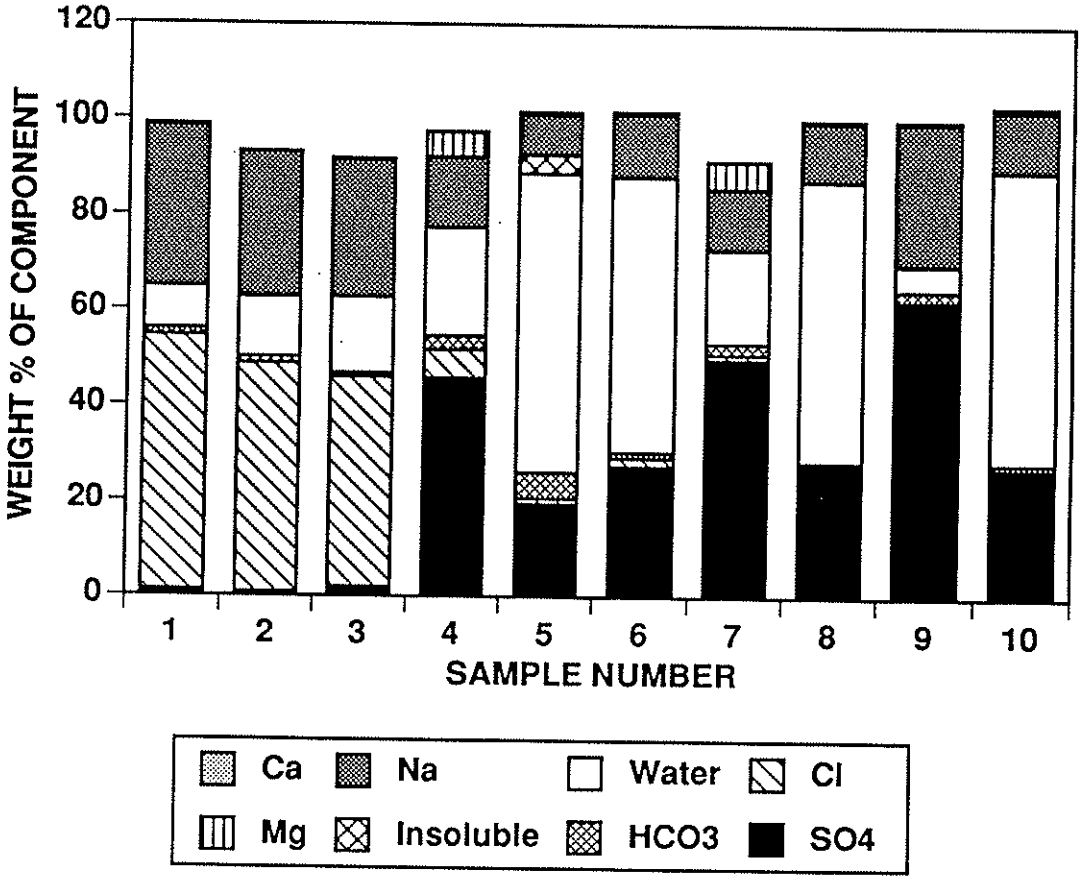

Figure 8. Chemical compositions of evaporite samples from evaporation ponds collected on February 2, 1991

The chemical composition of pond waters is shown for the August 1990 and February 1991 sampling in **Figures 9** and **10**, respectively. Concentrations of chloride were elevated, while sodium and sulfate concentrations were reduced in February. These differences are due to relative changes in halite and mirabilite solubility as a function of temperature.

The chemical composition of the evaporation pond waters were input for analysis by C SALT. Components used as input include Na, Ca, Mg, SO_4, Cl, temperature and pH. Several samples in February were collected at temperatures below 10°C (the minimum handled by C SALT) and these runs were conducted at 10°C.

The accompanying charts (**Figures 11-13**) show the degree with which the solutions were under-saturated with respect to the major mineral phases detected by x-ray diffraction. The pond sites are abbreviated as follows: LH...Lost Hills; PK..Peck; WLN...Westlake North; WLS...Westlake South. When the abbreviation is underlined, this indicates that the particular mineral phase (halite, thenardite or mirabilite) was found in contact with the solution. Annotations to the data points indicate the date of collection (1...August 1990; 2...February 1991). The dashed line at log $(IAP/K_{eq}) = 0$ indicates the saturation point. Above this line, the solution is saturated with respect to the mineral phase, while below this line indicates undersaturation.

* DISCUSSION

The three mineral phases dominating evaporite mineralogy at evaporite-forming evaporation pond were halite, mirabilite, and thenardite. Halite is readily identified at ponds in most cases by its cubic morphology. Electrical conductivity measurements above about 180 dS/m is another indicator of halite. X-ray diffraction analysis was useful in verifying evaporite identity from chemical analysis. Halite is characterized by a dominant peak at about 31.5° 2θ, and distinguished from the sulfate evaporites by the absence of a peak at 59.5° 2θ. Thenardite is characterized by a dominant peak at about 18.8° 2θ, and has a simpler pattern, that is fewer peaks, than mirabilite. In some evaporites, the weight contribution from water was greater than 50% due to the presence of the hydrated mineral phase mirabilite.

The chemical equilibrium modeling done with C SALT indicated that none of the solutions were saturated with respect to the evaporites found: halite, thenardite, or mirabilite. This may have arisen either because (1) the ionic strengths involved are not applicable to the activity coefficient formula used in the model; (2) the solutions were not in fact in equilibrium with the evaporites at the time of sampling; and/or (3) the thermodynamic database does not accurately depict the field evaporites.

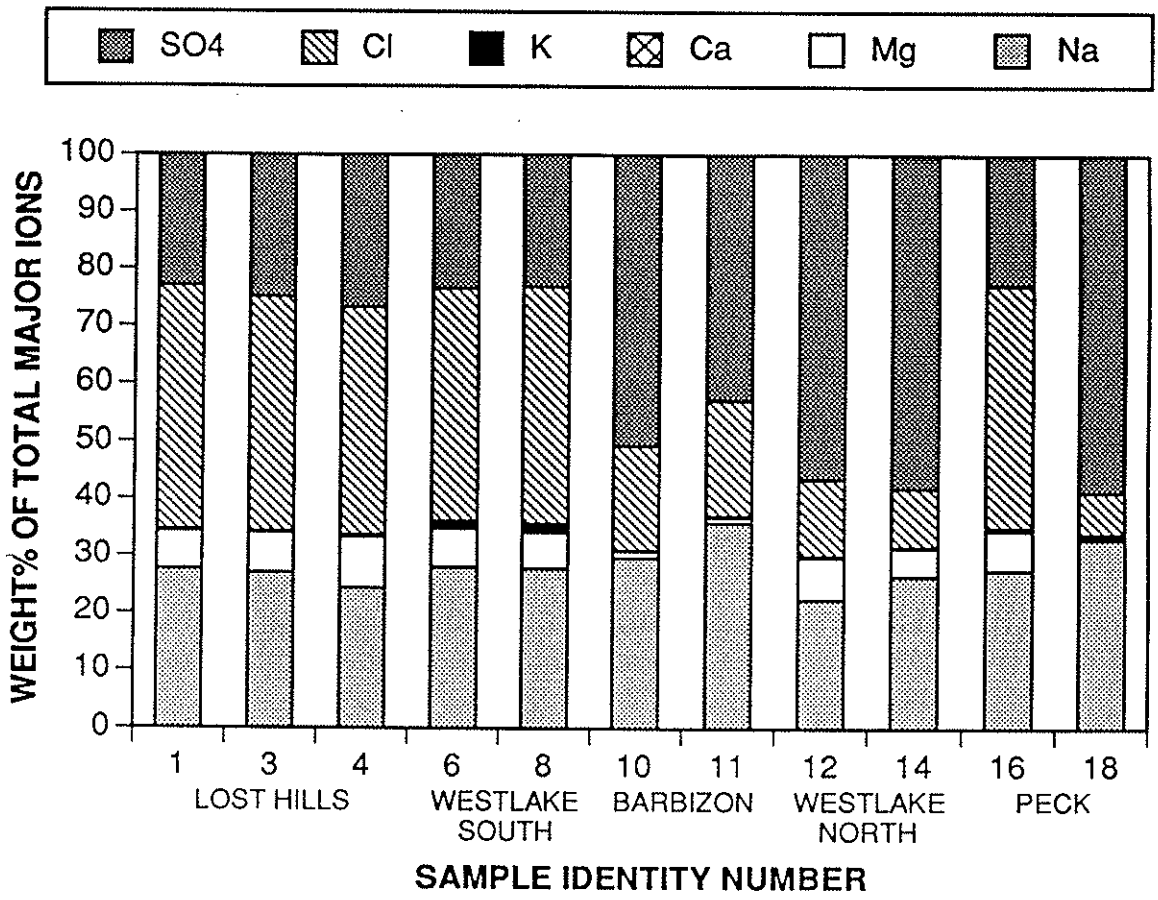

Figure 9. Weight percent composition of major ions in solution samples collected from evaporation ponds on August 17 and 18, 1990.

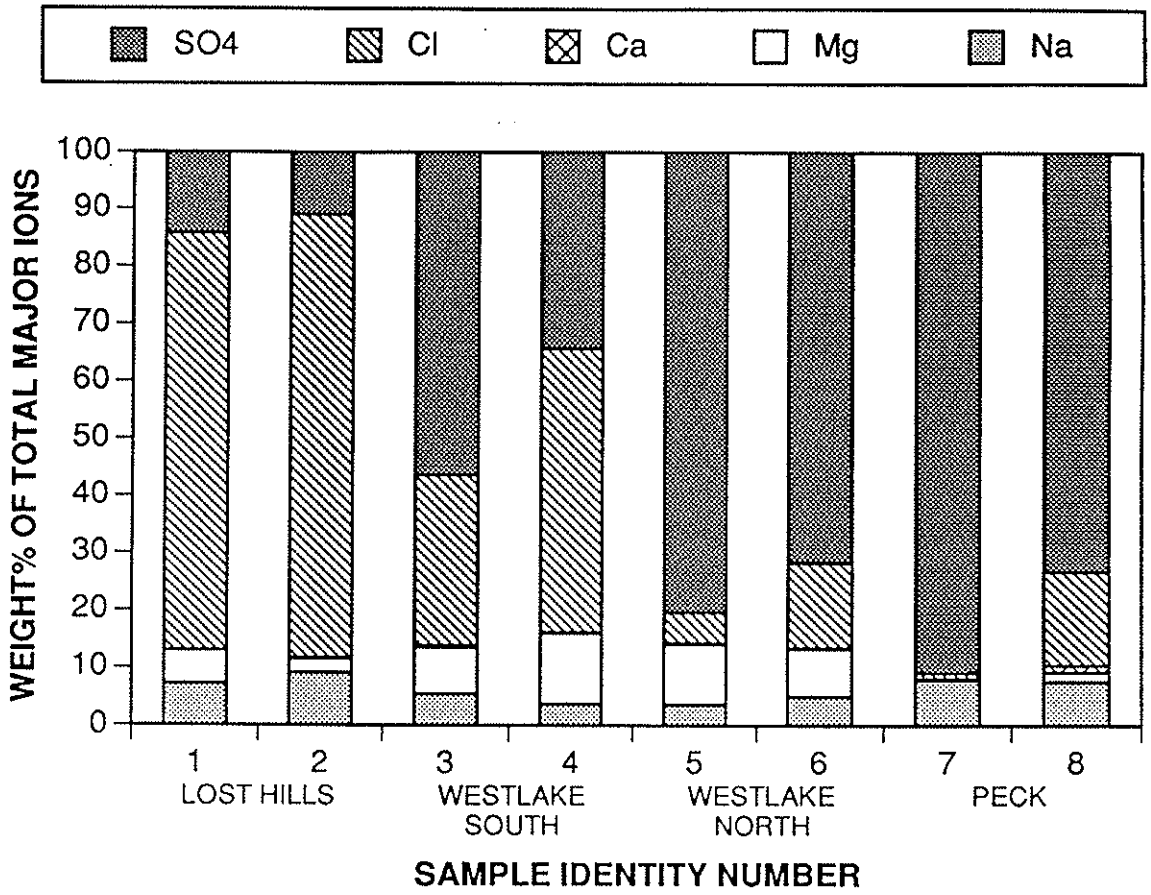

Figure 10. Weight percent composition of major ions in solution samples collected from evaporation ponds on February 2, 1991.

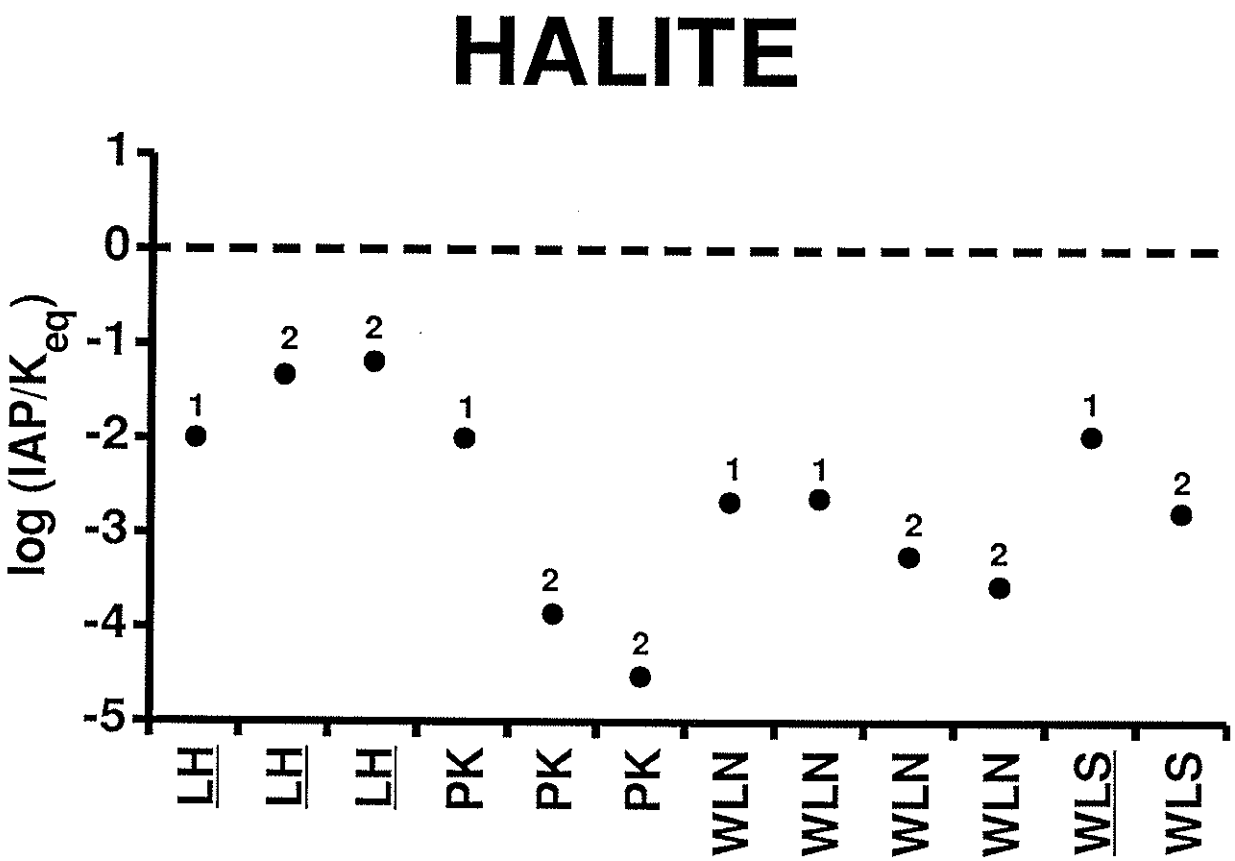

Figure 11. Saturation indices calculated by C SALT for halite (NaCl) in field soltuion sample (Notations 1 and 2 respectively refer to August 1990 and February 1991 sample; and LH=Lost Hills, PK=PeaK, WLN=Westlake North; WLS=Westlake South pond facilities)

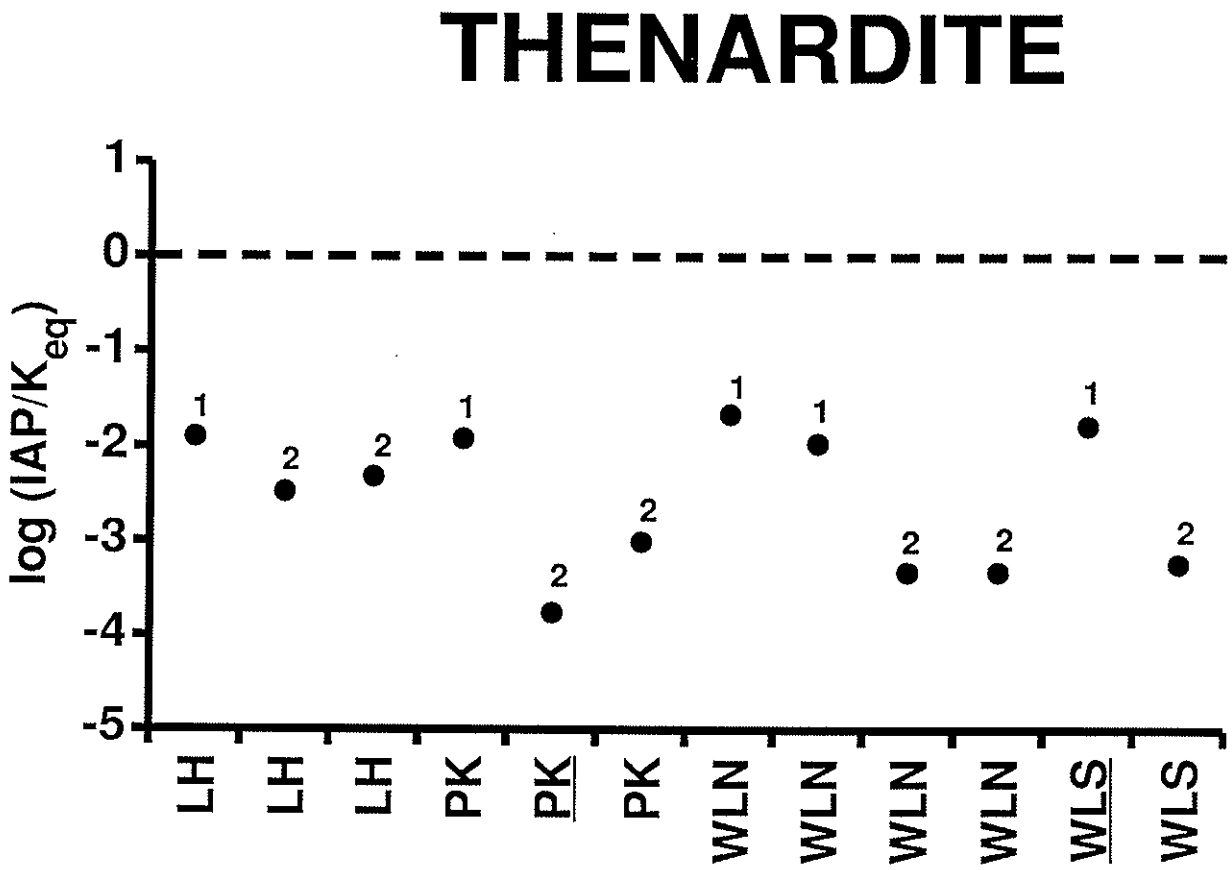

Figure 12. Saturation indices calculated by C SALT for thenardite (Na_2SO_4) in fileld solution samples (Notations 1 and 2 respectively refer to August 1990 and February 1991 sample; and LH=Lost Hills, PK=PeaK, WLN=Westlake North; WLS=Westlake South pond facilities)

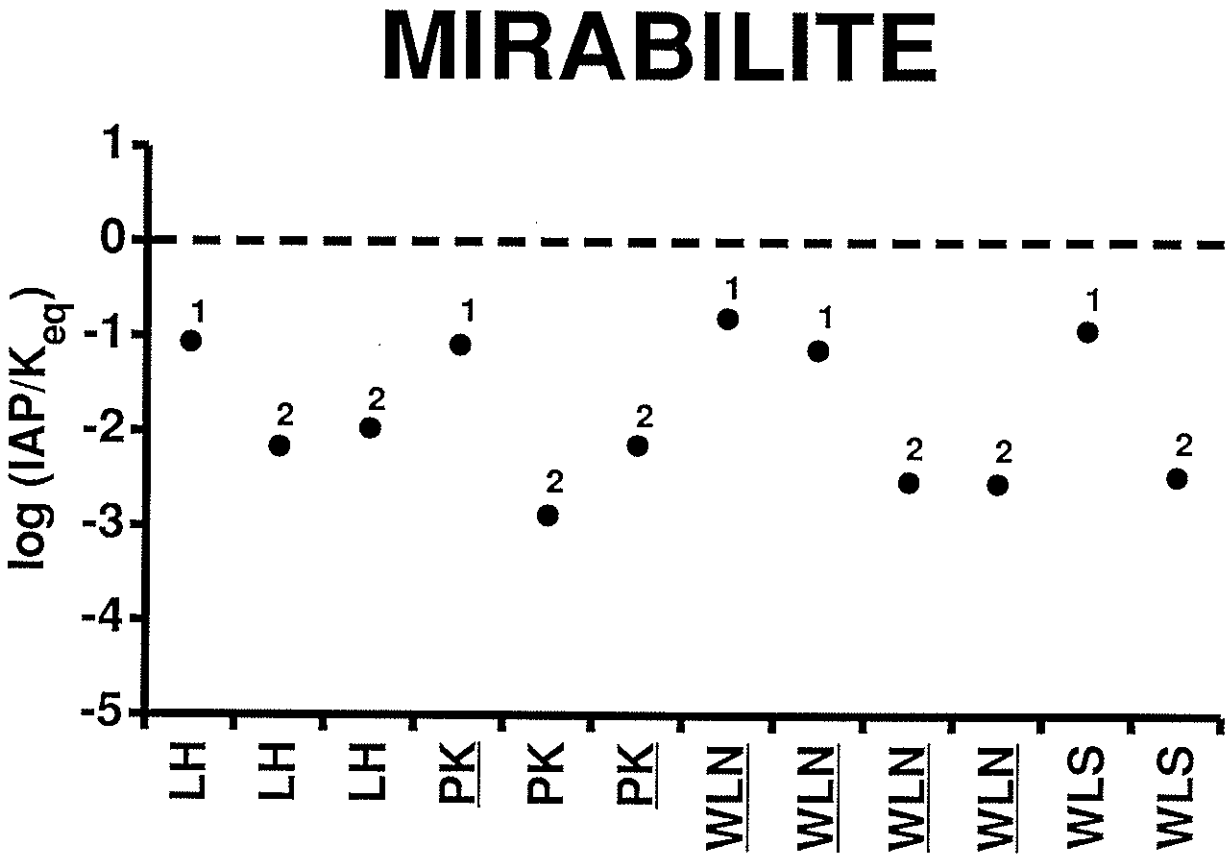

Figure 13. Saturation indices calculated by C SALT for mirabilite ($Na_2SO_4 \cdot 10H_2O$) in fileld solution samples (Notations 1 and 2 respectively refer to August 1990 and February 1991 sample; and LH=Lost Hills, PK=PeaK, WLN=Westlake North; WLS=Westlake South pond facilities)

PARTITIONING OF TRACE ELEMENTS BETWEEN EVAPORITE MINERALS AND POND WATERS

Agricultural evaporation ponds have become a common option for disposal of agricultural drainage waters. The major concern with this method is the accumulation of potentially toxic trace elements, such as Se, As, Mo and B. These trace elements persist in evaporation pond waters over the evaporative concentration process (Ong, 1991) while others are short-lived in the water column. However, information about the fate of these trace elements during the evaporite salt formation stage has not been available since the evaporation ponds have only reached this latter stage recently. The concern arises over salt disposal since evaporite salts contaminated with trace elements may be classified as hazardous waste and thus have low to no economic and commercial value, which would leave the burial alternative (Ford, 1988).

Bromide (Br) has been used as an indicator of brine stage in chloride salt deposits (Moretto, 1988). Chloride (Cl) may be substituted by Br within the crystal lattice, and also along dislocations and grain boundaries. The same mechanisms may extend to Se, As, Mo, and B in evaporation pond evaporite mineral salts including thenardite, mirabilite and halite. Substitution of SO_4 in mirabilite or thenardite crystal lattices by Se oxyanions, especially SeO_4, is possible since element periodicity, as in the case of Br and Cl, would suggest similar chemical properties. Incorporation of trace elements by fluid inclusion is also a possibility and may occur in cavities or along grain boundaries housing a thin solution film. Adsorption may play a major role either as a step towards SeO_4 coprecipitation or surface sorption of B. Any salt coexisting in a solution containing these trace elements may also be expected to contain some level of the trace elements due to surface wetness.

The primary objectives of this portion of the study were to measure Se, As, Mo, and B levels in evaporite mineral salts collected from several evaporation ponds located in the San Joaquin Valley of California. Distribution coefficients describing the proportion of Se, As, Mo, or B relative to the major components are calculated. The ratio of distribution coefficients in the salt and solution leads to a partition coefficient, a value indicating enrichment or depletion of the trace element in the solid phase.

* MATERIALS AND METHODS

Evaporite mineral samples and solutions in contact with these minerals were collected from seven evaporation ponds (Peck, Pryse, Meyers, Barbizon, Lost Hills, West Lake South and West Lake North). The evaporites were dissolved in distilled deionized water and filtered through a 0.45 m membrane filter. Major cations (Na, Ca, Mg, and K) were analyzed by ICP and major anions (Cl, NO_3, and SO_4) by ion chromatography. The dissolved evaporite samples and pond waters were analyzed for total Se by hydride vapor generation-atomic absorption spectrophotometry (HVG-AAS), and B by a colorimetric

method, azomethine-H, on a HP 8452A Diode Array Spectrophotometer (Herbel, 1991). The HVG-AAS method is discussed by Fio and Fujii (1990). Preparative sample digestion for total Se determination was done using the nitric and perchloric acid mixture procedure (Ogle and Knight, 1989). The hydride was generated with a Varian VGA-76 Vapor Generation Accessory and fed into a Varian AA-1275 Atomic Absorption Spectrophotometer for analysis. Arsenic and Mo were determined using graphite furnace atomic absorption spectrometry.

Distribution coefficients were calculated on a mole fraction basis (after Driessens, 1986):

$$D_x^{solution} = \frac{m_x^{solution}}{\sum_{y=cations} m_y^{solution} + \sum_{z=anions} m_z^{solution}}$$

$$D_x^{solid} = \frac{m_x^{solid}}{\sum_{y=cations} m_y^{solid} + \sum_{z=anions} m_z^{solid}}$$

where x = Se, As, Mo, or B. The distribution coefficients describe the proportion of the trace element to all other solutes in the solution or solid phases. Values for cation and anion concentrations used in the distribution coefficient calculations are reported in Ong (1991).

In contrast, the partition coefficient describes the phase selectivity and is given by:

$$K_x = \frac{D_x^{solid}}{D_x^{solution}}$$

* RESULTS AND DISCUSSION

Pond water concentrations of Se, As, B, and Mo were highly variable between the four ponds that contained pond waters in association with evaporite minerals (**Table 1**). Solution concentrations (on a molar basis) of these trace elements followed the order: B >> Mo > As > Se. A statistical summary of trace element concentration is given in **Table 2.** The trace element composition is a function of the chemical composition of the drainage waters entering the ponds which is related to the geologic parent material of the soil. Once the drainage waters enter the pond environment, processes such as reduction by the pond bottom sediments, sorption to pond sediments, and volatilization further alter trace element concentrations.

TABLE 2

Trace Element Concentration in Pond Waters

	Mean	Std. Error	Minimum	Maximum	Hazardous Limit
	----------	----------	mM	----------	----------
Se	0.016	0.06	1.68E-4	1.01E-1	0.013*
As	0.023	0.009	4.16E-4	1.59E-1	0.067*
B	9.61	0.978	7.51E-1	18.5	6.48**
Mo	0.608	0.127	4.88E-2	2.94	3.65*

* threshold limit concentration for soluble species according to Title 22, California Administrative Code.

** designated waste level for total species according to Title 23, California Administrative Code.

The solution concentrations presented in this study represent the final stages of evapo-concentration and therefore the highest levels to be found at any given pond. During the final stages of evaporite formation, only small pools of solutions exist within the pond. As a result of evapo-concentration, many trace element solution concentrations exceed limits set for hazardous waste. Selenium, arsenic, and boron in all solution samples exceeded the hazardous waste limits according to Title 22 of the California Administrative Code. Only soluble Mo concentrations were less than hazardous waste limits for all samples examined. With regard to potential toxicities to waterfowl and wildlife, these pools of highly concentrated solute do not appear to be a serious problem due to their small size and the small volume of solution that they contain.

Concentrations of trace elements in evaporite minerals found in contact with pond water solutions (wet) and in dry pond beds (dry) are shown in **Table 3** and summarized in **Table 4.** As with the solution concentrations, there was large variability between the various evaporite samples. Selenium and boron were more concentrated in the wet samples while arsenic and molybdenum were more concentrated in the dry evaporite samples. No explanation for these differences is apparent from our preliminary analysis. All the evaporites examined in this study had trace element concentrations well below the hazardous waste criteria. Therefore, the salts forming in evaporation ponds do not appear to be a potential environmental hazard and do not require special precautions for their ultimate disposal. Given the chemical composition of the evaporation pond waters, the conversion of solutions exceeding hazardous trace elements limits to solids containing these same components results in creation of a nonhazardous solid material.

To examine the interaction of soluble trace elements with evaporite minerals, partition charts were constructed to compare the mole fraction of a particular trace element in the solution-phase with that in the solid-phase. This analysis shows whether trace elements are selectively incorporated into the solid-phase by mechanisms such as occlusion, sorption, and coprecipitation or excluded from the solid-phase. The partition diagrams are shown in **Figure 14-17.** Data points falling in the region above the dashed line indicate evaporite minerals in which the trace element is depleted in the solid-phase relative to the solution-phase, while points falling below the line indicate enrichment of the trace element in the solid-phase. Points falling on the line indicate that the proportion of trace element in the solid- and solution-phases are identical.

For selenium, only one point falls distinctly in the region of solid-phase enrichment while the majority of the points lie in the region indicating depletion in the solid-phase. A number of the points are in the area immediately surrounding the dashed line indicating nearly equal proportions of Se in the solid- and solution-phases. Arsenic partitioning showed a clearer trend with most points clustering in the solid-phase depletion zone. One point fell very close to the dashed line indicating equal proportions in the solid- and solution-phases. Boron partitioning showed a wide scattering of data points within the region indicating solid-phase depletion. Molybdenum showed a tighter clustering of data points with all points indicating solid-phase depletion. There were no distinct differences between chloride and sulfate dominated evaporites for any of the trace elements. The 20-30° temperature difference occurring between August and February did not appear to affect trace element partitioning.

Partition coefficients were also calculated to provide a numerical representation of trace element incorporation in evaporite minerals (**Table 3**). The partition coefficient is defined as the $\log_{10}$ of the ratio of the mole fraction of the trace element in the solid-phase to the mole fraction of the trace element in the solution-phase. Positive values indicate solid-phase enrichment, negative values indicate solid-phase depletion, and a value of zero indicates equal proportions in the solid- and

TABLE 3. Trace Element Concentrations in Evaporite Minerals

				Dominating		SOLID PHASE (mg/kg)			SOLUTION PHASE (mM)					Partition Coeff		
SITE	CODE	WET/DRY	Solution T, °C	Anion in Salt	Se	As	B	Mo	Se	As	B	Mo	Insoluble%	Se	As	B	Mo
LOST HILLS	4	w		Cl	0.675	ND	525	27.59	5.07E-3	4.16E-4	7.10E+0	5.57E-1	0.2	-0.72		-0.07	-1.24
LOST HILLS	5	d		Cl	0.067	ND	114	2.14					0.2				
LOST HILLS	6	d		Cl	0.612	ND	822	17.30					0.2				
LOST HILLS	7	w		Cl-SO4	0.324	ND	741	12.85					0.8				
LOST HILLS	8	w	35.3	Cl	0.387	ND	731	13.14	2.36E-3	6.51E-4	7.44E+0	8.32E-1	0.3	-0.76		-0.12	-1.87
LOST HILLS	12	w	39.1	Cl	0.521	ND	975	13.18	4.09E-3	2.00E-3	9.71E+0	8.32E-1	0.2	-0.89		-0.13	-1.88
LOST HILLS	14	w	39.1	Cl	0.927	ND	922	29.09	4.09E-3	2.00E-3	9.71E+0	8.32E-1	0.0	-0.51		0.06	-1.41
WESTLAKE S	17	w	40.2	Cl	0.121	0.138	495	7.00	3.14E-4	3.61E-3	1.71E+1	1.45E-1	0.1	-0.18	-1.21	-0.44	-1.17
WESTLAKE S	21	w	40.2	Cl-SO4	0.133	0.134	86	1.53	3.14E-4	3.61E-3	1.71E+1	1.45E-1	0.3	-0.26	-1.34	-1.32	-1.95
WESTLAKE S	22	d		SO4	0.106	0.400	20	0.57					0.4				
WESTLAKE S	23	d		SO4	0.334	0.402	88	1.68					0.4				
WESTLAKE S	24	d		SO4	0.339	0.557	64	1.09					0.0				
WESTLAKE S	25	w		Cl-SO4	0.143	0.425	165	1.70					0.3				
WESTLAKE S	26	w	41.1	Cl	0.218	0.102	554	7.74	3.35E-4	4.55E-3	2.49E+0	1.79E-1	0.1	0.02	-1.42	0.42	-1.24
WESTLAKE S	30	d		SO4	1.759	0.504	56	0.73					0.4				
WESTLAKE S	31	d		SO4	0.223	0.403	50	1.07					0.1				
PRYSE	33	d		SO4	ND	8.092	74	7.77					0.0				
PRYSE	34	d		Cl-SO4	0.045	8.589	92	11.69					0.0				
PRYSE	35	d		SO4	0.287	2.867	44	30.87					3.4				
PRYSE	36	d		SO4	0.244	3.421	180	20.40					16.3				
PRYSE	37	d		Cl-SO4	0.550	3.179	192	32.00					29.8				
BARBIZON	39	d		Cl-SO4	0.721	0.767	196	15.51					63.6				
BARBIZON	40	d		SO4	0.377	1.146	244	17.06					12.7				
BARBIZON	42	d		SO4	0.344	0.000	83	0.00					6.4				
BARBIZON	43	d		SO4	0.113	0.000	16	5.96					0.2				
MEYERS	45	d		SO4	0.325	0.879	115	93.58					2.3				
MEYERS	46	d		SO4	0.651	0.133	173	8.37					7.5				
MEYERS	47	d		SO4	ND	ND	88	0.00					4.8				
WESTLAKE N	48	d		SO4	0.318	0.502	141	1.87					2.6				
WESTLAKE N	49	d		SO4	0.329	1.692	184	3.21					25.6				
WESTLAKE N	50	d	25.3	SO4	0.077	0.537	191	4.11	1.68E-4	1.52E-2	1.16E+1	9.35E-2	0.0	0.00	-1.09	-0.58	-1.11
WESTLAKE N	53	w	25.3	SO4	0.100	0.827	288	4.33	1.68E-4	1.52E-2	1.16E+1	9.35E-2	0.7	0.14	-0.87	-0.37	-1.05
WESTLAKE N	57	w	25.3	SO4	0.330	0.171	97	2.00	1.68E-4	1.52E-2	1.16E+1	9.35E-2	0.2	0.50	-1.71	-1.01	-1.55
WESTLAKE N	58	w	25.3	SO4	9.248	0.276	123	1.70	1.68E-4	1.52E-2	1.16E+1	9.35E-2	0.0	2.13	-1.33	-0.72	-1.44
WESTLAKE N	60	w	28.4	SO4	0.004	0.055	46	0.59	1.01E-1	1.59E-1	7.12E+0	1.24E+0	0.1	-1.31	-3.02	-1.25	-2.98
WESTLAKE N	62	w	28.4	SO4	0.038	0.058	44	0.78	1.01E-1	1.59E-1	7.12E+0	1.24E+0	0.5	-3.00	-2.99	-0.92	-2.86
WESTLAKE N	66	w	28.4	SO4	0.030	0.054	90	1.05	1.01E-1	1.59E-1	7.12E+0	1.24E+0	0.1	-3.10	-3.01	-0.60	-2.72
WESTLAKE N	67	w		SO4	0.354	0.124	104	1.41					1.6				
WESTLAKE N	68	d		SO4	0.114	0.292	239	11.64					18.2				
PECK	69	w	32.9	Cl-SO4	33.216	ND	326	3.55	2.31E-4	4.46E-4	1.59E+1	1.00E-1	0.1	2.52		-0.46	-1.17
PECK	73	w	32.9	Cl	5.491	ND	60	0.79	2.31E-4	4.46E-4	1.59E+1	1.00E-1	0.3	1.37		-1.56	-2.19
PECK	76	d		SO4	11.516	ND	ND	0.13					0.5				
PECK	77	d		SO4	11.029	ND	26	0.96					0.2				
PECK	78	w	31.0	SO4	5.221	ND	15	0.25	2.76E-2	2.58E-3	2.91E+0	4.75E-1	0.4	-0.36		-1.07	-3.00
PECK	80	w	31.0	SO4	2.972	ND	13	0.14	2.76E-2	2.58E-3	2.91E+0	4.75E-1	0.0	-0.94		-1.47	-3.57
LOST HILLS	1	w	6.0	Cl	0.166	ND	328	4.38	5.86E-3	0.00E+0	1.85E+1	1.40E+0	0.0	-1.15		-0.49	-2.19
LOST HILLS	2	w	6.0	Cl	ND	ND	294	3.99	5.86E-3	0.00E+0	1.85E+1	1.40E+0	0.0			-0.49	-2.18
LOST HILLS	3	w	6.0	Cl	0.649	ND	225	3.99	4.67E-3	2.08E-3	9.67E+0	7.63E-1	0.0	-0.48		-0.58	-2.16
WESTLAKE S	4	w	6.0	Cl-SO4	0.019	0.680	43	0.94	4.67E-3	2.08E-3	9.67E+0	7.63E-1	0.0	-1.66	0.28	-0.76	-2.27
WESTLAKE S	5	N/A		SO4	0.389	0.913	43	0.87					3.9				
WESTLAKE S	6	w	8.3	SO4	ND	0.049	18	0.34	5.44E-4	8.81E-3	6.33E+0	6.80E-2	0.1		-1.79	-1.22	-1.94
WESTLAKE N	7	w	7.0	SO4	ND	1.126	117	1.62	2.10E-4	2.66E-2	7.50E+0	4.91E-2	0.0		-1.08	-0.67	-1.29
WESTLAKE N	8	w	5.8	SO4	ND	0.129	20	0.90	7.11E-4	1.89E-2	9.30E+0	4.88E-2	0.0		-1.76	-1.42	-1.44
PECK	9	w	14.6	SO4	6.051	ND	3	0.61	2.57E-2	5.87E-3	7.51E-1	2.14E-1	0.2	-0.79		-1.70	-2.79
PECK	10	w	11.5	SO4	8.193	ND	1	0.23	1.49E-2	8.53E-3	3.15E+0	2.94E+0	0.2	-0.37		-2.65	-4.30

solution-phases. Mean partition coefficients for Se, As, Mo, and B were -0.43, -1.60, -0.80, and -2.04, respectively. This indicates that trace element affinity for evaporite minerals follows Se > B> As > Mo. The mean values were all negative indicating trace element depletion in the solid-phase relative to the solution-phase. Therefore, trace elements prefer to remain in the solution rather than being incorporated into the evaporite minerals.

TABLE 4.

Summary of Trace Element Concentrations in Evaporate Minerals

	Mean	Std. Error	Minimum	Maximum	Hazardous Limit
			mg/kg		
Se wet	3.02	1.37	ND	33	100*
dry	1.33	0.66	ND	11.5	100
As wet	0.13	0.05	ND	1.1	500*
dry	1.43	0.48	ND	8.6	500
B wet	256	54	1	975	7000**
dry	146	33	ND	82	7000
Mo wet	5.1	1.4	0.14	29	3500*
dry	11.6	9	ND	94	3500

* threshold limit concentration for soluble species according to Title 22, California Administrative Code

** designated waste level for total species according to Title 23, California Administrative Code

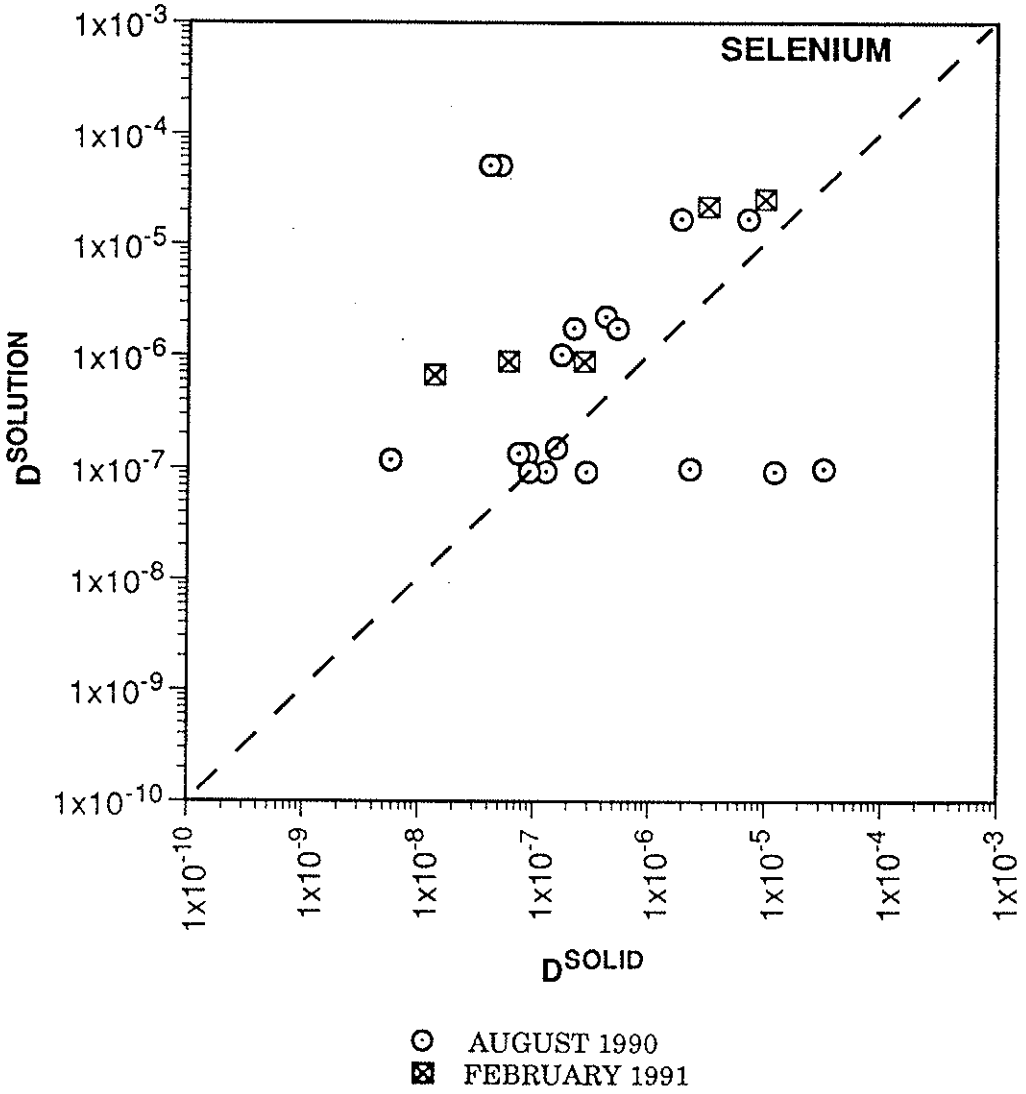

Figure 14. Selenium distribution coefficients in evaporites and associated contact solutions.

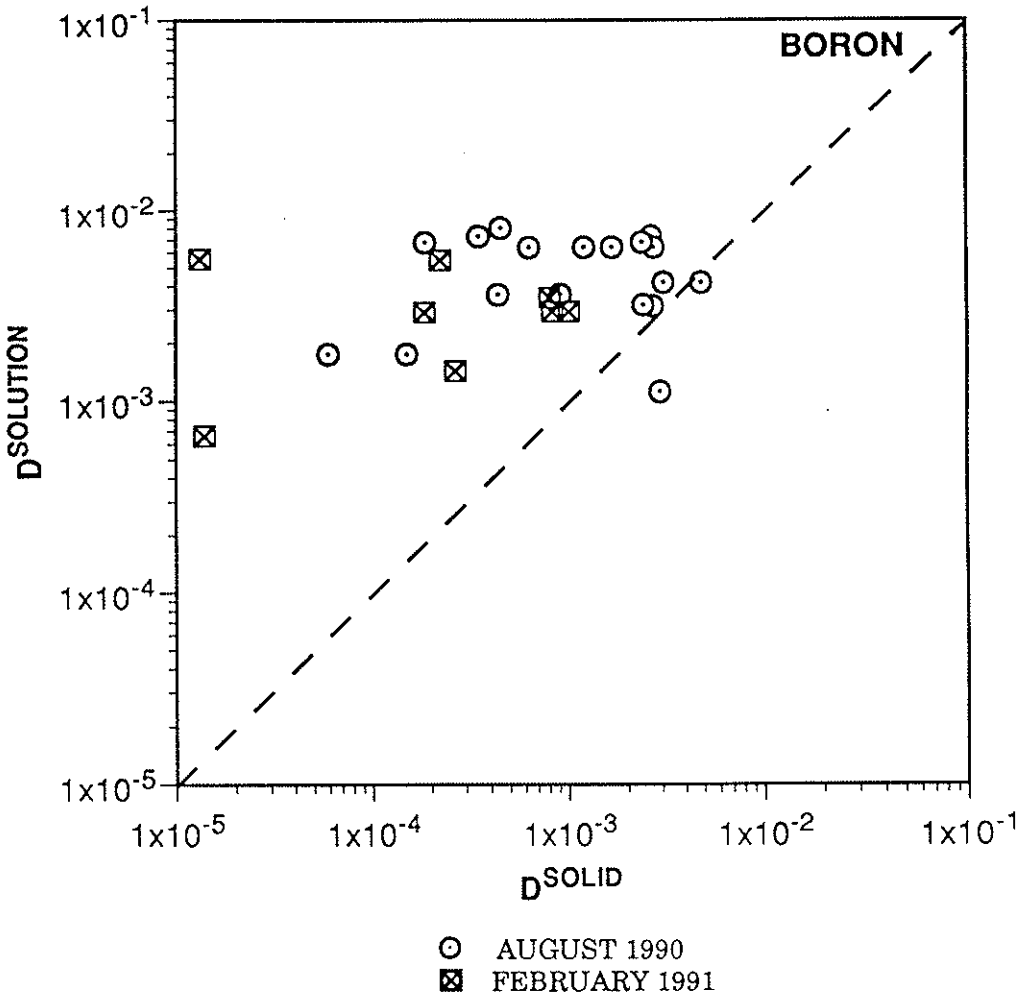

Figure 15. Boron distribution coefficients in evaporites and associated contact solutions

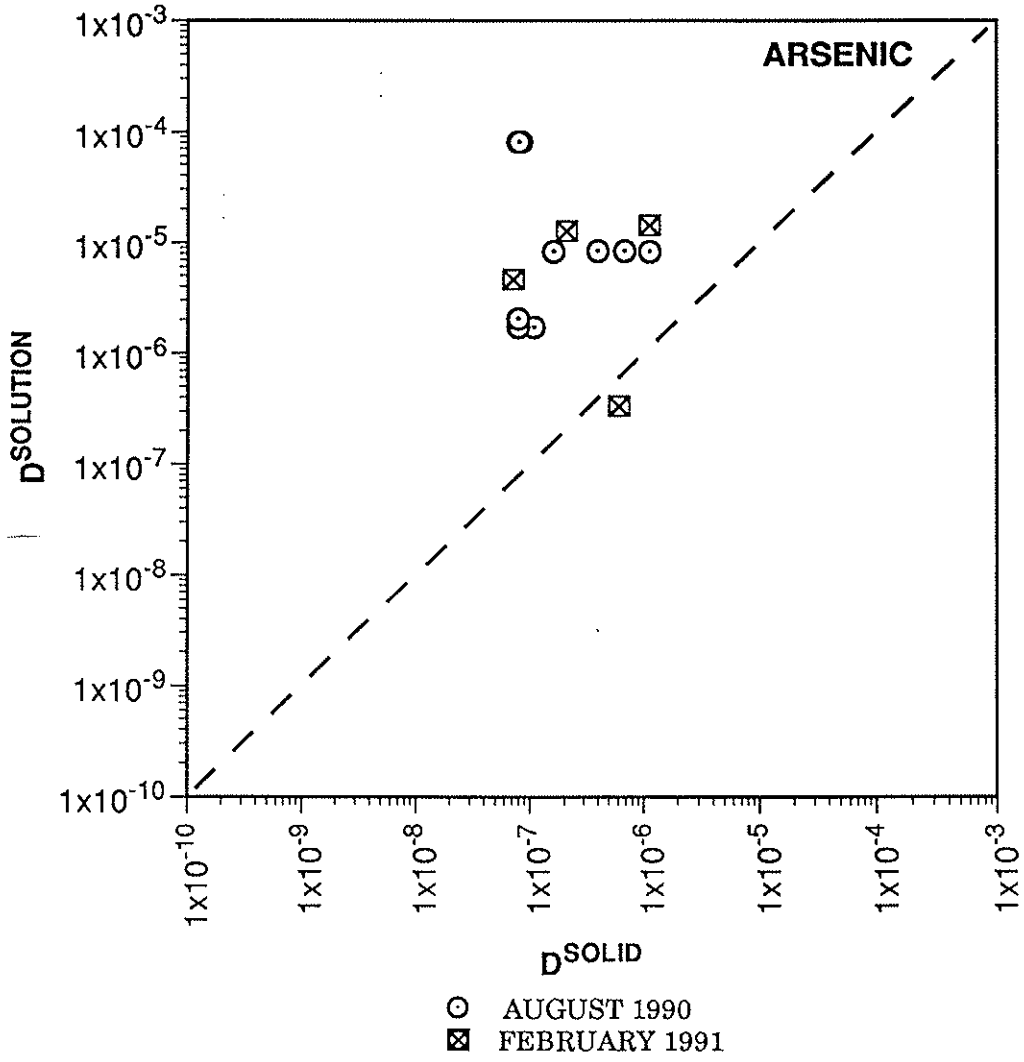

Figure 16. Arsenic distribution coefficients in evaporites and associated contact solutions.

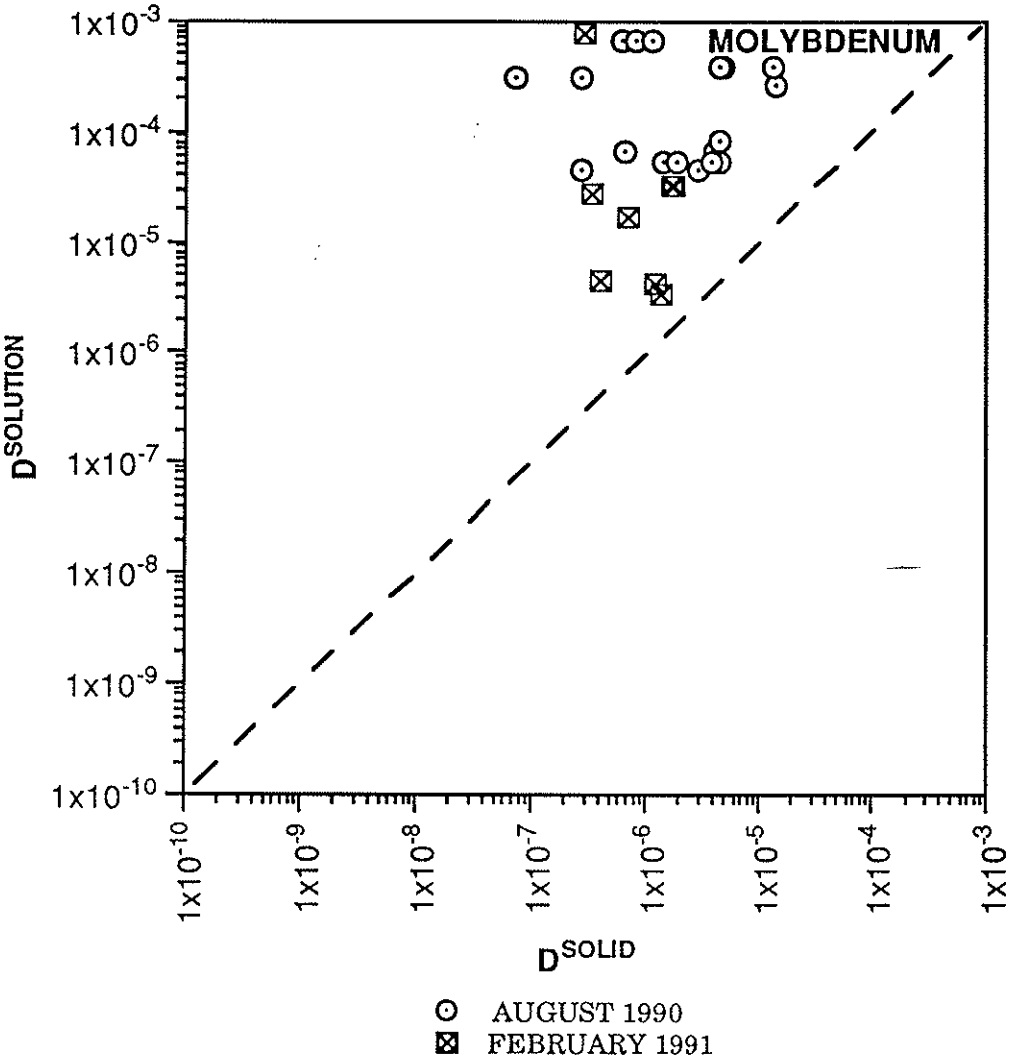

Figure 17. Molybdenum distribution coefficients in evaporites and associated contact solutions.

DESICCATION OF $Na\text{-}SO_4\text{-}SeO_3$ AND $Na\text{-}SO_4\text{-}SeO_4$ SOLUTION

Sodium sulfate evaporite salts, thenardite (Na_2SO_4) and mirabilite ($Na_2SO_4 \bullet 10H_2O$), are common evaporite minerals in agricultural evaporation ponds. Selenium (Se) is commonly present in trace quantities and its chemical interaction in the Na_2SO_4 salt formation process is of great interest since selenium potentially toxic action may determine the toxicological impact of the evaporite salts in the environment, and have a detrimental effect on the commercial usage of an otherwise less harmful substance. Characterization of the aqueous systems $Na\text{-}SO_4\text{-}SeO_3$ and $Na\text{-}SO_4\text{-}SeO_4$ under evaporite-forming conditions is important in predicting the fate of Se during the evaporite forming stage in evaporation ponds.

The chemical periodicity of elements would suggest that S and Se, both group VIA elements, have similar chemical properties. This study investigates the desiccation pathways and crystallization isotherms that result from solutions containing S and Se oxyanions ultimately leading to the formation of Na salts. It also identifies the salts that arise from desiccation to total dryness in order to determine whether pure or transitional solid phases are favored.

Differences between Se(IV) and Se(VI) interactions are expected. Similar to Na_2SO_4, Na_2SeO_3 and Na_2SeO_4 salts exist in hydrated as well as unhydrated forms. The salt Na_2SeO_3 is stable as the pentahydrate, $Na_2SeO_3 \bullet 5H_2O$. The salt Na_2SeO_4 mimics thenardite-mirabilite in that the decahydrate, $Na_2SeO_4 \bullet 10H_2O$, is also stable.

* MATERIALS AND METHODS

The following experimental methods involve the isothermal evaporation of $Na_2SO_4\text{-}Na_2SeO_3\text{-}H_2O$ and $Na_2Se_4\text{-}Na_2SO_4\text{-}H_2O$ solution mixtures. Stock solutions were comprised of reagent grade 0.5 *M* Na_2SO_4, 0.5 *M* Na_2SeO_3 and 0.5 *M* Na_2SeO_4, all prepared in distilled-deionized water.

Samples of the desired composition (**Table 5**) were prepared in 400 mL Fisherbrand PTFE dishes using the stock solutions to obtain 200 mL final volumes, and placed in a desiccation chamber (**Figure 18**) designed after Keller et al. (1986a). The weights of the empty dishes were recorded beforehand, as well as the initial weights of the dishes with solution. The dimensions of the plexiglass experiment chamber were 28" x 20" x 20". Holes in the wall were cut to insert needle valves with two hose tips as dry air inlets, a platinum RTD probe and a heating lamp.

The probe and heating lamp were used in combination with a Scientific Instruments Dyna-Sense indicating, proportional temperature controller (Markson Science). The dry air supply was obtained by constructing a plexiglass desiccation chamber containing anhydrous calcium chloride and aquarium diaphragm pumps to take in air from the lab and pass it out through Tygon tubing. The tubing was attached to a series of polyethylene drying tubes; one contained activated carbon for removal of

organics and the other indicating Drierite. Access to the inside of the chamber was facilitated by a removeable side and a pair of bare hand entry iris ports (Fisher Scientific) on the front. Weight measurements were made with a Mettler PM460 DeltaRange electronic balance equipped with XPac-M cassette and keyboard, and connected for data output to a Macintosh computer.

One dish of solution was placed in the chamber on a balance, positioned under the heat lamp. The temperature was maintained at 40°C which was approximately the maximum solution temperature found during summer field sampling at the evaporation ponds. Weight readings were recorded at 15 minute intervals until the weight difference was less than 0.001 g over an hour. The salt residue was collected and the mineral composition identified by x-ray powder diffraction (XRPD).

The first derivative of the weight data against time was calculated and plotted. The break in the curve (**Figure 19b**) was used to mark the end of water loss. The second derivative of the weight data against time was also calculated, and the break was taken as the point at which crystallization began (**Figure 19c**). The crystallization points were calculated in ternary coordinates on a weight percent basis and plotted. These points were connected to create a crystallization isotherm. The terminal points were used to calculate the mass of water loss and check that solute mass had been conserved in the dishes. Several runs were repeated to test the reproducibility.

TABLE 5.

Pre-desiccation solution anionic compositions

Sample Code	Na_2SO_4	Na_2SeO_3 or Na_2SeO_4
	mole %	
A	100	0
AB	87.5	12.5
B	75	25
BC	62.5	32.5
C	50	50
CD	37.5	62.5
D	25	75
DE	12.5	87.5
E	0	100

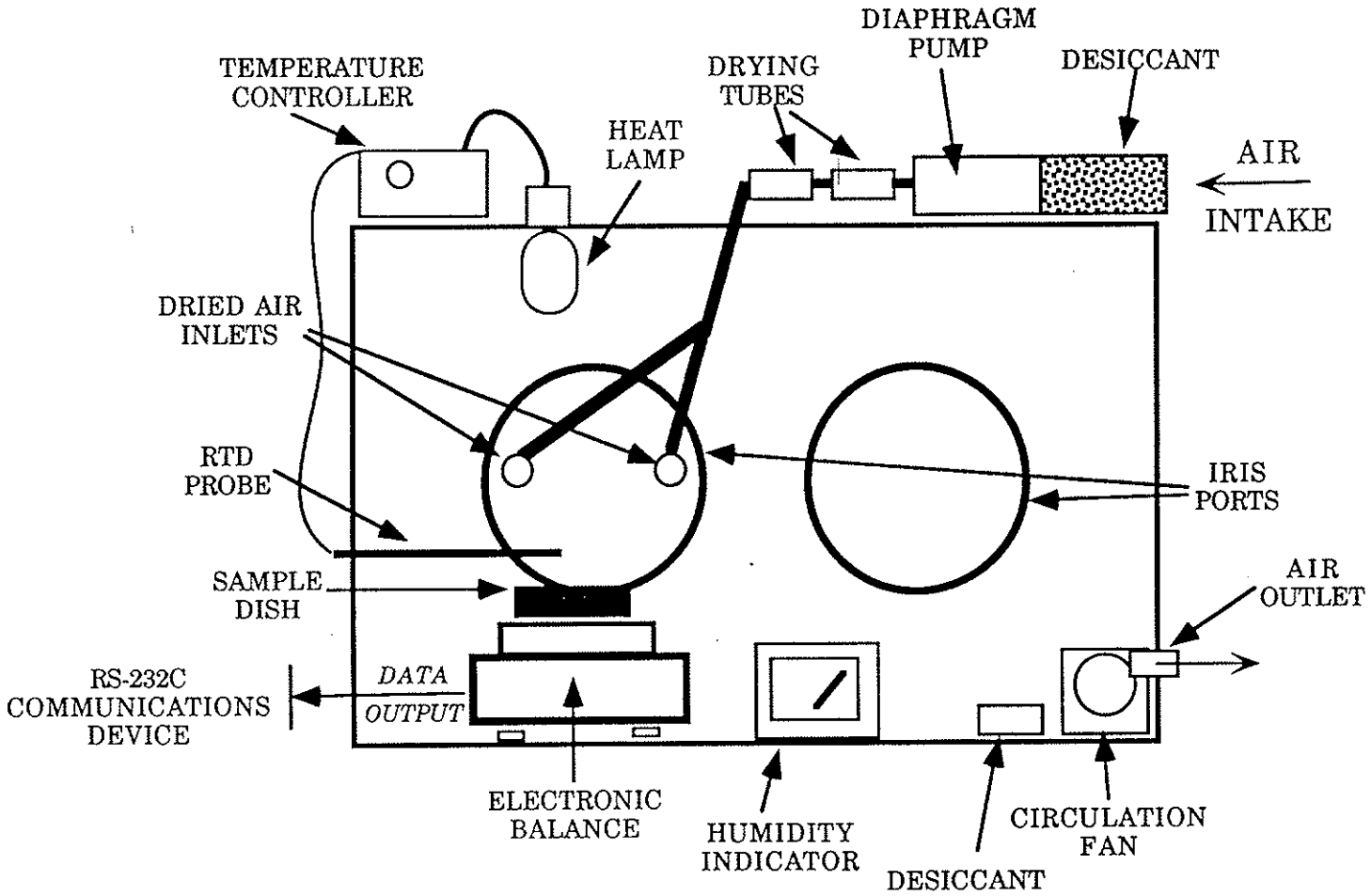

Figure 18. Desiccation chamber schematic

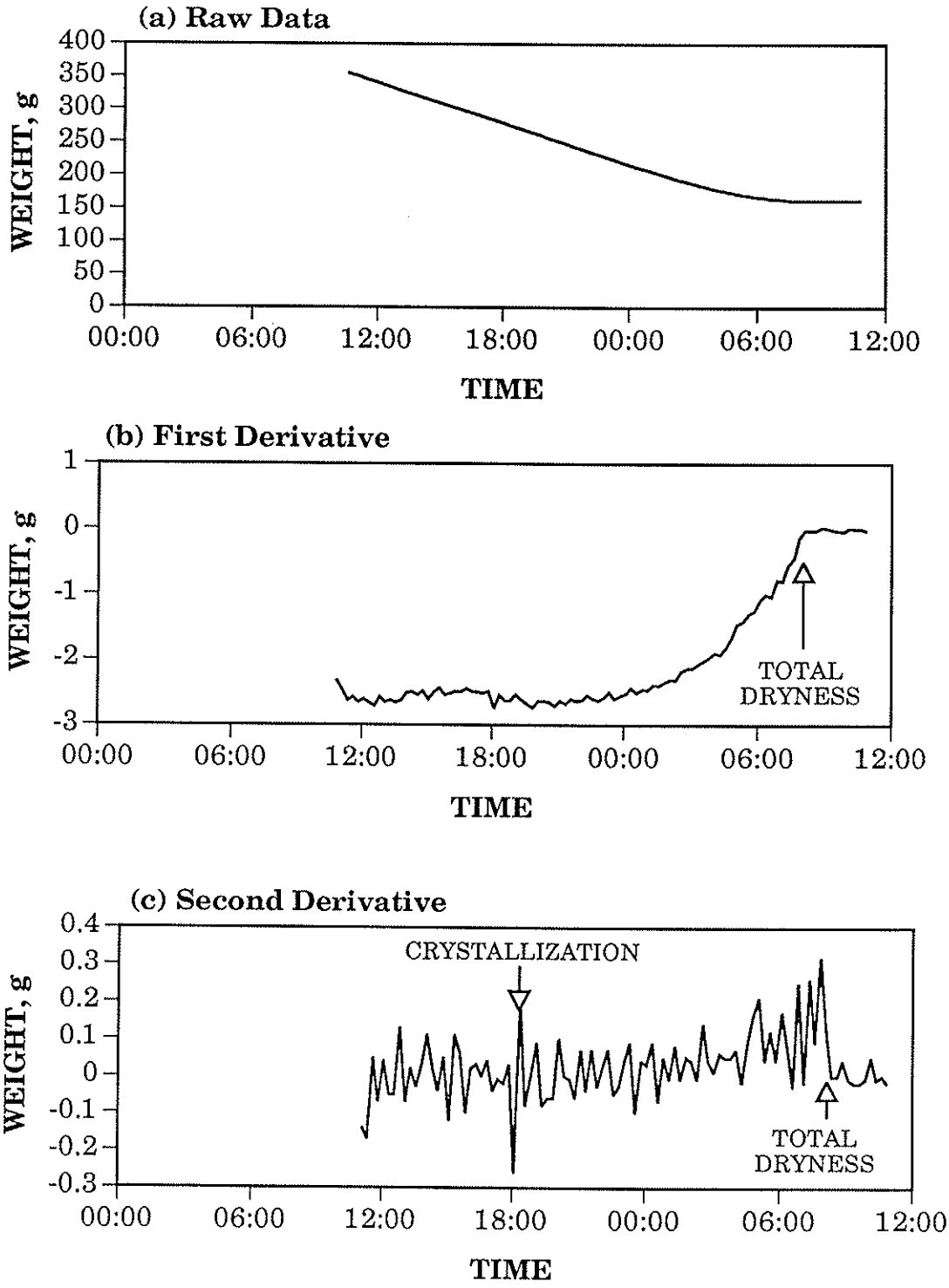

Figure 19. Derivatization with respect to time for determining breaks in weight change trends

* RESULTS

Figure 20 illustrates the desiccation pathways and crystallization isotherm for the system Na_2SeO_3-Na_2SO_4-H_2O. The crystallization point for the BC composition is high in H_2O because crystallization was significantly slower relative to the other runs (see first derivative charts in appendix). This may be due to immiscibility of the anionic components in the crystallization process.

The desiccation pathways and crystallization isotherm for the system Na_2SeO_4-Na_2SO_4-H_2O are shown in **Figure 21**. The gradual trend of the isotherm from Na_2SO_4-H_2O to the Na_2SeO_4-H_2O axis indicates that the anionic components were relatively miscible. The amount of water that had to be lost to attain crystallization, that is the length of the desiccation pathway, increased from Na_2SO_4-rich to Na_2SeO_4-rich solution composition. In contrast, the desiccation pathway lengths were fairly even except for solution composition BC.

The x-ray diffraction patterns of desiccated samples were reduced to line peak spectra. **Figure 22** contains the patterns of samples in the Na_2SeO_3-Na_2SO_4-H_2O experiment. Peaks characteristic of the Na_2SO_4 end-member, in this case thenardite because the experimental temperature was 40°C which favors the formation of thenardite, include those at about 18.9° and 32.2° 2θ. The Na_2SeO_3 end member is characterized by peaks at about 37.3° and 21.8° 2θ. The spectra of mixed composition samples yield a greater number of peaks and appear complex compared to the spectra of the pure end-members. The most complex spectra is of the DE sample which contains peaks characteristic of both members indicating that both end members are present.

The complexity of the intermediate composition sample spectra is not apparent for the Na_2SeO_4-Na_2SO_4-H_2O system (**Figure 23**) as it was for the Na_2SeO_3-Na_2SO_4-H_2O system. This suggests that the anions interacted miscibly and formed a mixed salt of the type $Na_2(SO_4)_x(SeO_4)_{1-x}$. While the peaks were not extremely intense, the Na_2SeO_4 end-member may be characterized by the medium-sized peaks at 47.2°, 48.7° and 52.8° 2θ. The Na_2SeO_4 end member peak at 19.1° 2θ dominates the spectrum but is only medium sized at 19.8° 2θ in the Na_2SO_4 end member spectrum. Medium to high intensity peaks differing slightly in position and appreciable in intensity differences may be useful as an indicator of crystal structure similarity arising from ion substitution.

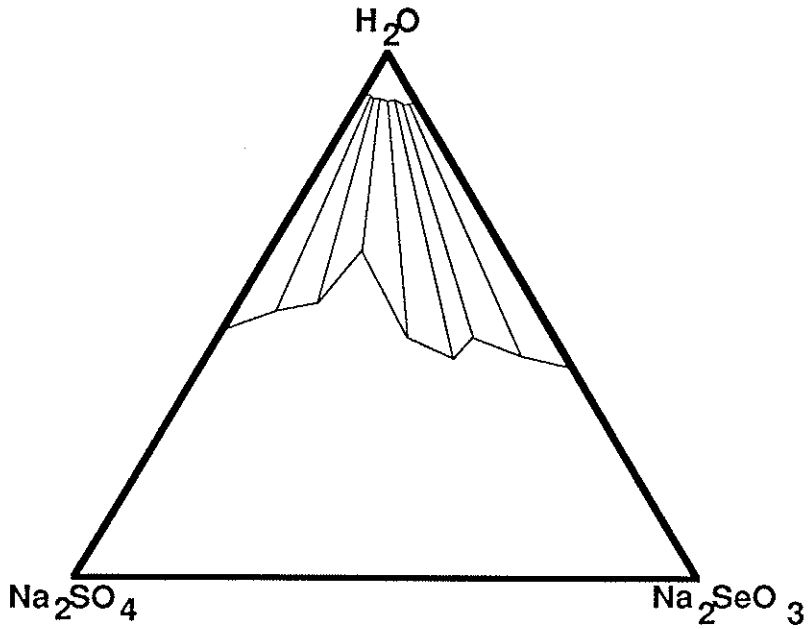

(Axial units are in terms of weight% of solution)

Figure 20. Experimental desiccation pathways in the system Na_2SeO_3 - Na_2SO_4 - H_2O.

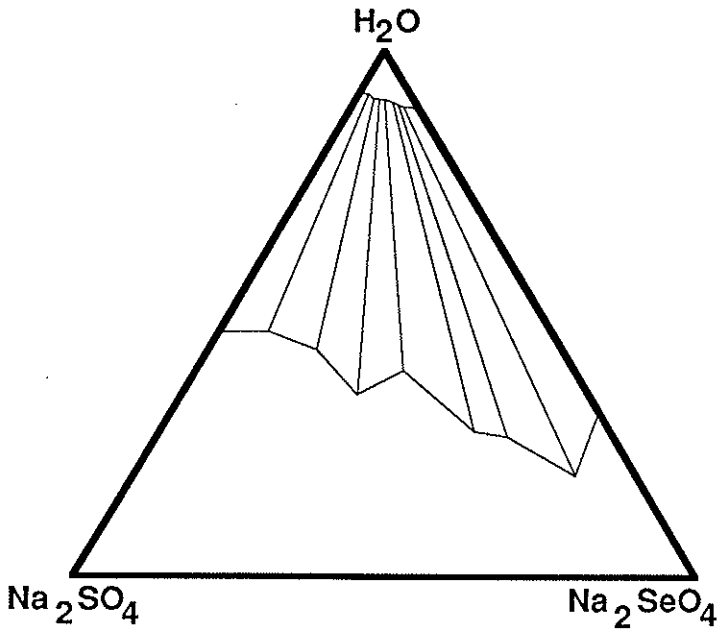

(Axial units are in terms of weight% of solution)

Figure 21. Experimental desiccation pathways in the system Na_2SeO_4 - Na_2SO_4 - H_2O.

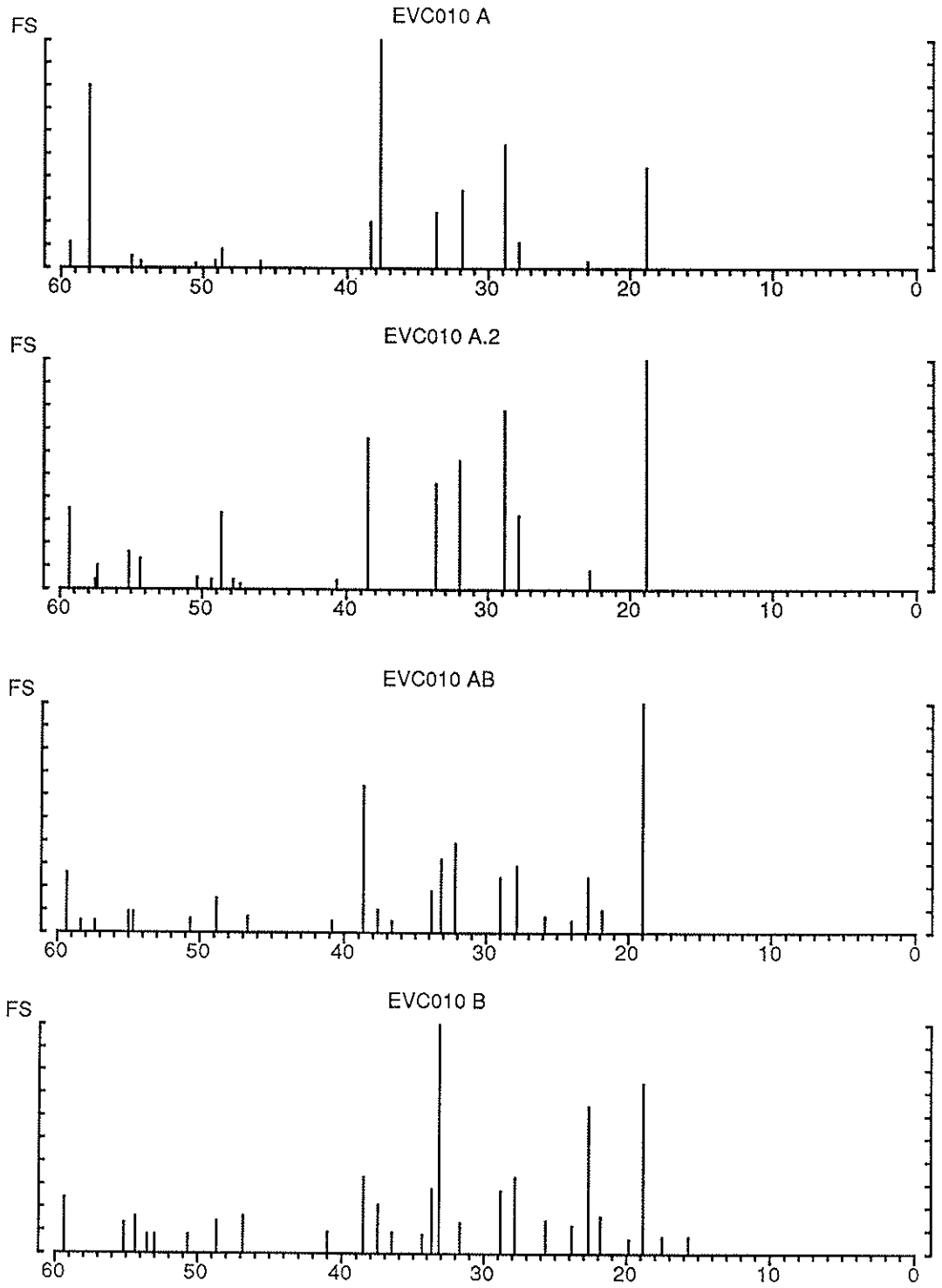

Figure 22. Line peak spectra representation of x-ray diffraction patterns for selenite-sulphate anion system.

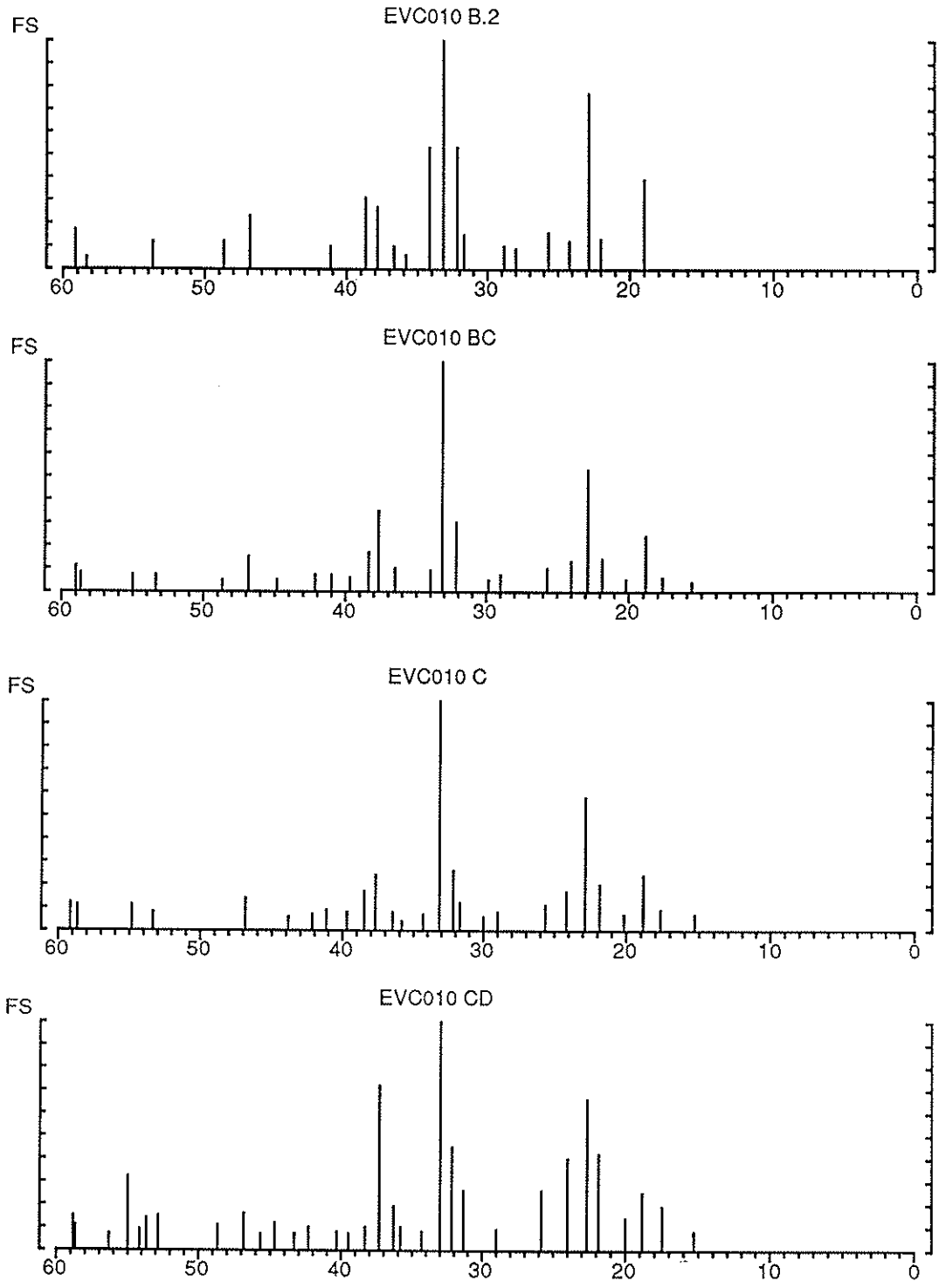

Figure 22 (continued). Line peak spectra representation of x-ray diffraction patterns for selenite-sulphate anion system.

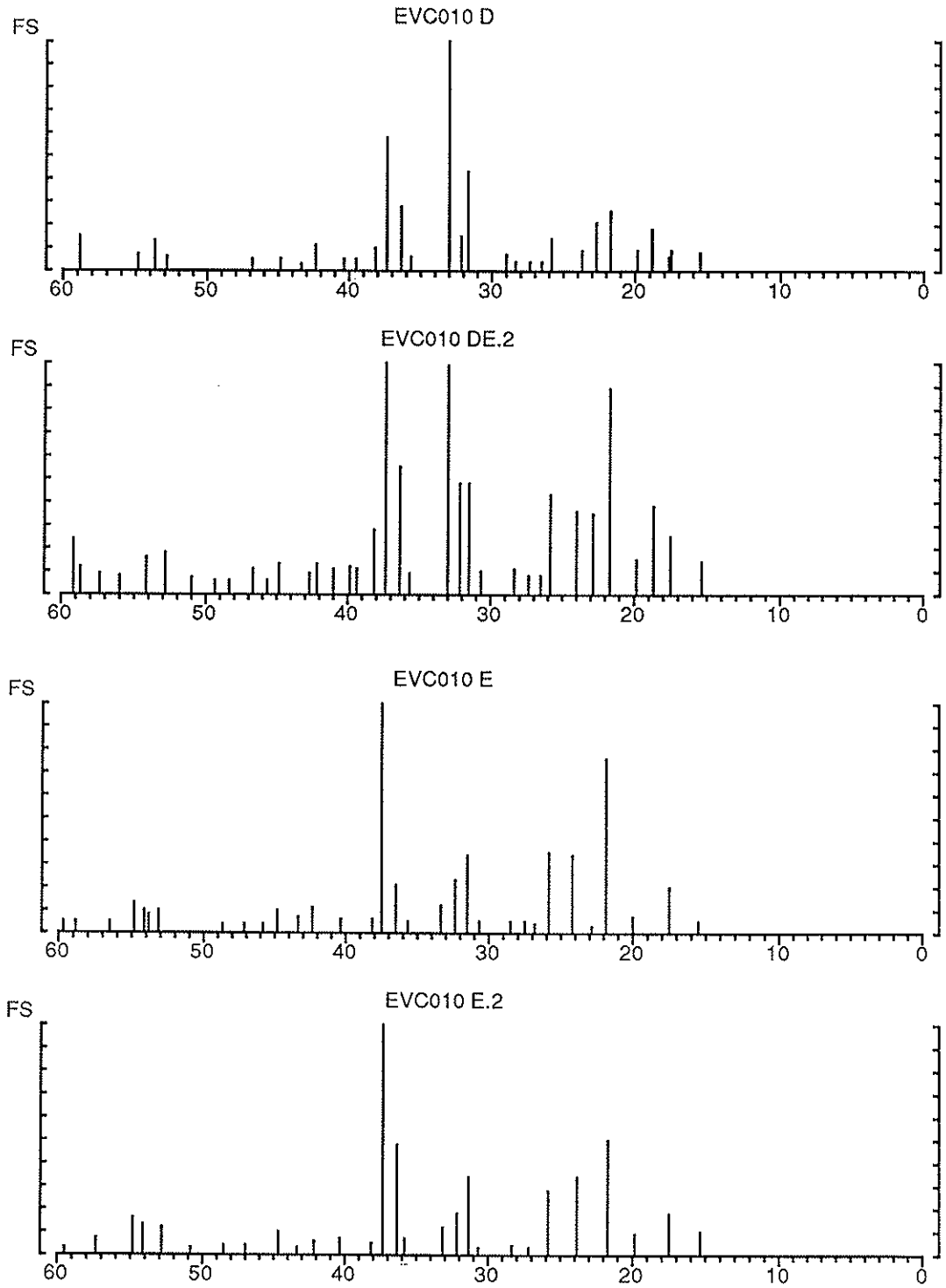

Figure 22 (continued). Line peak spectra representation of x-ray diffraction patterns for selenite-sulphate anion system.

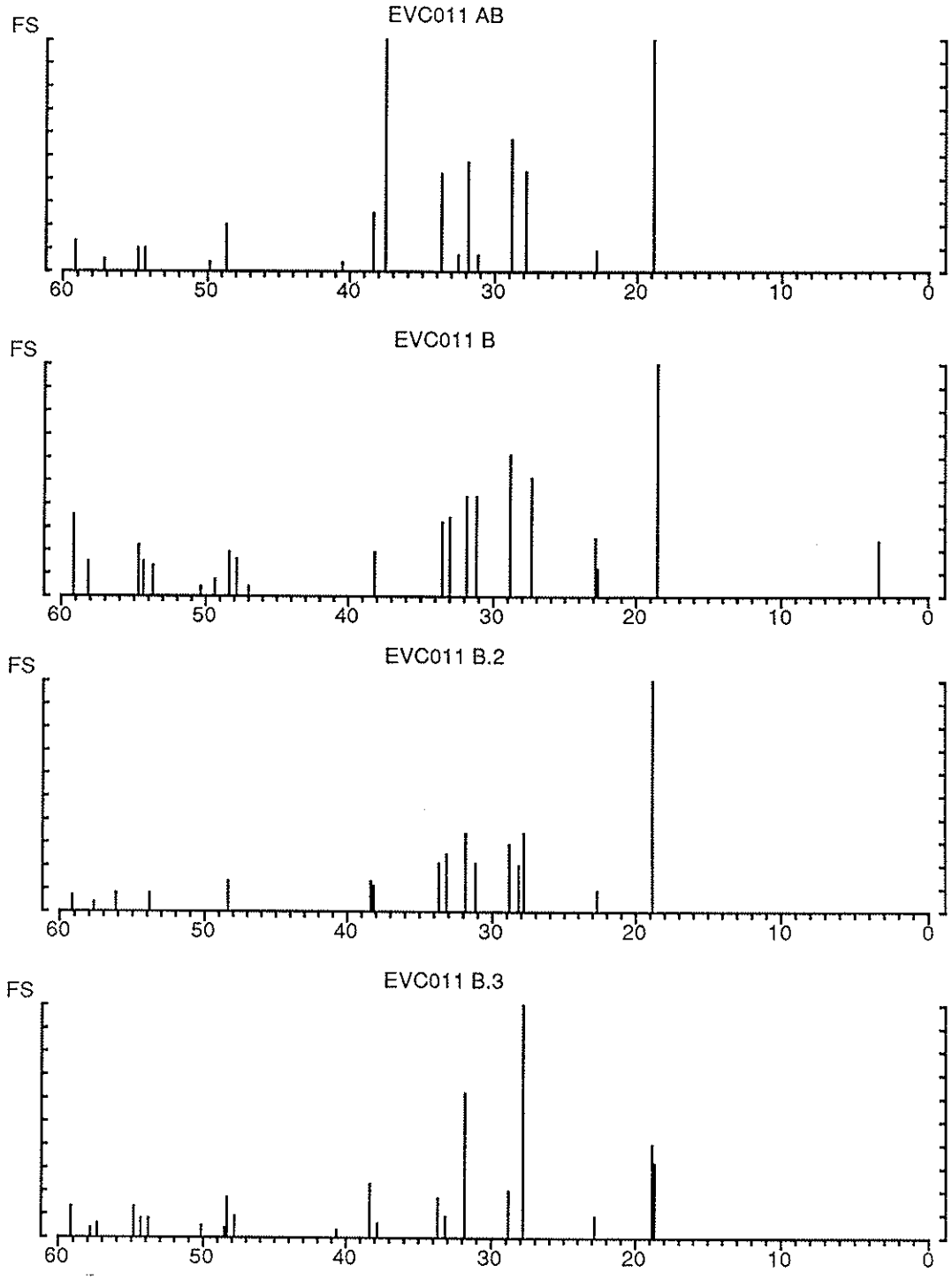

Figure 23. Line peak spectra representation of x-ray diffraction patterns for selenate-sulphate anion system.

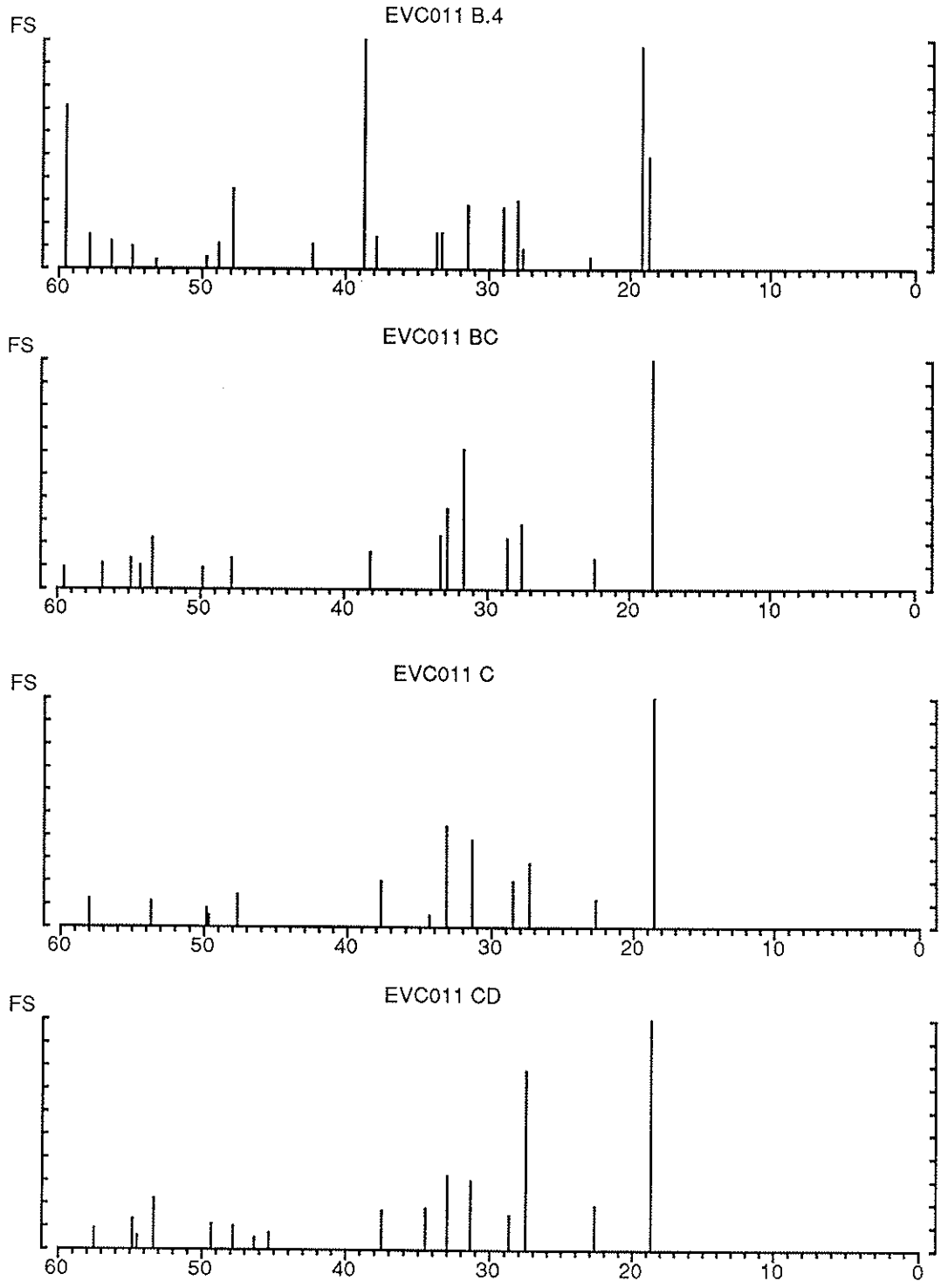

Figure 23 (continued). Line peak spectra representation of x-ray diffraction patterns for selenate-sulphate anion system.

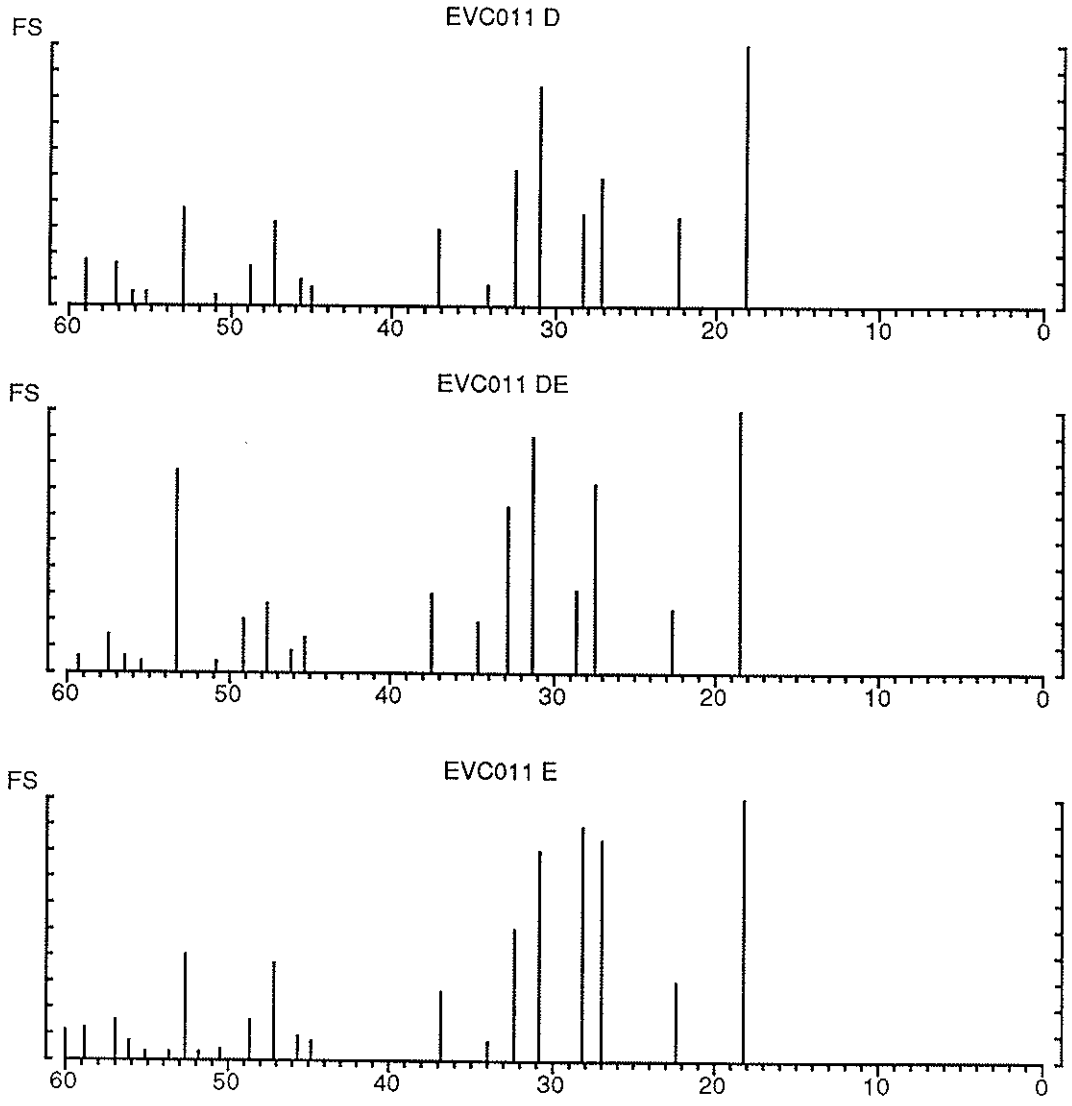

Figure 23 (continued). Line peak spectra representation of x-ray diffraction patterns for selenate-sulphate anion system.

* DISCUSSION AND CONCLUSIONS

The results from this experimental study can be used to test hypersaline models that utilize Pitzer equations (Smith, 1989; Kurilenko et al., 1990). In evaporation ponds, much of the modeled desiccation will occur towards the Na_2SO_4-H_2O axis since SeO_3 and SeO_4 are found at trace levels. While the environmental composition is far more complex than in the laboratory system, the liquid-solid chemistry findings here enable a first cut at modeling Se interaction with evaporite formation. Much work has yet to be done to investigate the competitiveness of Se with other ions for solid phase partitioning.

The field data from several evaporite-forming evaporation ponds indicate that Se is incorporated, albeit inconsistently, in the solid phase. Speciated Se data would be necessary to directly relate the findings of this study to the field results. However, it would be expected that SeO_4 concentrations in evaporites would vary according to the SO_4/SeO_4 ratio in solution, while SeO_3 in evaporites would be limited in most cases because the tendency for SeO_3 incorporation is low from trace SeO_3 solutions. In addition, SeO_3 readily undergoes adsorption to various mineral surfaces such as iron hydroxides (Gilliom, 1989) such that its availability would already be diminished.

The Na_2SO_4-Na_2SeO_4-H_2O system produced a continuous solid solution. In contrast, the Na_2SO_4-Na_2SeO_3-H_2O system possesses a discontinuous solid solution. Under Roozeboom's classification scheme (Driessens, 1986), the discontinuous solid solution is a type II, while the continuous solid solution is most likely a type III. A type I solid solution is ideal which when considering the chemical similarity, that is miscibility, of SO_4 and SeO_4, the Na_2SO_4-Na_2SeO_4-H_2O system would be a good candidate for type I classification. The data for the Na_2SO_4-Na_2SeO_4-H_2O system does not preclude type I classification. However, the SeO_4 ion may be deterred from substitution by less than ideal crystal class matching; SeO_4 ion forms a specific rhombic salt, while SO_4 could form several rhombic classes within the orthorhombic system. Further work monitoring the solution composition between crystallization and complete dryness would be needed to extend the desiccation pathways along the crystallization isotherm.

This experiment could be performed at a lower temperature favoring mirabilite formation. The solid solution results could be similar to those studied here with thenardite since the sulfate and selenate decahydrate minerals are both monoclinic, whereas the selenite pentahydrate mineral is tetragonal. However, the temperature range in which the various hydrated phases are stable is presently unknown and could conceivably create a system in which one mineral end member is hydrated and the other not.

The dehydration step played, on occasion, a mechanistic role in determining the total time taken to desiccate a sample. Assuming that unhydrated minerals were being formed at 40°C, the secondary weight loss pattern observed between crystallization and complete dehydration was due to gradual evaporative loss of physically trapped water. Reducing physically trapped water to insignificant

levels would be important to the study of the hydrated minerals in case multiple hydrated states form and transitions between such phases would be observable.

While current evaporation pond water quality conditions would utilize only a minute portion of the chemistry investigated here, final disposal of Se enriched solutions may be necessary if partitioning of Se into sinks is minimal. Further detailed studies of the Na_2SO_4-Na_2SeO_3-H_2O and Na_2SO_4-Na_2SeO_4-H_2O systems are necessary to determine the ultimate fate of Se in evaporite-forming evaporation ponds.

COPRECIPITATION OF SELENIUM OXYANIONS WITH MIRABILITE

The trace level presence of selenium (Se) in agricultural evaporation ponds at the evaporite-forming stage yields the question as to whether evaporites could serve as a Se sink through coprecipitation with mirabilite ($Na_2SO_4 \bullet 10H_2O$). Factors that affect the coprecipitation reaction include the precipitation rate, agglomeration, and miscibility (Walton, 1967). The miscibility factor suggests that Se may actively coprecipitate in a sulfate mineral since Se and S, both group VIA elements, share several common properties.

Inorganic oxyanion forms of S and Se include sulphite (SO_3) and selenite (SeO_3), as well as sulfate (SO_4) and selenate (SeO_4). The oxidation states are also shared and result in all these oxyanions possessing a -2 charge. The oxyanion sizes are also similar because they are largely determined by the surrounding oxygen atoms coordinated similarly. Both SeO_3 and SO_3 both form pyramidal groups (Wyckoff, 1964; Naray-Szabo, 1969); SeO_4 and SO_4 form tetrahedrons of similar sizes (Naray-Szabo, 1969). The polarizabilities are expected to be similar too because S and Se are from the same periodic group, and would thus have similar electronegativities. The above commonalities indicate that S and Se oxyanions are indeed miscible especially between those with the same oxidation states.

This section investigates the partitioning of Se into mirabilite when supersaturation leading to crystallization is created by a temperature drop. This is in contrast to supersaturation and crystallization resulting from evaporative concentration. The final temperature of 15°C favors formation of mirabilite rather than thenardite (Na_2SO_4), (Keller et al., 1986b). The solubility of mirabilite increases with temperature until thenardite becomes favored at about 32°C (Doner and Lynn, 1989).

Mirabilite formation under cool conditions is likely to occur due to temperature drops in the diurnal solution temperature cycle which may reach as low as 6°C (Tanji and Dahlgren, 1990). Evaporites in evaporation ponds have been reported to form during the night time low temperatures and disappear during the day (Chip Eulis, personal communication). In addition to daily variations, monthly and seasonal variations have also been reported (Smith et al., 1987) in other saline water bodies.

Formation of thenardite in this way is unlikely because thenardite solubility hardly changes in the range 32 to 50°C.

***MATERIALS AND METHODS**

A saturated solution of Na_2SO_4 at 60°C was prepared by combining an excess of reagent Na_2SO_4 (Fisher Scientific) with distilled-deionized water. Stock solutions of 1 *M* Na_2SeO_3 and Na_2SeO_4 were prepared in distilled-deionized water and kept in the water bath at 60°C.

Mixtures of Na_2SO_4-Na_2SeO_3-H_2O (**Table 6**) and Na_2SO_4-Na_2SeO_4-H_2O (**Table 7**) were made by combining 40 mL of the saturated Na_2SO_4 solution with 0, 2, 4, 6, 8 and 10 mL of either Se stock solution. Volumes were made up to 50 mL with distilled-deionized water. All samples were prepared in triplicate and maintained at 60°C for 24 hours. The samples were then transferred to a constant temperature bath cooled to 15°C.

A seeding mixture to induce precipitation was prepared by adding a few crystals of reagent Na_2SO_4 to 100 mL of the saturated Na_2SO_4 solution cooled to room temperature. After 24 hours at 15°C, the samples were seeded with 0.05 mL of the seeding solution which was well shaken to obtain an evenly distributed suspension. The seeded samples were gently shaken to ensure that crystallization occurred homogeneously. Samples stood for another 24 hours, during which time the crystals settled to the container bottom.

The natant solutions were sampled and filtered and the crystals collected for analysis. About 1 g of each crystalline sample was then dissolved in one liter of distilled-deionized water. The natant solution and redissolved crystal samples were then analyzed for SO_4, SeO_3 and SeO_4 using a Dionex Model 4000 ion chromatograph with conductivity detector.

The same procedure was applied to Na_2SO_4-Na_2SeO_3-Na_2SeO_4-H_2O mixtures (**Table 8**) to ascertain the effects of the simultaneous presence of Se(IV) and Se(VI).

A similar experiment using Na_2SO_4-NaCl-H_2O mixtures (**Table 9**) was done to determine the rise in solute, specifically Cl, concentrations that may be expected when H_2O molecules are consumed in the formation of the hydrated mineral, mirabilite ($Na_2SO_4 \cdot 10H_2O$). The amount of chloride bound to the crystallized phase is assumed to be insignificant, and allows the experiment to serve as a control.

Distribution coefficients are calculated on a mole fraction basis (after Driessens, 1986):

$$D_{SeO_x}^{solution} = \frac{m_{SeO_x}^{solution}}{m_{Na}^{solution} + m_{SO_4}^{solution}}$$

$$D_{SeO_x}^{solid} = \frac{m_{SeO_x}^{solid}}{m_{Na}^{solid} + m_{SO_4}^{solid}}$$

The partition coefficient describing the phase selectivity is given by:

$$K_{SeO_x} = \frac{D_{SeO_x}^{solid}}{D_{SeO_x}^{solution}}$$

TABLE 6.
Mean (n = 3) salt and solution compositions in selenite-sulfate system.

	WEIGHT % OF TOTAL ANIONS							
	Initial Solution		Final Solution			Final Solid		
	SO_4	SeO_3	SO_4	SeO_3	σ	SO_4	SeO_3	σ
I	100.00	0.00	100.00	0.00	0.00	100.00	0.00	0.00
II	97.84	2.16	85.57	14.43	1.15	99.78	0.22	0.03
III	95.78	4.22	74.93	26.44	0.27	99.63	0.37	0.08
IV	93.80	6.20	65.82	35.55	0.42	99.44	0.56	0.08
V	91.90	8.10	57.43	43.94	0.03	98.84	1.16	0.22
VI	90.07	9.93	51.30	50.07	0.31	98.74	1.26	0.11

TABLE 7.

Mean (n = 3) salt and solution compositions in selenate-sulfate system.

	WEIGHT % OF TOTAL ANIONS							
	Initial Solution		Final Solution			Final Solid		
	SO_4	SeO_3	SO_4	SeO_3	σ	SO_4	SeO_3	σ
I	100.00	0.00	100.00	0.00	0.00	100.00	0.00	0.00
II	97.58	2.42	94.49	5.51	0.57	98.88	1.12	0.14
III	95.27	4.73	88.61	11.39	*	97.59	2.41	0.35
IV	93.07	6.93	84.27	15.73	0.62	96.29	3.71	0.31
V	90.97	9.03	78.81	21.19	0.09	94.57	5.43	0.07
VI	88.96	11.04	75.32	24.68	0.81	93.25	6.75	0.71

TABLE 8.

Mean (n = 3) salt and solution compositions in selenite-selenate-sulfate system.

WEIGHT % OF TOTAL ANIONS

SO_4

	Initial Solution	Final Solution		Final Solid	
	Wt %	Wt %	σ	Wt %	σ
I	90.07	69.76	0.31	97.92	0.39
II	89.85	71.71	0.13	96.11	1.27
III	89.62	73.17	0.21	94.71	0.54
IV	89.40	74.28	0.20	93.69	0.93
V	89.18	74.73	0.37	91.61	1.26
VI	88.96	74.82	0.19	89.89	1.66

SeO_3

	Initial Solution	Final Solution		Final Solid	
	Wt %	Wt %	σ	Wt %	σ
I	9.93	30.23	0.31	2.08	0.39
II	7.92	24.04	0.22	2.19	0.96
III	5.93	17.54	0.19	1.55	0.26
IV	3.94	11.21	0.10	0.87	0.36
V	1.97	5.32	0.09	0.63	0.58
VI	0.00	0.00	0.00	0.00	0.00

SeO_4

	Initial Solution	Final Solution		Final Solid	
	Wt %	Wt %	σ	Wt %	σ
I	0.00	0.00	0.00	0.00	0.00
II	2.23	4.25	0.09	1.70	0.33
III	4.45	9.29	0.02	3.74	0.29
IV	6.66	14.52	0.10	5.44	0.58
V	8.86	19.95	0.28	7.75	0.76
VI	11.04	25.19	0.20	10.11	1.25

TABLE 9.

Mean (n = 3) salt and solution compositions in chloride-sulfate system.

	WEIGHT % OF TOTAL ANIONS							
	Initial Solution		Final Solution			Final Solid		
	SO_4	SeO_3	SO_4	SeO_3	σ	SO_4	SeO_3	σ
VII	97.01	2.99	89.93	10.07	0.02	97.91	2.09	0.27
VIII	98.18	1.82	94.21	5.79	0.07	98.47	1.53	0.16
IX	99.39	0.61	94.21	5.79	0.07	98.61	1.39	0.59

*** RESULTS**

The low standard deviations of the experimental data show that there was good reproducibility between triplicate samples (**Tables 6 - 9**). The mean composition of initial solutions may be compared to the mean composition of the final solutions and solids. The sulfate-chloride control experiment shows that hydration of the Na_2SO_4 solid enriches solute concentration by approximately three-fold.

Figure 24 shows the composition of solids formed from the crystallization in the selenite-sulfate solutions. The proportion of selenite associated with the solid is very low. In the selenate-sulfate solutions (**Figure 25**), the selenate proportion is in the range 0 to 2% w/w. Similar observations can be made in the mixed sulfate-selenate-selenite solutions (**Figure 26**). The results of the chloride-sulfate experiment (**Figure 27**) show that low quantities of chloride are associated with the sampled solid and follow the trend of solution concentration.

The calculated partition coefficients (**Tables 10 and 11**) show that both selenium oxyanion species are depleted in the solid phase relative to the solution phase similar to the field collected mirabilite samples. When both Se oxyanion species are present in the same solution along with SO_4, the partition coefficients are lower as a result of competition (**Table 12**).

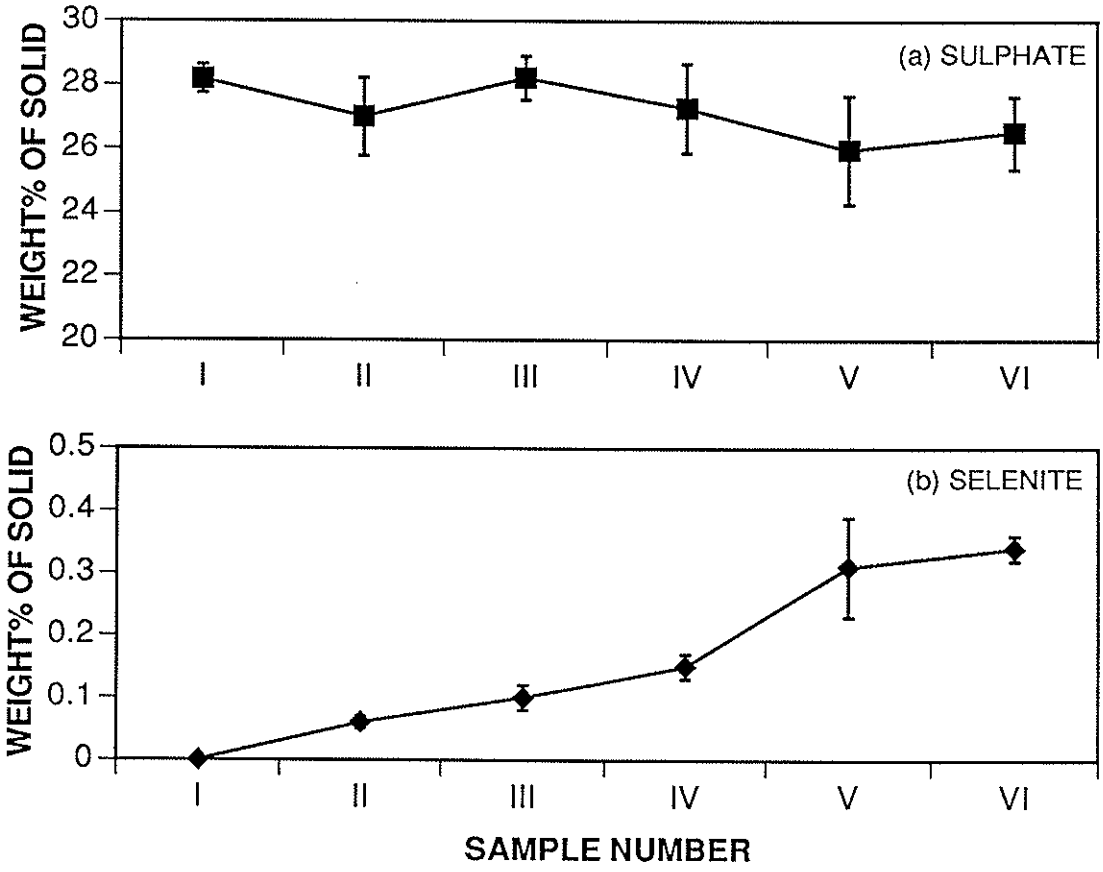

Figure 24. Weight percent of total salt of sulphate and selenite in salts formed from selenite-sulphate solutions.

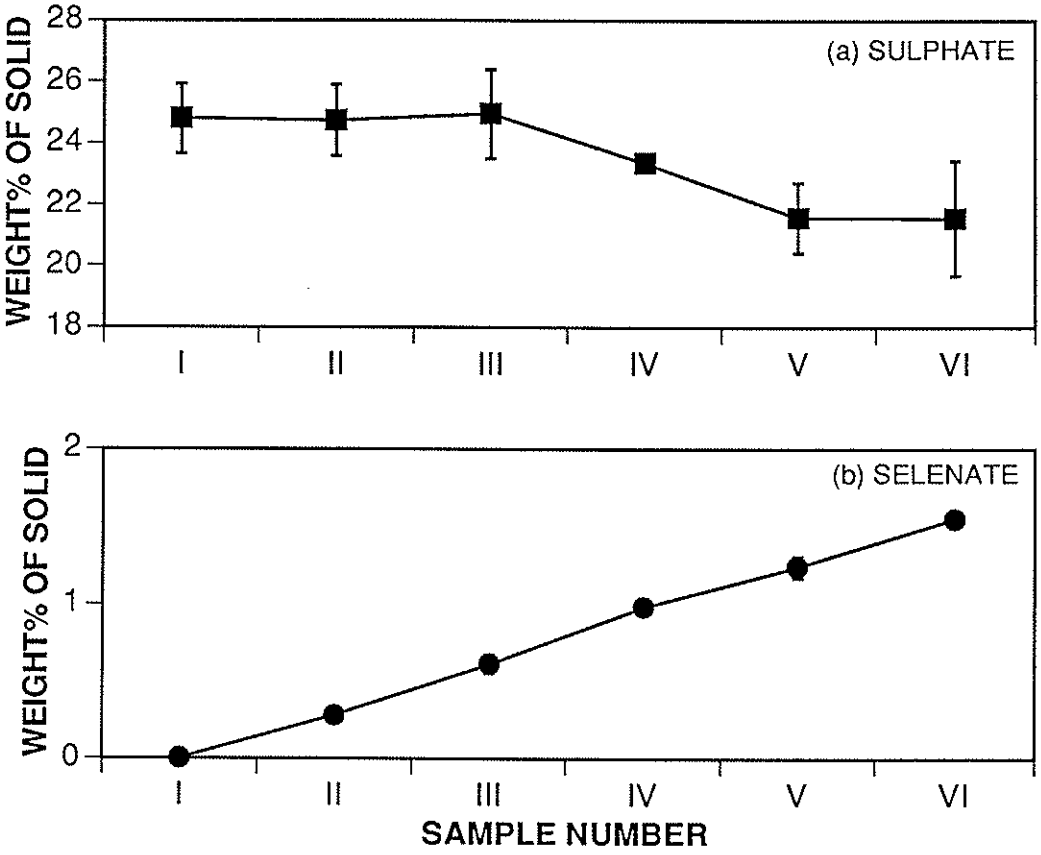

Figure 25. Weight percent of total salt of sulphate and selenate in salts formed from selenate-sulphate solutions.

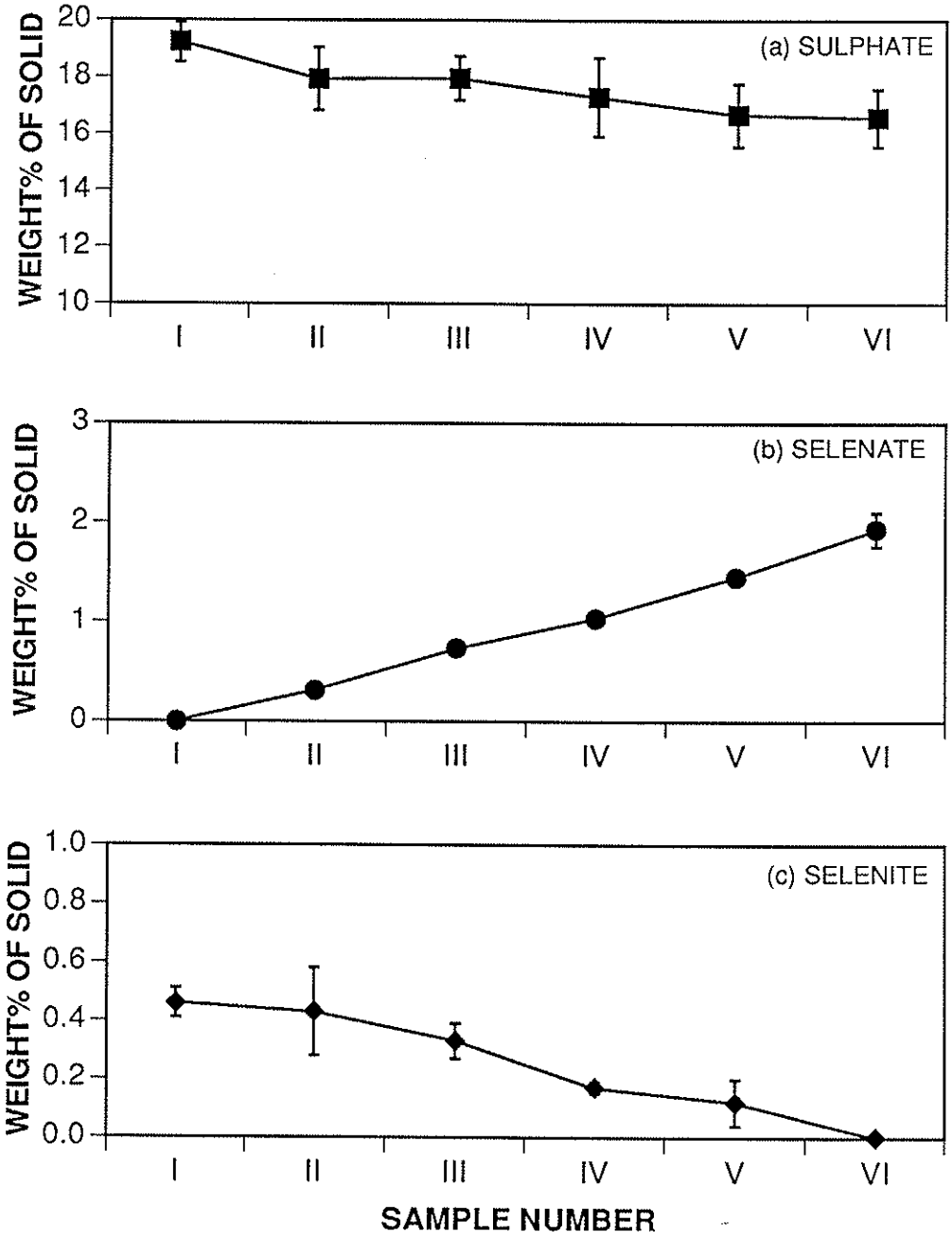

Figure 26. Weight percent of total salt of sulphate, selenate and selenite in salts formed from selenite-selenate-sulphate solutions.

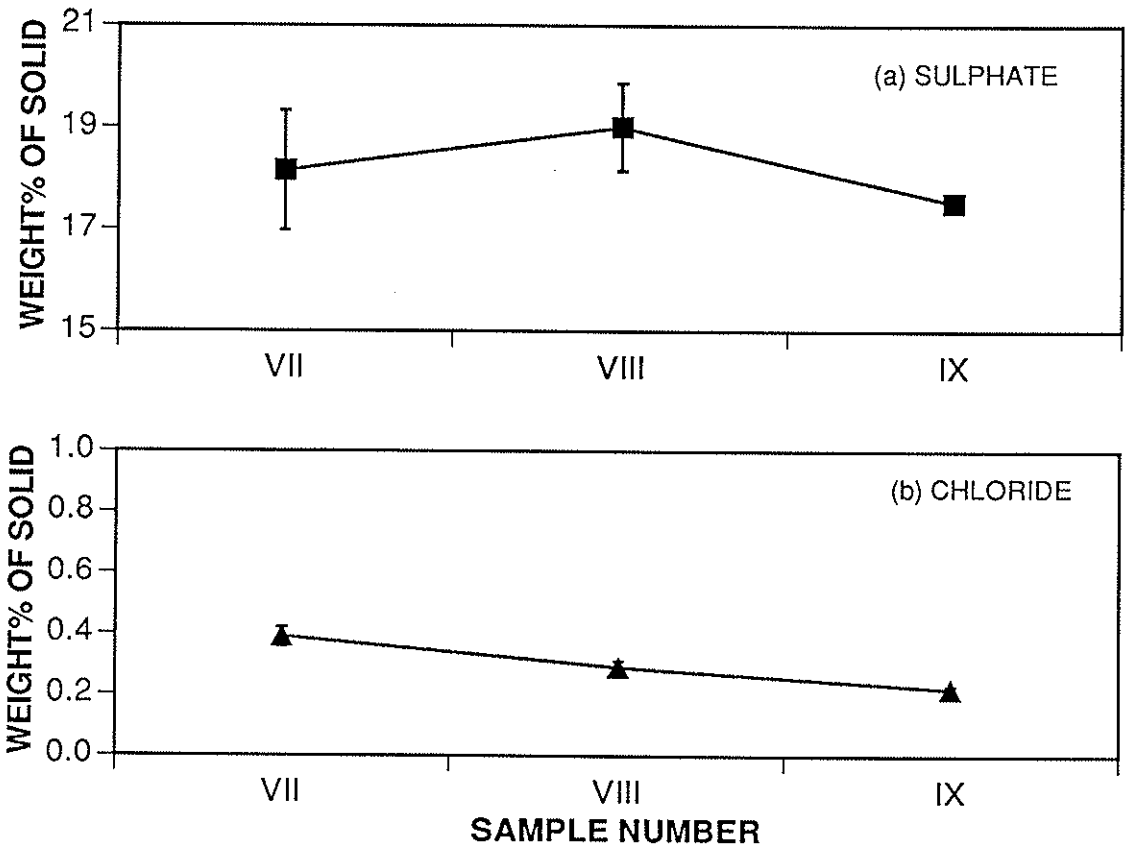

Figure 27. Weight percent of total salt of sulphate and chloride in salts formed from chloride-sulphate solutions.

TABLE 10.

Calculated partition coefficients in selenite-sulfate system.

Sample Number	log K_{SeO_3}
I	*
II	-1.59
III	-1.62
IV	-1.58
V	-1.37
VI	-1.40

* Not applicable since no SeO_3 in system

TABLE 11.

Calculated partition coefficients in selenate-sulfate system.

Sample Number	log K_{SeO_4}
I	*
II	-0.36
III	-0.33
IV	-0.31
V	-0.29
VI	-0.27

* Not applicable since no SeO_4 in system.

TABLE 12.

Calculated partition coefficients in selenite-selenate-sulfate system.

Sample Number	log K_{SeO_3}	log K_{SeO_4}
I	-0.96	**
II	-0.84	-0.09
III	-0.86	-0.09
IV	-0.91	-0.13
V	-0.73	-0.12
VI	*	-0.11

* Not applicable since no SeO_3 in system
** Not applicable since no SeO_4 in system

* DISCUSSION AND CONCLUSIONS

It is possible that while SeO_3 or SeO_4 do not appreciably substitute in the mirabilite crystal lattice, these oxyanions may cause a common ion effect or at least contribute to an ionic strength significantly greater than in the control experiment such that more mirabilite forms hence consuming more water molecules for hydration. This would account for the greater degree of concentration observed for the selenite-sulfate systems which also indicates that SeO_3 did not substitute for SO_4 in the solid. Solution phase SeO_3 appears to have concentrated about six times.

Coprecipitation of SeO_3 with mirabilite was not detected whereas SeO_4 coprecipitation could be proposed because of the much smaller partition coefficients than those of either SeO_3 or Cl. However, partitioning of SeO_4 into the solid was not reflective of the solution composition. Recognizing that some SeO_4 in the solid arose from occlusion or surface film, the amount that did coprecipitate was small. Rate studies on aging mirabilite in selenate solutions would be needed to determine whether coprecipitation occurs during crystallization or solid-solution equilibration.

Mirabilite may be a sink for Se in evaporation ponds especially under oxidizing conditions where SeO_4 is the dominant form. However, the partitioning would still leave the solution enriched in Se while the solid is depleted, potentially raising the toxicological danger of the desiccating solutions. The concentration of solutes provided by the consumption of water molecules in mirabilite could significantly be alleviated if thenardite would form instead. Thenardite, which is favored under dry conditions and above about 32°C, could be induced to form during summer months when drainage inputs and water levels are low, evaporation rates are high, and solution temperatures reach as high as 40°C.

The rate of crystallization is a factor in determining mixed crystal composition (Walton, 1967). The rapid rate induced in this experiment represents one extreme. Temperature drops at evaporation ponds occur over a period of about 12 hours. Experiments utilizing a temperature ramp could be performed to determine if different enrichment pathways are taken.

DESICCATION OF Na_2SO_4-B AND NaCl-B SOLUTIONS

Synthetic salt solution desiccation procedure

The study of boron association with mirabilite and halite examined the possible uptake mechanisms of coprecipitation, sorption, and occlusion. In order to study these mechanisms, evaporite formation was induced by desiccating synthetic saline solutions in an evaporating chamber, which used a flow of dry air to remove water vapor at room temperature. The variables under consideration were the major salt ion constituents, solution pH, degree of evaporation, and boron concentration. Equilibrium solutions and dissolved evaporites were analyzed for boron by complexation with azomethine-H and an acetate - EDTA buffer using a HP8452A UV-Visible Spectrophotometer (John et al., 1975). Boron concentrations were determined by absorbance at 420 nm.

In order to prevent accidental precipitation with drop in temperature, the boron - salt solutions were made by mixing a stock solution of boron in distilled, deionized water (DDW) with saturated salt solution, so that the degree of saturation was at 90%, rather than 100%. The 500 m*M* B stock solution was made by adding boric acid [$B(OH)_{3(s)}$] to DDW. Stock solutions of 50 and 5 mM B were made by 1:10 and 1:100 dilutions with DDW. Saturated Na_2SO_4 or NaCl solutions were made by heating DDW and dissolving a predetermined amount of anhydrous $Na_2SO_{4(s)}$ or $NaCl_{(s)}$ as determined from solubility data in Linke (1965) and the CRC Handbook of Chemistry and Physics (1982-83), respectively. The solutions were allowed to reach ambient temperature, and, if precipitation did not commence, the supersaturated solution was seeded with a small amount of solid Na_2SO_4 or NaCl. The precipitate or excess reagent salt remained in the solution to ensure saturation as room temperature varied (± 3°C), and the containers were frequently shaken to prevent density effects on concentration in aged solutions.

The samples at each concentration were made in triplicate by adding a volume of $B(OH)_3$ solution that was less than or equal to 10 mL, then bringing to 10.0 mL with the addition of DDW, and finally adding 90 mL of saturated salt solution. This brought the volume of each sample to 100.0 mL.

The samples were put into preweighed polypropylene containers, and the starting solution weight was determined. After initial sample preparation, pH was adjusted using either standardized KOH (0.733 *M*) or HCl (1.021 *M*) solutions. Estimations for volumes of KOH or HCl were made by obtaining titration curves for variable amounts of boron in Na_2SO_4 or NaCl. While adding the acid or base, the

pH was monitored using a combination electrode until the desired pH level was obtained (± 0.1 pH units). The samples were reweighed following addition of acid or base.

The samples were uncapped and placed into the evaporation chamber with a dry air flow rate of 4.5 liters/minute. The air was dried by passing through $CaCl_2$ and $CaSO_4$ cylinders and circulated by an electric fan inside the evaporation chamber. At roughly 24 hour intervals, the pH was measured and the samples were rotated to encourage uniform evaporation.

After the volume of the samples decreased to approximately 50 mL, the containers were capped and the samples reweighed. The evaporites were then separated from the solution by filtering each through a 0.45 μm Millipore filter. The time of filtration was kept to under 10 minutes to prevent drying the salts and to keep potential volatilization of $B(OH)_3$ to a minimum. The separated evaporites were placed into preweighed polypropylene containers and weighed to obtain the wet mirabilite or halite weight. The filtrates were put back into the original evaporating container.

Quantification of boron in saline solutions and precipitates.

Solutions were diluted and the precipitates were dissolved to bring the concentration of boron into the linear detection range for the azomethine-H method. For the NaCl and Na_2SO_4 solutions, the 2, 10, 50, and 100 m*M* B (initial concentrations) were diluted by a factor of 10, 100, 500, and 1000, respectively. The boron standards used for the azomethine-H method ranged from 0.05 to 1.00 m*M* B in DDW.

For the precipitates, the high amounts of NaCl or Na_2SO_4 in the dissolved solutions would not accurately match with the boron standards prepared in DDW. This is due to potential interference by the ion pair $NaB(OH)_4^-$. For NaCl, a preweighed subsample (2.0 g) for the 2 and 10 m*M* B samples was dissolved in DDW and brought to volume of 10 mL with DDW. For 50 and 100 mM B samples, a 2.0 g subsample was dissolved in roughly 10 mL, then brought to 100 mL with 2 g : 10 mL solution of NaCl. This would keep the 2 g : 10 mL NaCl matrix consistent. The boron standards used for quantification were between 0.02 to 0.90 m*M* B in a matrix of 2.0 g : 10 mL NaCl.

For the acidic Na_2SO_4 samples, the 2 and 10 m*M* B precipitates were dissolved in a ratio of 10 g : 100 mL DDW, and the 50 and 100 m*M* B were dissolved in a ratio of 6.2 and 5.1 g : 100 mL DDW in order to keep the boron concentration as high as possible for quantification. For the alkaline Na_2SO_4 samples, the 2 and 10 m*M* B precipitates were again dissolved in a 10 g : 100 mL ratio, and the 50 and 100 mM B precipitates were dissolved in a 2 g : 100 mL ratio. The standards used were between 0.02 to 0.80 m*M* B in a 1 g Na_2SO_4 : 10 mL DDW matrix. Although this is not exactly the same matrix as the dissolved salts, it does approximate the influence of Na^+ on ion pair formation with $B(OH)_4^-$, which is minor at the buffered pH of 5.1 (John et al., 1975).

The azomethine-H method was used for measuring boron in the standards and samples. The azomethine-H solution was made by dissolving 1.00 g of ascorbic acid in DDW, then bringing up to

100 mL with DDW. To this ascorbic acid solution, 0.45 g of the powdered, sodium salt of azomethine-H was dissolved. The buffer solution consisted of 250 g ammonium acetate dissolved in 400 mL DDW, followed by the addition of 15 g of disodium ethylenediamine tetraacetate (EDTA) and 125 mL of glacial acetic acid. One mL of each standard or sample was placed in a plexiglass test tube. Two mL of the buffer solution was added, and the test tubes were vigorously mixed. This was followed immediately by adding two mL of the azomethine-H solution, again mixing thoroughly. The standards and samples were allowed to sit for 30 minutes before measuring the absorbance at 420 nm in a 1 cm quartz cuvet. The HP3452A spectrophotometer, interfaced with a Macintosh® IIci computer by National Instruments Labview™ software, was used for quantifying the amount of boron in each sample.

The QA/QC protocol (Taylor, 1987) was followed in order to provide a measure of accuracy. The standards were run, followed by the samples, duplicates (every 6th sample) and a recovery sample for every 12 samples.

Sorption experiments using desiccated NaCl and Na_2SO_4 solutions

In order to compare sorption reactions directly to the coprecipitation-sorption-occlusion reactions provided by the desiccation experiments, the solutions saved from the desiccation experiments were used for sorption onto boron-free halite or mirabilite. This was to keep the solutions very close, if not exactly the same, in the two different studies. One main difference would be that the desiccation samples had increasing concentrations of ions during evapoconcentration, and subsequently, during growth of mirabilite. The sorption samples would have mirabilite free of boron influence, which would not be in exact equilibrium with the desiccated boron solutions. Nevertheless, this was the closest method devised to compare the retention mechanisms.

The preparation of the boron-free mirabilite or halite was the same as the boron desiccation sample preparation described above, except no boron stock solution was added. The pH was adjusted similarly, and the samples were desiccated over a comparable time period to induce similar crystal morphologies. The pH was monitored occasionally for the acidic samples, but daily for the alkaline samples. After desiccation to about 50 mL, the precipitates were separated from the solutions.

The procedure was to add a specified volume of the desiccated boron solution to a container having a preweighed, boron-free sample of halite or mirabilite. The ratio of volume to precipitate weight was determined by the calculations of the desiccated samples. For each boron concentration, the average volume remaining and average precipitate (wet) weight was calculated. Then, based on either a 10 or 20 mL volume of solution, the weight of the boron-free precipitate was determined. By using this technique, the degree of retention of boron would not change due to inconsistent volumes of solutions or weights of solid. Therefore, a direct comparison of sorption mechanism versus coprecipitation-sorption-occlusion could be made.

After combining the precipitates with the desiccated solutions, the samples were placed in a temperature controlled bath (25°C) to prevent excessive dissolution or precipitation. The samples were not stirred so that the crystals would not abrade or change surface area substantially. The reaction time for the sorption studies was five days, and afterwards, the solutions were diluted 1:10, 1:100, 1:500, or 1:1000 depending on concentration. The precipitates were separated, reweighed, and dissolved in a manner similar to the desiccated sample salts. Boron was quantified by the azomethine-H method. Three samples for each boron concentration and pH level were used for the sorption studies. Sorption experiments were carried out for acidic and alkaline NaCl and Na_2SO_4 solutions.

Description of the partition coefficient, K_d.

The partition coefficient, K_d, is the term used to express the relative amount of boron removed from solution by the solid phase as compared to the amount in the solution. In the case of the synthetic, laboratory investigations of boron association with mirabilite or halite, the partition coefficient was expressed by

$$K_d = \frac{\left(\frac{\mu\text{moles B}}{\text{gram Mirabilite or Halite}}\right)}{\left(\frac{\text{mmoles B}}{\text{liter of } Na_2SO_4 \text{ or NaCl solution}}\right)}$$

C SALT model use for boron species and evaporite mineral predictions

Smith (1989) developed an equilibrium model that simulates the evapoconcentration of solutions and precipitation of salts in environments similar to the agricultural evaporation ponds of the San Joaquin Valley. The model simulates solution and mineralogical changes from dilute to highly evapoconcentrated solutions. By using the Pitzer equations in a similar manner as Felmy and Weare (1986) and Harvie et al. (1980), singular, binary, and tertiary ion associations are accounted for, thereby adjusting the ionic strength, pH and density of the solution. Felmy and Weare (1986) provided thermodynamic data concerning the likely boron polymer formation as well as ion pair associations in hypersaline solutions. By using these thermodynamic constants and values, C SALT incorporates boron interactions with the saline evaporation pond solutions and precipitates. Precipitation of salts is also predicted and accounted for in the calculations.

The constituents important in this study were Na^+, SO_4^{2-}, Cl^-, $B(OH)_3$, and K^+. The Na^+ and SO_4^{2-} concentrations were based on the pK_{sp} (-log K_{sp}) of thenardite at 25°C, which was 0.288 as found in the Compound.dat file. At 90% saturation, this gave a $[Na^+]$ = 1.44 moles/liter and a $[SO_4^{2-}]$ = 0.72 moles/liter. These values were used since Na_2SO_4 was dissolved in water in the anhydrous form (thenardite). For the NaCl solutions, the Na^+ and Cl^- concentrations were based on the pK_{sp} of halite

at 25°C, which was -1.570, as found in the Compound.dat file. At 90% saturation, this gave both [Na^+] and [Cl^-] = 5.49 moles/liter. **Table 13** lists the ion concentrations used for C SALT, as well as the concentration factors. These evapoconcentration factors were based on preliminary data not reported in this study, yet they accurately approximate the desiccation experiments.

The results of the calculations by C SALT indicate that the model under-predicted the amount of mirabilite precipitation, especially for boron concentrations above 2.0 mM. The input values for the Na^+ and SO_4^{2-} may be too low, since the values were determined by the thenardite calculations. If the K_{sp} (1.288) for mirabilite was used, the value of Na^+ and SO_4^{2-} would be much lower, 0.78 *M* for Na^+ and 0.39 *M* for SO_4^{2-}.

TABLE 13.

Input data for C SALT calculations.

	Concentration (*M*)						
Sample	Na^+	SO_4^{2-}	K^+	$B(OH)_3$	Cl^-	ECF	pH
Na_2SO_4 alk							
2.00 m*M* B	1.44	0.72	0.023	0.002	-	4.29	10.0
10.00 m*M* B	1.44	0.72	0.034	0.010	-	4.54	10.0
50.0 m*M* B	1.44	0.72	0.066	0.050	-	4.63	10.0
100.0 m*M* B	1.44	0.72	0.115	0.100	-	3.77	10.0
Na_2SO_4 acid							
2.00 m*M* B	1.44	0.72	-	0.002	0.015	3.48	2.7
10.00 m*M* B	1.44	0.72	-	0.010	0.013	4.12	2.7
50.0 m*M* B	1.44	0.72	-	0.050	0.013	3.66	2.7
100.0 m*M* B	1.44	0.72	-	0.100	0.013	3.82	2.7
Na_2SO_4 alk							
100 m*M* B	1.452	0.72	-	0.100	-	1 - 8	10.0
NaCl alk							
2.00 m*M* B	5.49	-	0.042	0.002	5.49	2.39	10.0
10.00 m*M* B	5.49	-	0.050	0.010	5.49	2.23	10.0
50.0 m*M* B	5.49	-	0.088	0.050	5.49	2.35	10.0
100.0 m*M* B	5.49	-	0.134	0.100	5.49	2.34	10.0
NaCl acid							
2.00 m*M* B	5.49	-	-	0.002	5.49	2.44	3.0
10.00 m*M* B	5.49	-	-	0.010	5.49	2.23	2.3
50.0 m*M* B	5.49	-	-	0.050	5.49	2.33	2.4
100.0 m*M* B	5.49	-	-	0.100	5.49	2.37	2.3

Output from initial and evapoconcentrated solutions.

The results of evapoconcentrating alkaline Na_2SO_4-B solutions are shown in **table 14** The calculated values for boron species neglected the ion pair $NaB(OH)_4^\circ$, which would likely be a major species for boron at high pH levels and high Na^+ concentrations. C SALT was not fully developed for boron speciation, especially ion pairs. The change in boron species for alkaline Na_2SO_4-B solutions is evident as the concentration factors increase. The higher boron concentrations in these solutions promotes the formation of the $B_4O_5(OH)_4^{2-}$ polymer, which is a likely precurser for borax formation.

The change in boron species for acidic Na_2SO_4-B solutions is not as dramatic as for the alkaline solutions (**table 15**). The monomer, $B(OH)_3$, remains essentially at 100% of the boron species regardless of initial concentration or evapoconcentration. Boron concentrations for NaOH-pH adjusted Na_2SO_4-B solutions with increasing evapoconcentration factors tend toward the $B(OH)_4^-$ monomer, the $B_4O_5(OH)_4^{2-}$ polymer, and borax (**Figure 28**). The $B_3O_3(OH)_4^-$ polymer is lower in concentration than the $B(OH)_3$ monomer. This indicates that $B_3O_3(OH)_4^-$ polymer formation is not favored in alkaline Na_2SO_4-B solutions.

There is a substantial difference in the prediction of polymer formation with the halite solutions. The desiccation of the NaCl solutions created halite precipitate, which is more dense and takes up less volume than mirabilite. Consequently, the remaining volume at the end of desiccation is mainly the solution, and not the precipitate. Thus, the evapoconcentration factors for the NaCl-halite samples were never greater than 3.0, with most being under 2.5. This may not give the alkaline, high boron solutions enough evapoconcentration to form significant amounts of boron polymers. The main boron species for the alkaline-NaCl solutions was $B(OH)_4^-$, which remained above 90% for all treatments and all evapoconcentration factors used (**table 16**). Similarly, the monomer of $B(OH)_3$ was the dominant form of boron for all desiccations of acidic NaCl solutions (**table 17**). Therefore, polymer formation for the NaCl-B systems was not significant for any of the studies performed.

TABLE 14.

C SALT predicted molar concentrations of boron species in solution during desiccation of alkaline 90%-saturated Na_2SO_4-B solutions.

$[B]_i$	ECF	$B(OH)_3$	$B(OH)_4^-$	$B_3O_3(OH)_4^-$	$B_4O_5(OH)_4^{2-}$
2.00 m*M*	1.00	1.175E-4	1.886E-3	1.160E-9	8.065E-11
	4.29	7.129E-4	6.989E-3	3.279E-7	2.867E-7
10.0 m*M*	1.00	5.891E-4	9.427E-3	1.458E-7	5.068E-8
	4.54	3.893E-3	3.468E-2	5.906E-5	3.159E-4
50.0 m*M*	1.00	2.941E-3	4.691E-2	1.816E-5	3.198E-5
	4.63	1.071E-2	8.892E-2	1.127E-3	2.236E-2
100.0 m*M*	1.00	5.788E-3	9.177E-2	1.381E-4	4.877E-4
	3.77	1.277E-2	1.233E-1	1.441E-3	6.567E-3
				*Borax :	3.021E-1

TABLE 15.

C SALT predicted molar concentrations of boron species in solution during desiccation of acidic 90%-saturated Na_2SO_4-B solutions.

$[B]_i$	ECF	$B(OH)_3$	$B(OH)_4^-$	$B_3O_3(OH)_4^-$	$B_4O_5(OH)_4^{2-}$
2.00 m*M*	1.00	1.999E-3	1.381E-9	3.032E-13	7.513E-21
	3.48	6.713E-3	4.616E-9	1.251E-11	2.308E-18
10.0 m*M*	1.00	1.000E-2	6.91E-9	3.809E-11	4.715E-18
	4.12	3.960E-2	2.693E-8	2.72E-9	3.228E-15
50.0 m*M*	1.00	5.012E-2	3.48E-8	4.896E-9	3.038E-15
	3.66	1.736E-1	1.131E-7	3.011E-7	2.205E-12
100.0 m*M*	1.00	1.006E-1	7.025E-8	4.057E-8	5.052E-14
	3.82	3.642E-1	2.501E-7	3.474E-6	6.898E-11

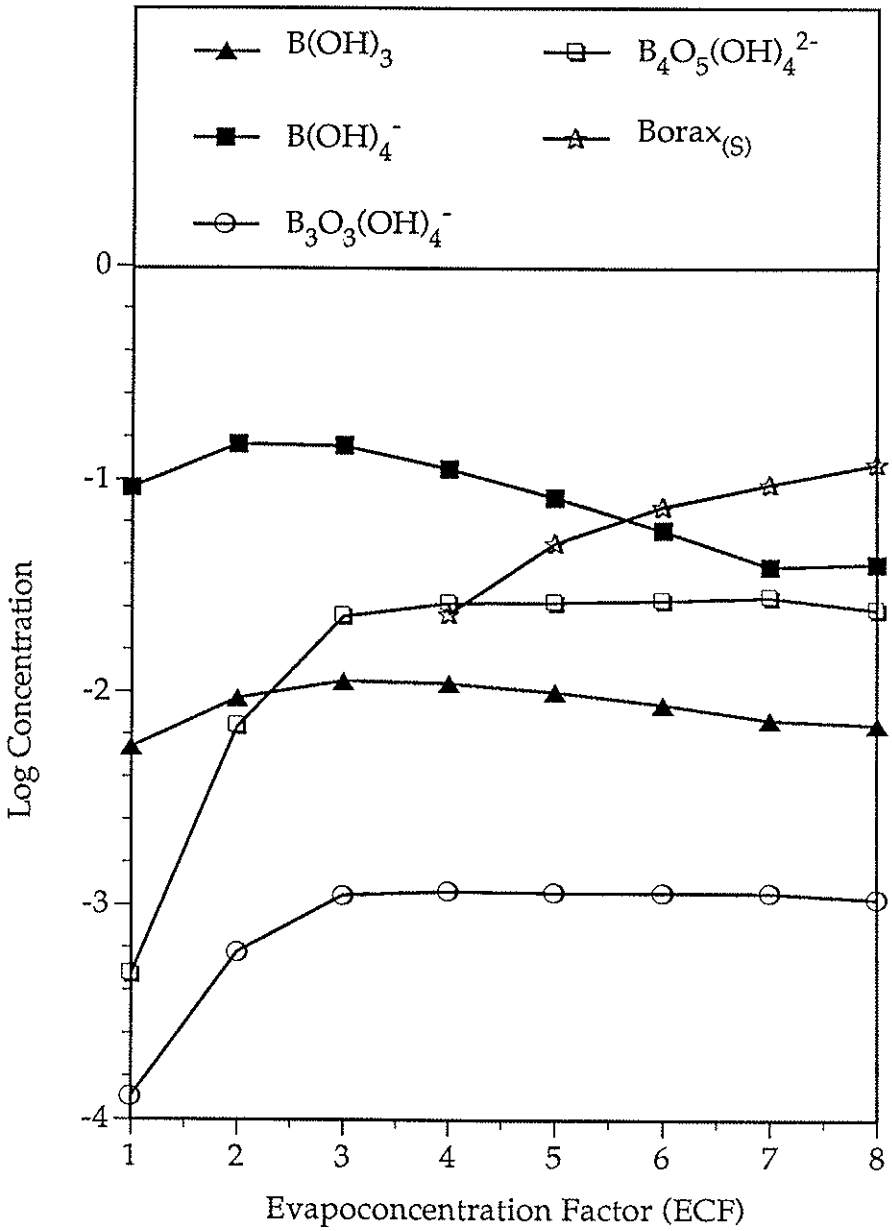

Figure 28. Changes in C SALT predicted boron species during desiccation of an alkaline, 100 mM B - sodium sulfate solution.

TABLE 16

C SALT predicted molar concentration of boron species in solution during desiccation of alkaline 90%-saturated NaCl-B solutions.

$[B]_i$	ECF	$B(OH)_3$	$B(OH)_4^-$	$B_3O_3(OH)_4^-$	$B_4O_5(OH)_4^{2-}$
2.00 m*M*	1.00	5.435E-5	2.093E-3	1.089E-10	1.751E-11
	2.39	1.310E-4	5.01E-3	1.439E-9	5.645E-10
10.0 m*M*	1.00	2.727E-4	1.046E-2	1.372E-8	1.101E-8
	2.23	6.142E-4	2.337E-2	1.48E-7	2.698E-7
50.0 m*M*	1.00	1.386E-3	5.228E-2	1.779E-6	7.053E-6
	2.35	3.335E-3	1.223E-1	2.296E-5	2.148E-4
100.0 m*M*	1.00	2.814E-3	1.041E-1	1.473E-5	1.148E-4
	2.34	6.592E-3	2.330E-1	1.722E-4	3.030E-3

TABLE 17

C SALT predicted molar concentration of boron species in solution during desiccation of acidic 90%-saturated NaCl - B solutions.

$[B]_i$	ECF	$B(OH)_3$	$B(OH)_4^-$	$B_3O_3(OH)_4^-$	$B_4O_5(OH)_4^{2-}$
2.00 m*M*	1.00	2.146E-3	8.48E-9	6.901E-13	4.325E-19
	2.44	5.247E-3	2.128E-8	9.751E-12	1.593E-17
10.0 m*M*	1.00	1.074E-2	8.47E-9	1.729E-11	1.08E-17
	2.23	2.401E-2	1.944E-8	1.877E-10	2.786E-16
50.0 m*M*	1.00	5.385E-2	5.365E-8	2.787E-9	1.091E-14
	2.33	1.263E-1	1.293E-7	3.583E-8	3.429E-13
100.0 m*M*	1.00	1.081E-1	8.59E-8	1.826E-8	1.129E-13
	2.37	2.593E-1	2.119E-7	2.595E-7	3.912E-12

RESULTS AND SIGNIFICANCE OF BORON STUDIES

Desiccation of Na_2SO_4-B solutions.

In the first series of experiments, the Na_2SO_4-B solutions were acidified with the same amounts of 1.0 *M* HCl, regardless of the concentration of boron, since boron's buffer range is between pH 8.0 and 11.0. The pH of the samples remained below 3.0 during the entire experiment. The samples were desiccated so that the ECF was between 2.7 to 4.1, depending on the amount evaporated, the weight of the wet mirabilite (and subsequent volume), and the milliliters of solution remaining. The ECF was calculated by

$$ECF = \frac{100\ mL}{100\ mL - Amt.\ Evap - \frac{Mirabilite\ wt.}{1.464\ g/cm^3}}$$

where the density of mirabilite is 1.464 g/cm^3 (CRC Handbook of Chemistry and Physics, 1982-83). The amount evaporated was determined by sample weight loss before separation of the precipitate from the solution, and was assumed to be due to pure H_2O loss, with a density of 1 g/cm^3. Thus, the numerator 100 mL is the solution volume before HCl addition and desiccation, and the denominator is the calculated solution volume remaining after desiccation. The mean and standard deviation for the calculated partition coefficient, K_d, is indicated in **Figure 29**. The designation for K_d in the desiccation experiments was $K_{d(cso)}$. This is in contrast for the later described K_d from the sorption experiments $K_{d(s)}$.

The second set of desiccation experiments with Na_2SO_4 were performed under alkaline conditions. Variable amounts of 0.871 *M* KOH were added, depending on the boron concentration, to bring the pH of all samples to 12.0. During the subsequent desiccation, the pH dropped most rapidly in the samples containing the least amount of boron. For the 2.0 m*M* B samples, the pH dropped to 9.6 after 7 days of desiccation. The pH dropped to 9.7, 10.1, and 10.4 for 10.0, 50.0, and 100.0 m*M* B samples, respectively. This is due to the buffering ability of boron in solutions. Nevertheless, the main form of boron in solution with pH > 9.0 is $B(OH)_4^-$, with smaller amounts of $NaB(OH)_4^\circ$ ion pair and boron polymers. The evapoconcentration factors for the alkaline study ranged from 2.37 to 3.37.

The results of the desiccation experiment indicate a fairly consistent value of $K_{d(cso)}$, which is slightly higher for the alkaline samples than it was for the acidic samples **(Figure 30)**. The lower standard deviations for the alkaline samples reflects a more well-behaved system or the technique for sample preparation and boron quantification became more refined than with the acidic samples.

Post - desiccation, sorption experiments with Na_2SO_4 (mirabilite) - B.

The K_d for the sorption experiments of the acidic and alkaline Na_2SO_4 samples are shown in **Figures 29 and 30**, respectively. The amount of boron in the solid phase was determined by direct measurement of boron in a dissolved subsample of mirabilite and using the final weight of the mirabilite samples after sorption to correct for any dissolution or precipitation during the experiment. The acidic mirabilite samples lost on average 10.53% of their original weight, while the alkaline mirabilite samples lost on average 26.59% of their original weight.

The sorption of boron was plotted against the initial boron concentration in order to view retention relationships. The acidic boron-mirabilite system shows a linear increase in boron removed as compared to initial boron concentrations **(Figure 31).** The alkaline boron-mirabilite system, on the other hand, seems to show a leveling off of boron removed from the solution phase with concentrations greater than 150 mM **(Figure 32).** The error bars represent one standard deviation of the triplicate samples for the boron concentration in the solid phase (y-direction) and in the initial solution phase (x-direction). The initial solution phase was measured for each triplicate sample, and the variation was caused by differences in the prior evapoconcentration of the desiccation experiments.

Discussion of Na_2SO_4 -mirabilite-B results.

The determination of the partition coefficient (K_d) for the coprecipitation-sorption-occlusion (CSO) and the sorption (S) experiments was an attempt to discriminate between these processes using wet chemical-solution principles. The sorption experiments included adsorption along with absorption. Occlusion was thought to happen only when the precipitates conglomerated, trapping solution in the voids between the particles. The CSO experiments were carried out under near equilibrium conditions. The sorption experiments were likely not as close to equilibrium, since the boron-free salts were grown under conditions different than the coprecipitation experiments.

For the acidic Na_2SO_4-mirabilite-B samples, the value for the partition coefficient was around 0.05 to 0.08, regardless of the experiment **(Figure 29)** and the sorption isotherm was linear with respect to initial boron concentrations **(Figure 31).** The initial boron concentrations for the sorption experiments averaged 7.0, 34, 146, and 297 m*M* B. The sorption isotherm **(Figure 31)** indicates that, at these concentrations, sorption of boron by mirabilite in acidic Na_2SO_4 solutions is rapid (occurring within the 5-day time span), due to the linear increase with boron concentration. This sorption is likely not differentiable from the coprecipitation or occlusion. Mirabilite is highly hydrated, and according to Walton (1967), this allows for rapid equilibrium of microcomponents in the precipitate with the solution microcomponents by diffusion. Yet, there are limits to this equilibrium. If the $B(OH)_3$ is part of the crystal structure of mirabilite (i.e., substituting for SO_4^{2-}, Na^+, or a structural H_2O), this diffusion-equilibrium process will take place over extended periods of time. If the $B(OH)_3$ resides in the crystal crevasses or structural defect regions, exchange with solution $B(OH)_3$ is probably more

rapid. Adsorption followed by absorption are the likely dominant mechanisms for $B(OH)_3$ uptake with mirabilite. It is not likely that $B(OH)_3$ is exchanged for structural SO_4^{2-}.

The alkaline mirabilite-B samples showed similar behavior as the acidic counterparts. Yet, the value of $K_{d(cso)}$ for the alkaline CSO study was slightly greater than the acidic samples. The $K_{d(cso)}$ values for the alkaline samples were consistently about 0.01 units greater than the acidic samples, indicating another possible, different mechanism of boron uptake. These differences may be meaningful, since the standard deviations for both data sets were low. This slight increase in $K_{d(cso)}$ may be due to minor amounts of coprecipitation or exchange of $B(OH)_4^-$ for SO_4^{2-} in the mirabilite lattice. The borate ion, $B(OH)_4^-$, is similar in size to SO_4^{2-}, and both are anionic and tetrahedral in shape. Sulfate (SO_4^{2-}) has a diameter of 2.3 Å (CRC Handbook of Chemistry and Physics, 1982-83), which is very similar to that calculated for borate based on the tetrahedral B-O bond distance of 1.48 Å (Ross and Edwards, 1967.). This increases the possibility of substitution, and distortion to the crystal structure is minimal. Yet, the ionic charges are different, and the net charge balance in the crystal is disrupted.

The K_d values for the CSO study of the alkaline mirabilite system are fairly consistent over the boron concentrations used **(Figure 30).** They range from 0.069 to 0.085, with only the slightest increasing trend from low to high boron levels. The main form of boron during mirabilite crystal growth during desiccation is $B(OH)_4^-$ for all boron concentrations. Another important form of boron under alkaline conditions is the ion pair, $NaB(OH)_4^\circ$ (Bloesch et al., 1987). The ECF of the samples ranged between 2.37 to 3.37, which makes boron polymer formation minor in the 2 m*M* B and 10 m*M* B samples throughout desiccation and in the 50 m*M* B and 100 m*M* B samples at the beginning of desiccation. As desiccation proceeds, the 50 m*M* B and 100 m*M* B samples have increasing amounts of boron polymers. Yet, during most of the evapoconcentration sequence, the monomer, $B(OH)_4^-$, is the predominant species, as indicated by C SALT calculations. These calculations showed that desiccating 100 mM B in alkaline, Na_2SO_4 solutions did not produce significant boron polymers until an ECF > 3. For lower boron concentrations, polymer formation is even more unlikely. The ion pair, $NaB(OH)_4^\circ$, may also be present in sizable quantities.

The sorption experiments for the alkaline mirabilite system, on the other hand, used the desiccated solutions with fresh, boron-free mirabilite. These samples were highly concentrated in boron relative to the desiccation samples during evapoconcentration. The 2 m*M* B and 50 m*M* B samples had similar values for K_d in both the CSO and sorption studies, whereas the 100 m*M* B samples had a noticeably lower $K_{d(s)}$ than $K_{d(cso)}$ **(Figure 30).** The 10 m*M* B samples had slightly lower values of $K_{d(s)}$ than $K_{d(cso)}$. The sorption isotherm data **(Figure 32)** also reflect the general trends of the $K_{d(s)}$. As the initial boron concentrations increased, the amount of boron removed tended to level off at concentrations greater than 150 m*M*. The sorption samples used the desiccated solutions, which started with boron

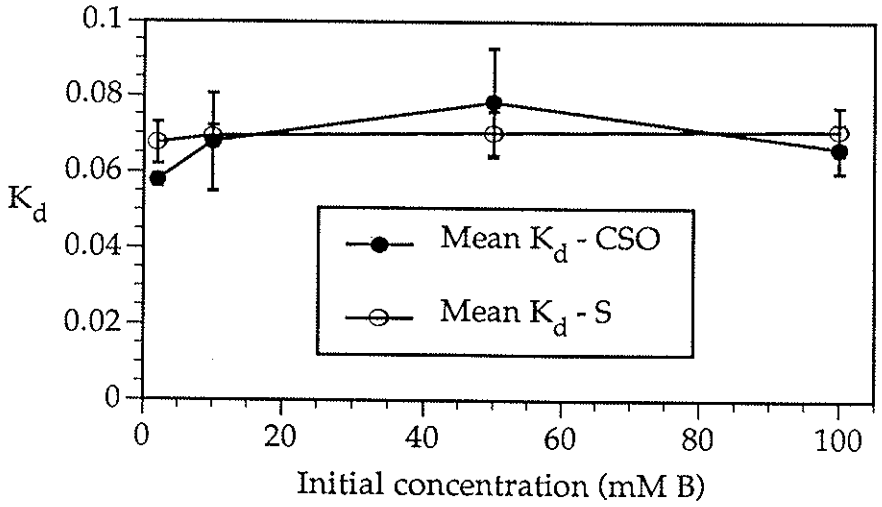

Figure 29. Partition coefficient (Kd) dependence on boron retention processes for acidic sodium sulfate-mirabilite samples. CSO=coprecipitation-sorption-occlusion; S = sorption.

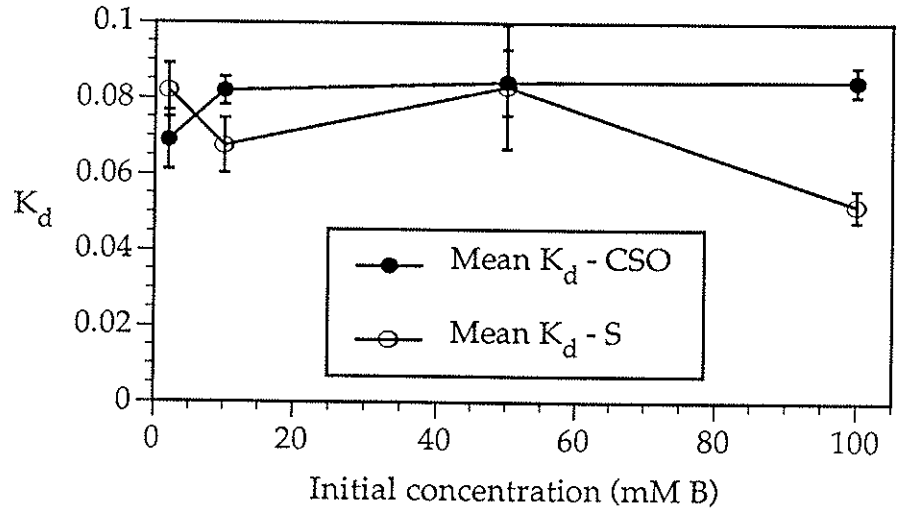

Figure 30. Partition coefficient (Kd) dependence on boron retention processes for alkaline sodium sulfate-mirabilite samples. CSO=coprecipitation, sorption, occlusion; S = sorption.

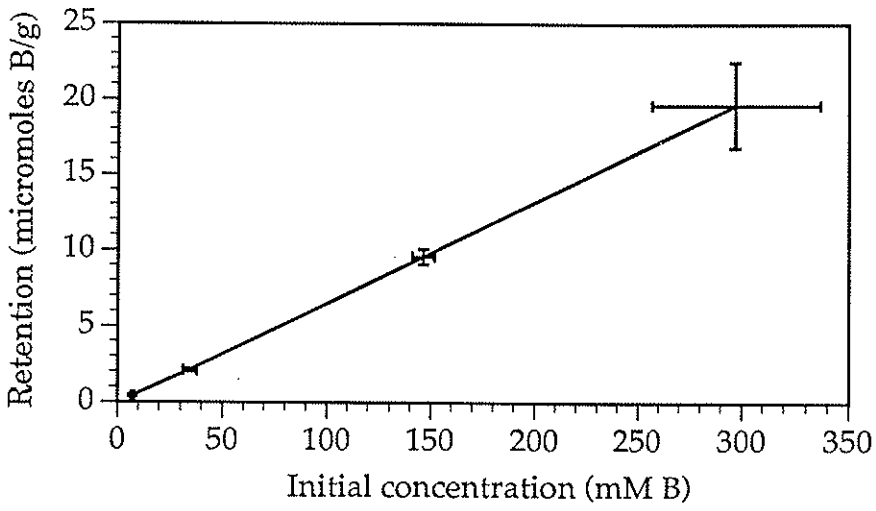

Figure 31. Boron sorption with acidic mirabilite.

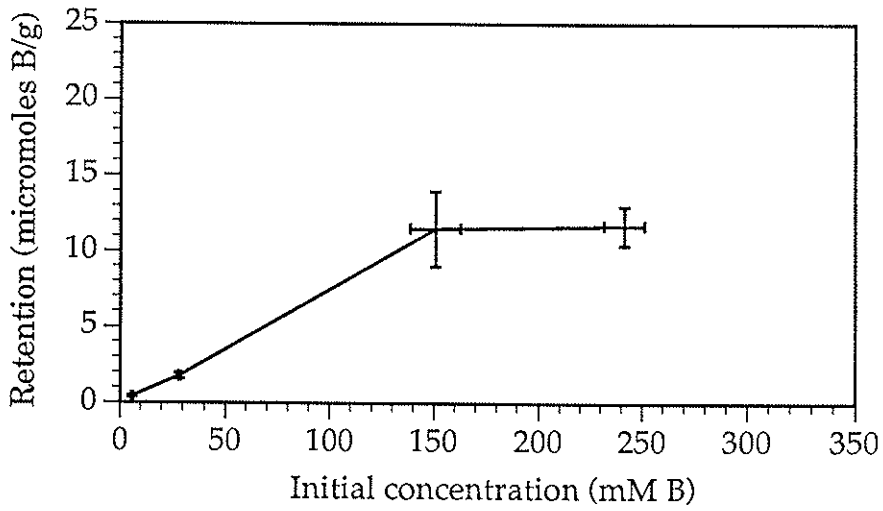

Figure 32. Boron sorption with alkaline mirabilite.

concentrations of about 6, 28, 150, and 241 m*M*, for the 2, 10, 50, and 100 m*M* B labelled samples, respectively.

The sorption results for the alkaline mirabilite system indicate that, especially for the 100 m*M* B samples, the degree of retention is lower than for the CSO desiccation results. The 50 m*M* B samples had very similar values of K_d for both experiments. This may be due to the high concentration of $B(OH)_4^-$, even though some polymers may be present. The retention is then dependent on mainly $B(OH)_4^-$, similar to the 2 m*M* B and 10 m*M* B samples. In the 100 m*M* B sorption samples, the polymers may be so predominant that borax could form. The polymers may diminish the $B(OH)_4^-$ sorption driving potential enough that, within 5 days, equilibrium is not reached for $K_{d(s)}$ to equal $K_{d(cso)}$. The polymers may also be excluded by charge repulsion from the potentially negative surface charge of mirabilite. The large size of the polymers would likely prevent any polymer incorporation into the mirabilite structure. Yet, polymer association with mirabilite by hydrogen bonding and van der Waal's attraction cannot be ruled out. Nevertheless, with less $B(OH)_4^-$ present compared to total boron (monomers and polymers), $K_{d(s)}$, which relies on monomers, may not be equal to $K_{d(cso)}$. Three boron sorption scenarios with mirabilite are depicted in **Figure 33.**

The importance of the ion pair, $NaB(OH)_4^\circ$, which may form whenever $B(OH)_4^-$ and high Na^+ are present, is not well known for the alkaline CSO or sorption experiments with mirabilite. It probably adsorbs by hydrogen bonding with surface H_2O and SO_4^{2-}, but it is likely to be excluded from absorbing into the mirabilite crystals. The sodium-borate ion pair most likely will not compete with $B(OH)_4^-$ for exchange of SO_4^{2-}- lattice sites. It is assumed to have no significant effect when compared to the acidic CSO or sorption experiments, since both $B(OH)_3$ and $NaB(OH)_4^\circ$ are neutral species.

Desiccation of NaCl - B solutions.

The NaCl (halite) desiccation samples were run with four replicates for each initial boron concentration at both acidic and alkaline pH values. Three of the sample precipitates were heated in the oven at 120°C for 2 hours to drive off any excess water after filtration, and thus were not used for determination of $K_{d(CSO)}$. The fourth precipitate was placed in a sealed vessel to prevent drying prior to XRD analysis. It was this fourth sample that was used for boron quantification in the solid phase, and therefore comparisons with replicates were not possible. The ECF was calculated in a similar manner as the mirabilite (Na_2SO_4) samples by the equation:

$$ECF = \frac{100\ mL}{100\ mL - Amt.\ Evap. - \frac{wt.\ halite}{2.165\ g/cm^3}}$$

with the density of halite being 2.165 g/cm^3. It was assumed that little or no excess surface water interfered with the ECF determinations, since halite weight measurements were not significantly

ACIDIC SODIUM SULFATE - MIRABILITE SOLUTIONS,
ALL BORON CONCENTRATIONS.

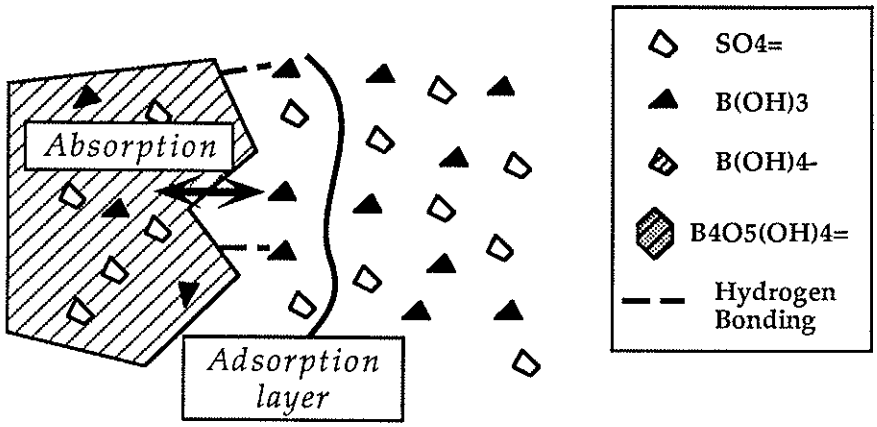

ALKALINE SODIUM SULFATE- MIRABILITE SOLUTIONS,
LOW BORON CONCENTRATIONS.

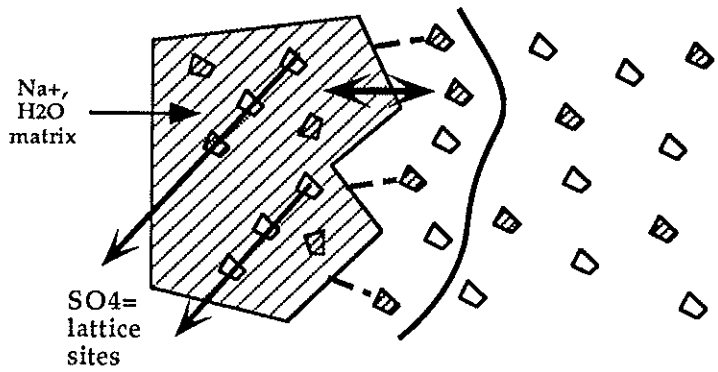

ALKALINE SODIUM SULFATE - MIRABILITE SOLUTIONS,
HIGH BORON CONCENTRATIONS.

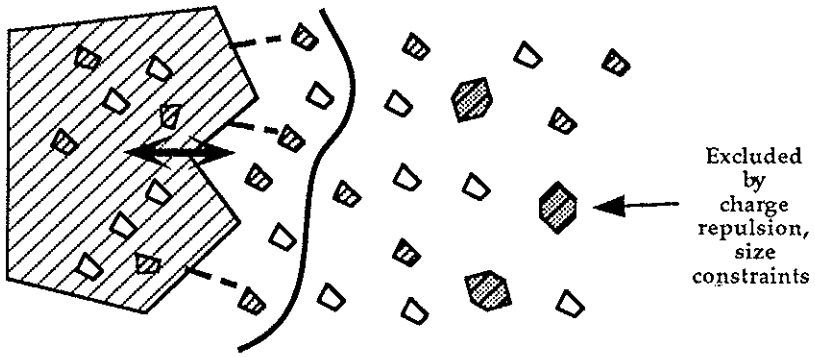

Figure 33. Sorption scenarios of boron with mirabilite.

different if moist or dried. The ECF was calculated to be between 2.2 and 2.5, and these values were used in C SALT input files.

The first set of NaCl desiccation experiments was performed under acidic conditions using HCl to adjust the pH to 3.0. Each sample had the same amount of acid added due to the inability of boron to buffer at low pH, and each of the samples in the different boron concentrations had a pH during desiccation between 2.6 to 3.0. The desiccation produced, on average, small, 2 mm-sized precipitates of halite that were cubic in form. Occasionally, the crystals would be larger in size, up to 10 mm in thickness. There was never any significant conglomeration as with the mirabilite precipitates. The calculation of K_d was done with only one replicate sample - that of the saved precipitate and its solution **(Figure 34)**. The lower boron concentration samples tended to have higher values of $K_{d(cso)}$ (about 0.08) while the higher concentrations had lower values (0.06). It appears that the average value of $K_{d(cso)}$ **(Figure 34)**, which is around 0.07, is similar to that of the acidic Na_2SO_4 (mirabilite) samples **(Figure 29)**. This may indicate similar boron uptake mechanisms.

The second set of NaCl - desiccation experiments was done under alkaline conditions using KOH to adjust the pH. Once again, different amounts of KOH were required to bring the samples to pH 12.0 due to the buffering ability of increasing amounts of boron. The value of $K_{d(cso)}$ was determined and found to be less (0.06), on average, than that of the acidic samples (0.07) **(Figure 35)**. As with the acidic samples, there was only one sample per data point, and the standard deviation could not be determined.

Post - desiccation, sorption experiments with NaCl (halite) - B.

The determination of $K_{d(s)}$ for the halite sorption samples was done in the same manner as the desiccation studies. The solutions and precipitates at the end of the experiment were measured for boron concentration by the azomethine-H method. The values of $K_{d(s)}$ are very similar regardless of the pH conditions **(Figures 34 and 35)**. Compared to the $K_{d(cso)}$, the acidic halite $K_{d(s)}$ is less for the low boron concentrations, but almost the same for the higher boron concentrations **(Figure 34)**. When comparing the two studies, it must be kept in mind that each of the desiccation results represent only one sample per data point. The alkaline halite sorption results tend to follow the desiccation results a little more closely **(Figure 35)**.

The sorption of boron onto halite was also plotted as boron removed versus initial concentrations **(Figures 36 and 37)**. The initial concentrations for the acidic sorption samples averaged 5, 24, 119, and 229 m*M* B, and the alkaline sorption samples averaged 5, 24, 128, and 229 m*M* B. As described for the sorption of boron with mirabilite, the error bars for figures 6.6.1 and 6.6.2 indicate one standard deviation for the measured boron concentration in the solid phase (y-direction) and for the measured boron concentration in the initial sorption solution (x-direction).

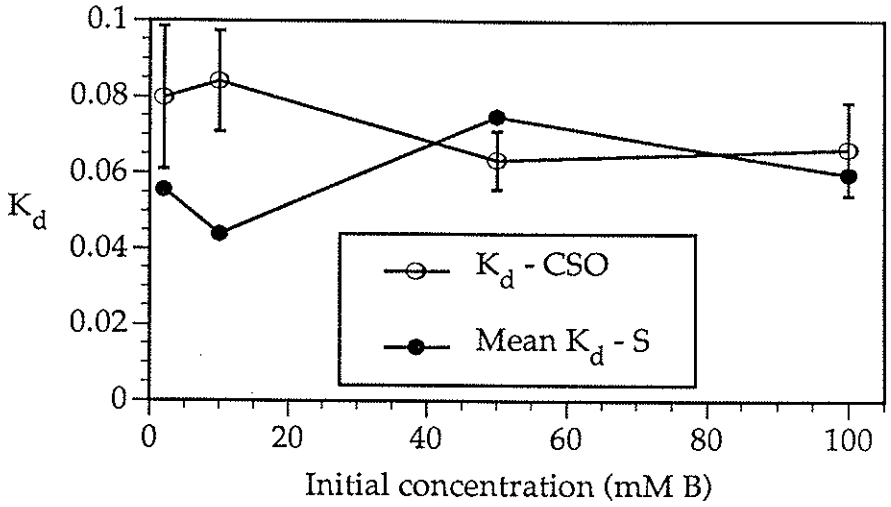

Figure 34. Partition coefficient (Kd) dependence on boron retention processes for acidic sodium chloride-halite samples. CSO = coprecipitation-sorption-occlusion; S = sorption.

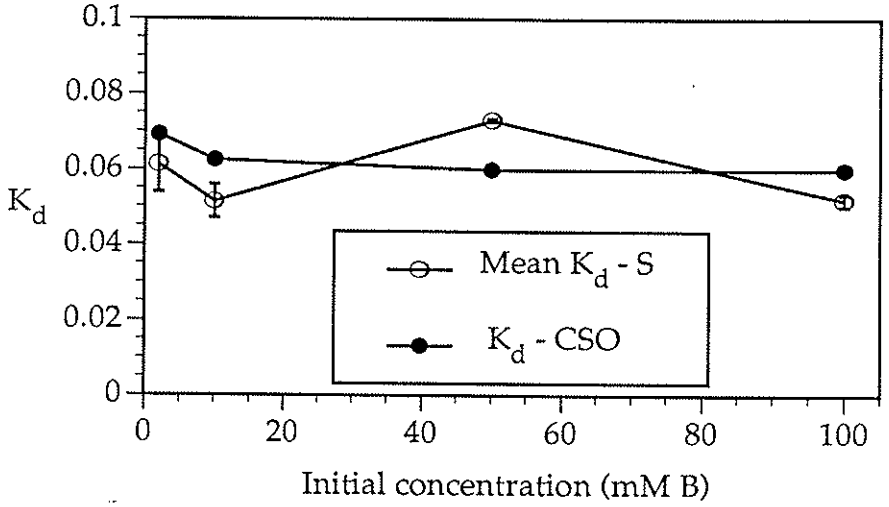

Figure 35. Partition coefficient (Kd) dependence on boron retention processes for alkaline sodium chloride-halite samples. CSO = coprecipitation, sorption, occlusion; S = sorption.

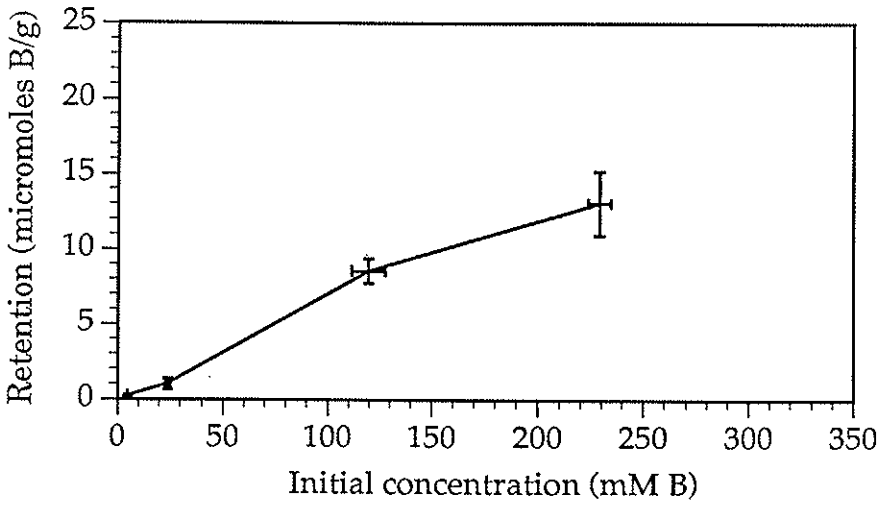

Figure 36. Boron sorption with acidic halite.

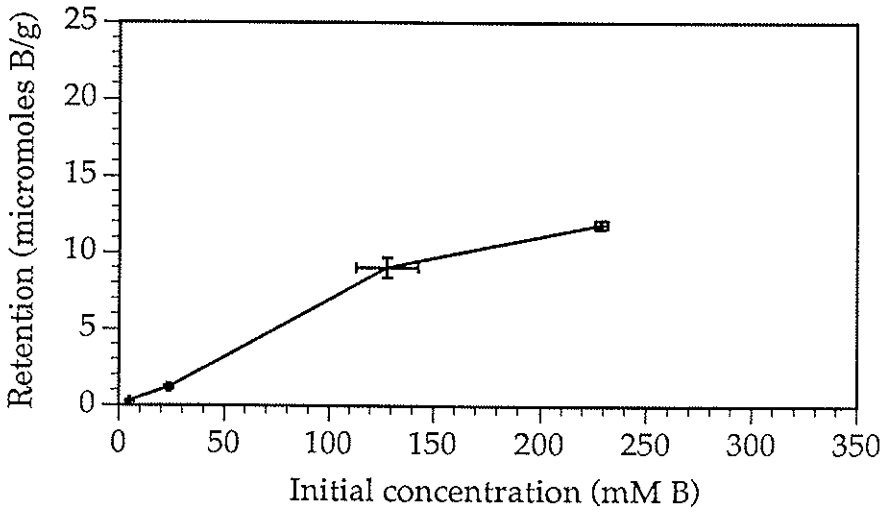

Figure 37. Boron sorption with alkaline halite.

Discussion of NaCl (halite)-B results.

The values of $K_{d(cso)}$ for the acidic NaCl samples were between 0.063 to 0.084 **(Figure 34)**. Since only one sample per data point was used for the $K_{d(cso)}$, it may not be as accurate as the $K_{d(s)}$, which had three replicate samples per data point. The $K_{d(s)}$ was lower than $K_{d(cso)}$ for low B concentrations, but approximately similar for the two higher B concentrations. These differences are likely not significant.

The prediction of boron species by C SALT in the NaCl-halite system shows that polymer formation is much less important than in the Na_2SO_4-mirabilite system, mainly because of the lower ECF values for the NaCl-halite system. Therefore, the main species are $B(OH)_3$ and $B(OH)_4^-$ for the acidic and alkaline NaCl solutions, respectively.

Because the $K_{d(cso)}$ and $K_{d(s)}$ are similar, it appears that $B(OH)_3$ reacts with halite mostly by sorption. The sorption study used the desiccated solutions for initial boron concentrations, and the sorption isotherms indicate a non-linear increase in uptake with an increase in initial boron concentrations **(Figure 36)**. Adsorption is probably the dominant sorption process, since halite is not well hydrated like mirabilite. This will deter the absorption or diffusion of boron into the halite structure. In an aqueous solution, halite has the Cl^- anions shifted toward the surface to decrease surface energy (Walton, 1967). With a slight negative charge at the surface, the Na^+ in solution, being hydrated as $[Na(H_2O)_6^+]$, will migrate and sorb to this negative surface. By having this hydrated-Na^+ layer surrounding the halite, the water molecules around the Na^+ may be oriented for sufficient periods of time to optimize hydrogen bonding with $B(OH)_3$. It may also produce a diffuse layer of positive charge surrounding the halite, which may affect ionic interaction. Yet, the diffuse double layer is likely to be very small due to the high ionic strength of the saturated solution. The sorption isotherm **(Figure 36)** may indicate a saturation of the adsorption sites once the concentrations increase above 100 m*M*.

The alkaline NaCl (halite) CSO and sorption studies showed relatively similar values of $K_{d(cso)}$ as boron concentration increases, with all values falling between 0.052 to 0.073 **(Figure 35)**. The CSO samples were lower than the acidic CSO samples, possibly indicating a slight repulsion of $B(OH)_4^-$ by the negatively charged halite surface due to Cl^- ion shifting. Coprecipitation appears to not be an important process in the CSO study. The $B(OH)_4^-$ is similar in charge to Cl^-, but is too large (2.3 Å) to easily substitute for Cl^- (1.81 Å) in the halite lattice.

The sorption isotherm for the alkaline halite system again shows a similar decrease from the linear relationship as boron concentration increases above 100 m*M* **(Figure 37)**. This may indicate a sufficient saturation of surface adsorption sites on the halite crystals to reduce the number of available sites for adsorption.

The relative importance of Cl^--$B(OH)_4^-$ repulsion overriding the $[Na(H_2O)_6^+]$-$B(OH)_4^-$ attraction in the solution near the surface layer is unknown. The data suggest that the anion repulsion at the surface

layer is more dominant than the electrostatic attraction at the sorbed layer. Yet, the value of $K_{d(s)}$ for both acidic and alkaline samples is nearly identical. Thus, hydrogen bonding and possibly minor amounts of $[Na(H_2O)_6^+]$-$B(OH)_4^-$ attraction are strong enough to attract boron to the surface of halite, regardless of anion repulsion (**Figure 38**).

The formation of the ion pair, $NaB(OH)_4^\circ$, under alkaline conditions will probably decrease the Cl^--$B(OH)_4^\circ$ repulsion to some extent, due to less free $B(OH)_4^\circ$ in solution. Sorption of $NaB(OH)_4^\circ$ may be due to hydrogen bonding, as with the neutral $B(OH)_3$, or van der Waal's attraction, as with the boron polymers. Thus, $NaB(OH)_4^\circ$ will likely have little debilitating effect on sorption of boron with halite in alkaline solutions.

Precipitate drying effects on boron partitioning

With oven drying of mirabilite to thenardite, earlier experiments showed the value of $K_{d(cso)}$ increased to about 0.20 for alkaline conditions, yet was only 0.06 to 0.10 for neutral (pH 5.9 to 7.4) conditions and 0.04 to 0.05 for acidic (pH 2.7) conditions (**Figure 39**). The inrease in $K_{d(cso)}$ for the dried alkaline-mirabilite samples was a result of loss of weight by H_2O volatilization, causing a concentration of $B(OH)_4^-$ in the precipitate. With the neutral and acidic conditions, the H_2O loss was accompanied by $B(OH)_3$ volatilization, keeping the value of $K_{d(cso)}$ around the 0.06 range.

the drying of the halite precipitate does not decrease the precipitate weight to the degree of mirabilite drying, since moist halite only loses weight from the surface layer of water. The value of $K_{d(cso)}$ slightly increases with the alkaline samples, but drops with the acidic samples (**Figure 40**). This change in $K_{d(cso)}$ upon drying is analogous to the mirabilite system, alhtough not as considerable.

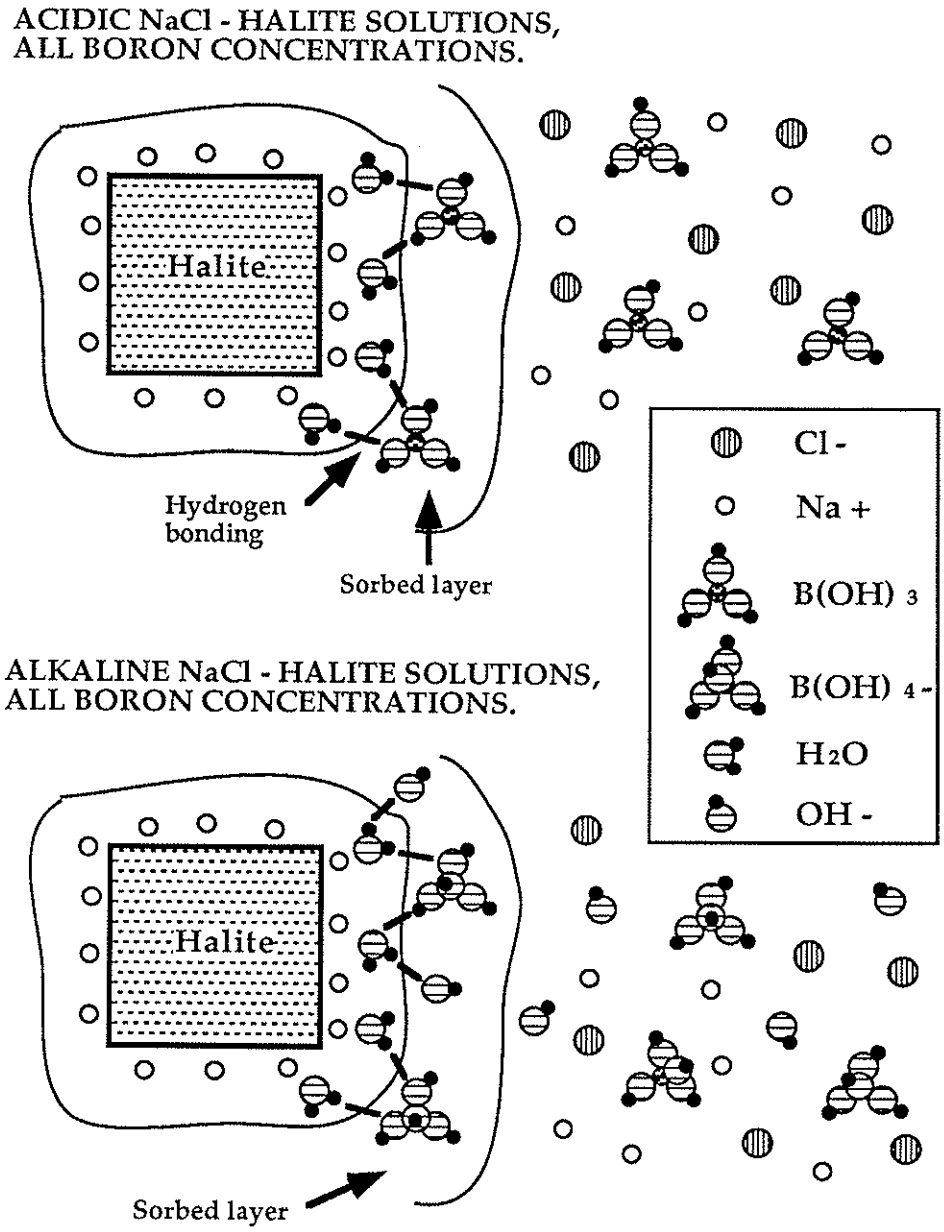

Figure 38. Adsorption scenarios of boron with halite.

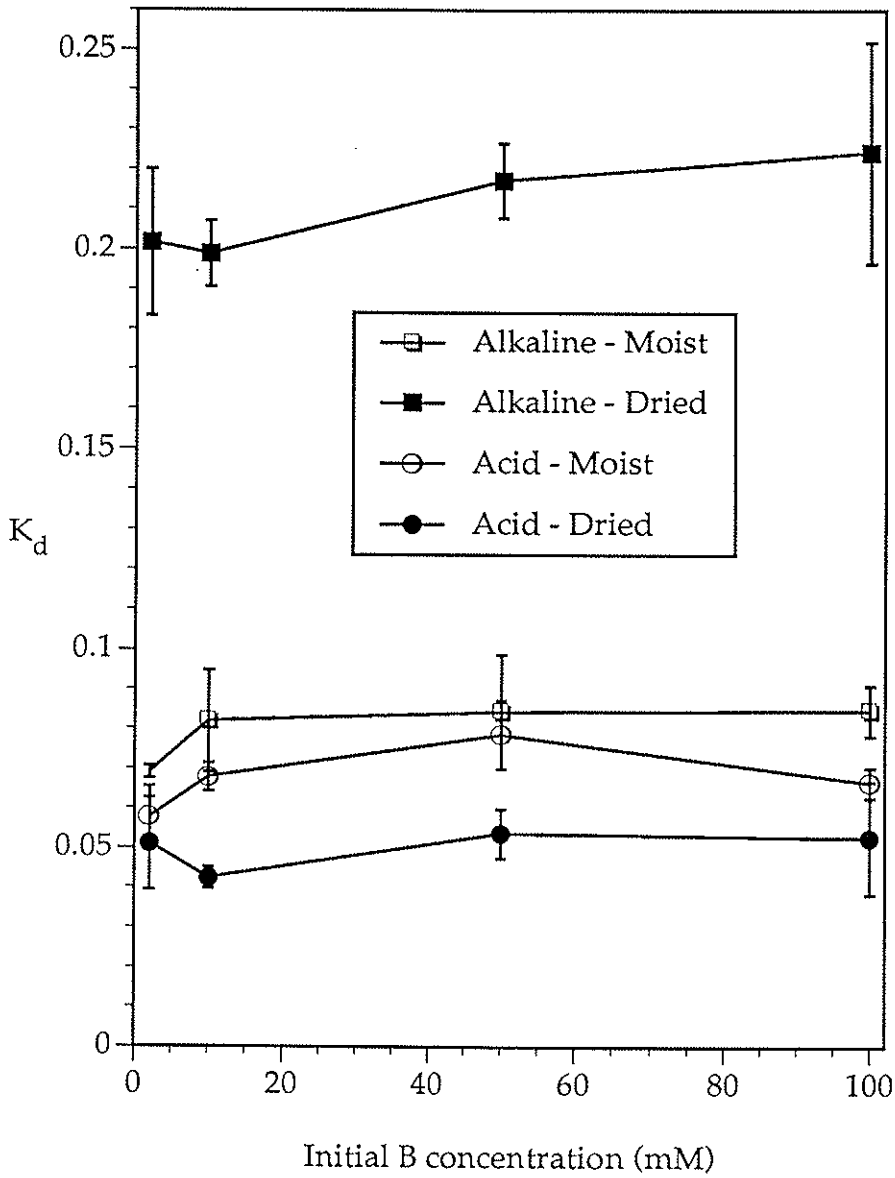

Figure 39. Partition coefficient comparison with moist or dried mirabilite from coprecipitation-sorption-occlusion (CSO) studies.

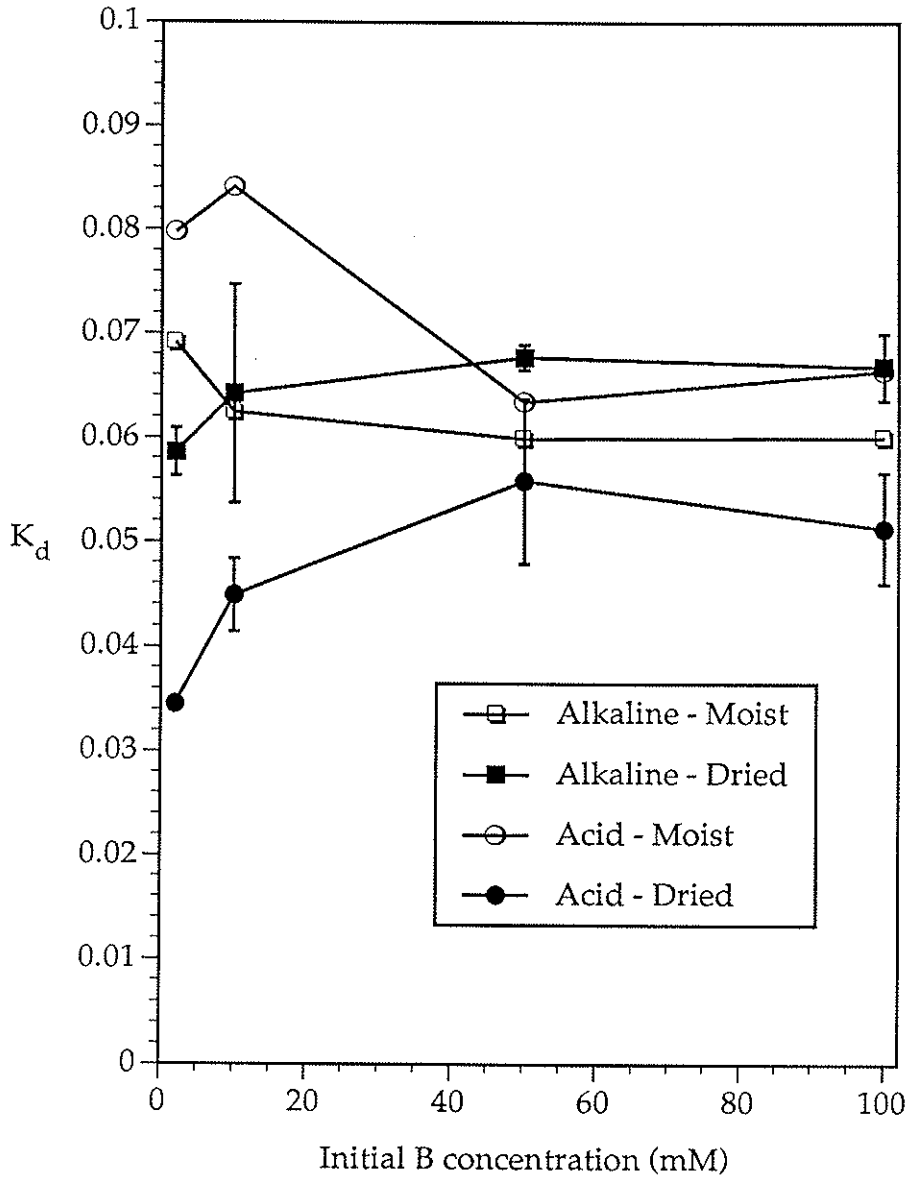

Figure 40. Partition coefficient comparison with moist or dried halite from coprecipitation-sorption-occlusion (CSO) studies.

* SUMMARY

Complex hypersaline environments, such as evaporation ponds, are not easily analyzed nor modeled by laboratory experiments. Nonetheless, a good beginning would involve a comparison to and simulation of simple systems. From this perspective, several projects were developed to address the issue of evaporite formation and the fate of selenium and boron.

The weight of salts accumulating in evaporation ponds within the San Joaquin Valley may be as high as 630,500 tons/year. This figure was derived with the assumption that all drainage water in containment would be desiccated completely.

An analysis of solute data shows that B could rapidly become excessive in pond waters. In contrast, dissipation mechanisms lower the concentrations of As, Mo and Se despite evapoconcentration. Dissolved B also behaves conservatively with respect to salinity which indicates that evaporation ponds with a series of progressively saline cells (multi-cell) will also possess a proportional range of B concentrations. In such multi-cell ponds, As dissipates to unquantifiable levels rapidly. Selenium levels also rise with salinity but the accumulation is in competition with dissipation which leads to a small but observable accumulation. The accumulation characteristics of Mo are different at the two times studied, exhibiting both rapid and slow dissipation.

Evaporites in evaporite-forming evaporation ponds may be chemically categorized into a halite group and a mirabilite/thenardite group. The salinities necessary for either group to be actively forming is so wide that these groups were found to coexist at the same pond facility in different cells. Evaporite management should accelerate desiccation of post-precipitation brines to minimize the time which enriched brines are exposed in the environment. Rate factors are important to predicting the existence of mineral phases which, in effect, reflect a quasi-equilibrium constantly adjusting to daily and seasonal changes.

Hazardous level criteria should be redefined for special application to evaporite beds. Under current hazardous waste guidelines, the evaporites in the evaporation ponds do not meet the threshold limit concentration (TLC) regarding classification as hazardous waste. The maximum amount of Se detected in evaporites was 35 mg/kg while the TLC was 100 mg/kg. The maximum B value was about 1000 mg/kg. These maximum values were found in halite-forming environments. Not all evaporites were in contact with solution. For those that were, partition coefficients were calculated. These partition coefficients describe the relative mole fractions in solid and solution. Selenium, B, As and Mo were consistently depleted in the solid phase.

Published research shows that Na_2SO_4 and Na_2SeO_4 share many chemical properties which suggest that SO_4 and SeO_4 should readily substitute for each other in the Na salt. The ternary system Na_2SO_4-Na_2SeO_4-H_2O behaves like a type III solid solution. The similarities are not as easily extended to SeO_3 and SO_4 which only share the same anionic charge. It is likely that SeO_3 acts immiscibly with SO_4 and does not participate in thenardite precipitation.

Partition coefficients for Se calculated similarly to those for the field study were calculated for an investigation of Se partitioning into mirabilite. Mirabilite was formed from seeding supersaturated Na_2SO_4 solutions. Only small quantities of SeO_3 were associated with the mirabilite while greater amounts of SeO_4 were detected. However, the solution always was enriched in Se after crystallization, and the solid and solution compositions did not reflect each other.

***Conclusions**

Trace elements in evaporite minerals from evaporation ponds.

1. Concentrations of Se, As, and B exceeded the hazardous waste limits for soluble species during the final stages of evapoconcentrations. This does not appear to be a serious problem from a wildlife and waterfowl perspective since the pools are too small to attract animal populations.

2. Concentrations of Se, As, B, and Mo in evaporite minerals do not exceed hazardous waste levels. The ultimate disposal of the evaporite minerals is therefore not complicated by high trace element concentrations.

3. Conversion of trace elements in these soluble form to those incorporated in solid-phases results in conversion of a hazardous solution to a non-hazardous solid-phase. However, environmental conditions favoring resolubilization may result in formation of a hazardous solution again.

4. In general, trace elements are excluded from evaporite minerals resulting in a solid-phase that is depleted in trace elements relative to the solution phase. As as result, management options could be developed to concentrate trace elements in the solution-phase in highly concentrated pond waters. This would leave the evaporite minerals relatively free from contamination by Se, As, B, and Mo.

5. Trace element incorporation into evaporite minerals showed no reponse to the composition of the evaporite formed or the temperature at which they formed.

6. The experimental values of $K_{d(s)}$ and $K_{d(cso)}$ for the mirabilite and halite samples are similar, ranging from 0.06 to 0.08. This may suggest that the mechanisms of B retention and uptake are similar in both experimental techniques and are mainly due to sorptive processes.

7. There are likely to be two or more uptake mechanisms for boron with mirabilite. the rapid adosprtion process occurs when the surface sorption sites are quickly filled by boron monomers, and to a lesser extent, polymers. The longer term uptake process can be attributed to sorption by boron

monomers diffusing into mirabilite through crystal defects and pathways between the conglomerated crystals, and also by the rapid exchange of the hydrated waters of mirabilite allowing boron transfer into the structure. Boron polymer formation decreases these sorptive processes, but increases the potential for precipitation of borax.

8. The retention of boron by halite is mainly by a rapid surficial, adsorptive process. It is likely that little excess sorption would occur after the initial adsorption process, since halite is not hydrated and the boric acid or borate ion do not exchange for sodium or chloride as it could with sulfate. Boron polymers may form in NaCl solutions, but will have little or no effect on boron uptake.

9. The implications of these boron laboratory investigations to evaporation pond management are that alkaline ponds (pH > 8) will have a large proportion of boron as $B(OH)_4^-$ and possibly as the polymers $B_4O_5(OH)_4^{2-}$ and $B_3O_3(OH)_4^-$. Boron in these forms will remain with the precipitates even if the ponds are completely dreid. If the salts were to be disposed, it would be most advantageous to transport dry thenardite or halite to decrease the precipitate weight. The neutral to acidic ponds (pH < 7) will have boron as $B(OH)_3$ at all concentration levels. With drying of the ponds, some of the $B(OH)_3$ will volatilize. This will decrease the boron mass in neutral to acidic, dried precipitates, especially for the mirabilite-thenardite system.

* REFERENCES

Bloesch, P.M., L.C. Bell, and J.D. Hughes. 1987. Adsorption and desorption of boron by geothite. *Aust. J. Soil Res.* 25:377-390.

Chilcott, J. E. D.W. Westcot, A.L. Toto and C.A. Enos. 1990. *Water quality in evaporation basins used for the disposal of agricultural subsurface drainage water in the San Joaquin Valley, California. 1988 and 1989.* California Regional Water Quality Control Board, Central Valley Region, 48p.

CRC Handbook of Chemistry and Physics. 1982-1983. 63rd Edition. CRC Press. Inc. Boca Raton, Florida.

Doner, H.E., and W.C. Lynn. 1989. Carbonate, halide, sulfate, and sulfide minerals. In *Minerals in Soil Environments.* 2nd ed. J.B. Dixon and S.B. Weed (eds.) Soil Science Society of America, Madison. Wisconsin, 279-330.

Driessens, F. C. M. 1986. Ionic solid solutions in contact with aqueous solutions. In *Geochemical Processes at Mineral Surfaces,* ACS Symposium Series 323, J. A. Davis and K. F. Hayes (eds) American Chemical Society, Washington, DC, 524-560.

Felmy. A.R., and J.H. Weare. 1986. The prediction of borate mineral equilibria in natural waters: Application to Searles Lake, California. *Geochim. Cosmochim. Acta.* 50:2771-2783.

Fio, J. L. and R. Fujii. 1990. Selenium speciation methods and application to soil saturation extracts froms San Joaquin Valley, California. *Soil Sci. Soc. Am. J.* 54:363-369.

Ford, S. 1988. *Investigation of Evaporation Ponds for the Disposal of Agricultural Drainage in the San Joaquin Valley.* Progress report. Department of Water Resources, State of California, 90p.

Gilliom, R. J. 1989. *Preliminary Assessment of Sources, Distribution, and Mobility of Selenium in the San Joaquin Valley, California.* U. S. Geological Survey, Water Resources Investigations Report 88-4186, 129p.

Harvie, C.E. J.H. Weare, L.A. Hardie, and H.P. Eugster. 1980. Evaporation of seawater: Calculated mineral sequences. *Science.* 208:498-500.

Herbel, M. J. 1991. *Geochemical Reactivity of Boron with Evaporites During Desiccation of Na-Cl and Na-SO_4 Solutions.* Master thesis. University of California, Davis.

John, M. K., H.H. Chuah and J.H. Neufeld. 1975. Application of improved azomethine-H method to the determination of boron in soils and plants. *Analytical Letters* 8(8):559-568.

Keller, L.P., G.J. McCarthy and J.L. Richardson. 1986a. Laboratory modeling of Northern Great Plains salt efflorescence mineralogy. *Soil Sci. Soc. Am. J.* 50:1363-1367.

Keller, L.P., G.J. McCarthy and J.L. Richardson. 1986b. Mineralogy and stability of soil evaporites in North Dakota. *Soil Sci. Soc. Am. J.* 50:1069-1071.

Kurilenko, V. V.,V. K. Filippov, N. A. Charykov and A A. Shvarts. 1990. Use of the Pitzer method for hydrogeochemical modeling of the development of modern evaporite basins. *Dokl. Akad. Nauk SSSR.* 31(1):193-196.

Linke, W.F. 1965. *Solubilities. Inorganic and Metal-Organic Compounds.* Volume II. 4th ed. American Chemical Society, Washington, D.C., 1914p.

Moretto, R. 1988. Observations on the incorporation of trace elements in halite of Oligocene salt beds, Bourf-en-Bresse basin, France. *Geochim. Cosmochim. Acta* 52:2809-2814.

Naray-Szabo, I. 1969. *Inorganic Crystal Chemistry.* [Translated by P. Hedvig and G. Zentai] Akademiai Kaido, Budapest, 479p.

Ogle, R.S. and A.W. Knight. 1989. Effects of elevated foodborne selenium on growth and reproduction of the fathead minnow (*Pimephales promelas*) Arch. *Eviron. Contam. Toxicol.* 18:795-803.

Ong, C.G.H. 1991. *Geochemical Dynamics of Selenium in Evaporite-Forming Agricultural Evaporation Ponds.* Ph. D. diss. University of California, Davis.

Ross, V.F., amd J.O. Edwards. 1967. The structural chemistry of the borates. In E.L. Muetteries (ed.) *The Chemistry of Boron and Its Compounds.* John Wiley & Sons, Inc., New York. pp, 155-207.

Smith, G.I., I. Friedman and R.J. McLaughlin. 1987. Studies of Quanternary saline lakes. III. Mineral, chemical, and isotopic evidence of salt solution and crystallization processes in Owens Lake, California, 1969-1971. *Geochim. Cosmochim. Acta* 51(4):811-827.

Smith, G.R. 1989. *Brine Chemistry Model for Agricultural Evaporation Ponds and Other Hypersaline Waters.* Ph. D. diss. University of California, Davis.

Tanji, K., and R. Dahlgren. 1990. *Efficacy of Evaporation Ponds for Disposal of Saline Drain Waters.* Final Report to San Joaquin Valley Drainage Program through the Department of Water Resources.

Taylor, J.K. 1987. *Quality Assurance of Chemical Measurements.* Lewis Publishers, Inc. Chelsea, Michigan. 328p.

Walton, A.G. 1967. *The Formation and Properties of Precipitates.* Robert E. Krieger Publishing Company, Huntington, New York, 232p. ???

Westcot. D., S. Rosenbaum and G. Bradford. 1989. Trace element buildup in drainage water evaporation basins, San Joaquin Valley. In *Proceedings of the Second Pan-American Regional Conference of the International Commission on Irrigation and Drainage.* U.S. Committee on Irrigation and Drainage, J.B. Summers and S.S. Anderson (eds) 123-135. Ottawa, Ontario, Canada.

Wyckoff, R.W.G. 1964. Crystal Structure. Vol. 2. 2nd ed. Interscience, New York, 588p.